"COMPARATIVE STUDY OF ELASTOGRAPHY AND ULTRASONOGRAPHY IN DIFFERENTIATING BENIGN AND MALIGNANT THYROID LESIONS WITH PATHOLOGICAL CORRELATION"

By

Dr. HITHISHINI H.

DISSERTATION SUBMITTED TO SRI DEVARAJ URS ACADEMY OF HIGHER EDUCATION AND RESEARCH, KOLAR, KARNATAKA

In partial fulfilment of the requirements for the degree of

DOCTOR OF MEDICINE
IN
RADIODIAGNOSIS

Under the Guidance of

Dr. N. RACHEGOWDA,
PROFESSOR & HOD
DEPT. OF RADIOLOGY

Under the Co-Guidance of

DR. SREERAMULU P. N,
PRINCIPAL & PROFESSOR,
DEPT. OF SURGERY

Under the Co-Guidance of

DR. KALYANI R.,
PROFESSOR & HOD,
DEPT. OF PATHOLOGY

DEPARTMENT OF RADIODIAGNOSIS, SRI DEVARAJ URS MEDICAL COLLEGE, TAMAKA, KOLAR-563101

APRIL 2020

SRI DEVARAJ URS ACADEMY OF HIGHER EDUCATION AND RESEARCH, TAMAKA, KOLAR, KARNATAKA

DECLARATION BY THE CANDIDATE

I hereby declare that this dissertation entitled **"COMPARATIVE STUDY OF ELASTOGRAPHY AND ULTRASONOGRAPHY IN DIFFERENTIATING BENIGN AND MALIGNANT THYROID LESIONS WITH PATHOLOGICAL CORRELATION"** is a bonafide and genuine research work carried out by me under the guidance of **Dr. N. RACHEGOWDA**, Professor & Head, Department of Radiodiagnosis, Sri Devaraj Urs Medical College, Kolar, in partial fulfilment of University regulation for the award "**M. D. DEGREE IN RADIODIAGNOSIS**", the examination to be held in April 2020 by SDUAHER. This has not been submitted by me previously for the award of any degree or diploma from the university or any other university.

Date:

Place: Kolar

Dr. HITHISHINI H.

Postgraduate in Radiodiagnosis

Sri Devaraj Urs Medical College

Tamaka, Kolar

SRI DEVARAJ URS ACADEMY OF HIGHER EDUCATION AND RESEARCH, TAMAKA, KOLAR, KARNATAKA

CERTIFICATE BY THE GUIDE & HOD

This is to certify that the dissertation entitled "**COMPARATIVE STUDY OF ELASTOGRAPHY AND ULTRASONOGRAPHY IN DIFFERENTIATING BENIGN AND MALIGNANT THYROID LESIONS WITH PATHOLOGICAL CORRELATION"** is a bonafide research work done by **Dr. HITHISHINI H.,** under my direct guidance and supervision at Sri Devaraj Urs Medical College, Kolar, in partial fulfilment of the requirement for the degree of "**M.D. IN RADIODIAGNOSIS"**.

Date:

Place: Kolar

Dr. N. RACHEGOWDA, MD, DMRD
Professor & HOD
Department Of Radiodiagnosis
Sri Devaraj Urs Medical College
Tamaka, Kolar

SRI DEVARAJ URS ACADEMY OF HIGHER EDUCATION AND RESEARCH, TAMAKA, KOLAR, KARNATAKA

CERTIFICATE BY THE CO-GUIDE

This is to certify that the dissertation entitled "**COMPARATIVE STUDY OF ELASTOGRAPHY AND ULTRASONOGRAPHY IN DIFFERENTIATING BENIGN AND MALIGNANT THYROID LESIONS WITH PATHOLOGICAL CORRELATION"** is a bonafide research work done by **Dr. HITHISHINI H.,** under my co-guidance and supervision at Sri Devaraj Urs Medical College, Kolar**,** in partial fulfilment of the requirement for the degree of "**M.D. IN RADIODIAGNOSIS"**.

Date:

Place: Kolar

Dr. DR. SREERAMULU P. N, MS, FMAS

Principal and Professor,

Department of Surgery

Sri Devaraj Urs Medical College

Tamaka, Kolar

SRI DEVARAJ URS ACADEMY OF HIGHER EDUCATION AND RESEARCH, TAMAKA, KOLAR, KARNATAKA

CERTIFICATE BY THE CO-GUIDE

This is to certify that the dissertation entitled "**COMPARATIVE STUDY OF ELASTOGRAPHY AND ULTRASONOGRAPHY IN DIFFERENTIATING BENIGN AND MALIGNANT THYROID LESIONS WITH PATHOLOGICAL CORRELATION"** is a bonafide research work done by **Dr. HITHISHINI H.,** under my co-guidance and supervision at Sri Devaraj Urs Medical College, Kolar**,** in partial fulfilment of the requirement for the degree of "**M.D. IN RADIODIAGNOSIS"**.

Date:

Place: Kolar

Dr. KALYANI. R, MD, FICP
Professor & HOD
Department Of Pathology
Sri Devaraj Urs Medical College
Tamaka, Kolar

SRI DEVARAJ URS ACADEMY OF HIGHER EDUCATION AND RESEARCH, TAMAKA, KOLAR, KARNATAKA

ENDORSEMENT BY THE HEAD OF THE DEPARTMENT AND PRINCIPAL

This is to certify that the dissertation entitled **" COMPARATIVE STUDY OF ELASTOGRAPHY AND ULTRASONOGRAPHY IN DIFFERENTIATING BENIGN AND MALIGNANT THYROID LESIONS WITH PATHOLOGICAL CORRELATION "** is a bonafide research work done by **Dr. HITHISHINI H.** under the direct guidance and supervision of **Dr. N. RACHEGOWDA,** Professor & Head, Department of Radiodiagnosis, Sri Devaraj Urs Medical College, Kolar, in partial fulfilment of University regulation for the award "**M.D. DEGREE IN RADIODIAGNOSIS**"**.**

Dr. N. RACHEGOWDA
Professor & HOD
Department Of Radiodiagnosis,
Sri Devaraj Urs Medical College,
Tamaka, Kolar

Date:
Place: Kolar

DR. SREERAMULU P. N
Principal,
Sri Devaraj Urs Medical College,
Tamaka, Kolar

Date:
Place: Kolar

SRI DEVARAJ URS ACADEMY OF HIGHER EDUCATION

AND RESEARCH TAMAKA, KOLAR, KARNATAKA

ETHICAL COMMITTEE CERTIFICATE

This is to certify that the Ethical committee of Sri Devaraj Urs Medical College, Tamaka, and Kolar has unanimously approved

Dr. HITHISHINI H.

Post-Graduate student in the subject of

RADIODIAGNOSIS at Sri Devaraj Urs Medical College, Kolar

to take up the Dissertation work entitled

"COMPARATIVE STUDY OF ELASTOGRAPHY AND ULTRASONOGRAPHY IN DIFFERENTIATING BENIGN AND MALIGNANT THYROID LESIONS WITH PATHOLOGICAL CORRELATION"

to be submitted to the

SRI DEVARAJ URS ACADEMY OF HIGHER EDUCATION AND

RESEARCH, TAMAKA, KOLAR, KARNATAKA,

Member Secretary

Sri Devaraj Urs Medical College,

Kolar–563101

SRI DEVARAJ URS ACADEMY OF HIGHER EDUCATION AND RESEARCH TAMAKA, KOLAR, KARNATAKA

COPY RIGHT

Dr. HITHISHINI H.

Date:

Place: Kolar

ACKNOWLEDGEMENT

I owe debt and gratitude to my parents ***Sri. HANUMANTHARAYAPPA A.*** *and* ***Smt. NIRMALA S DEVI****, along with my brother* ***Mr. CHIRAAG*** *and my husband* ***Mr. CHETAN R. H.*** *for their moral support and constant encouragement during the study.*

With humble gratitude and great respect, I would like to thank my teacher, mentor and guide, ***Dr. N. RACHEGOWDA,*** *Professor and Head, Department of Radiodiagnosis, Sri Devaraj Urs Medical College, Kolar, for his able guidance, constant encouragement, immense help and valuable advices which went a long way in moulding and enabling me to complete this work successfully. Without his initiative and constant encouragement this study would not have been possible. His vast experience, knowledge, able supervision and valuable advices have served as a constant source of inspiration during the entire course of my study. I would like to express my sincere thanks to* **Dr.SREERAMULU P. N***., Principal and Professor, Department of Surgery,* ***Dr. KALYANI R****., Professor and Head, Department of Pathology,* ***Dr. ANIL KUMAR SAKALECHA,*** *Professor, Department of Radiodiagnosis, Sri Devaraj Urs Medical College for their, valuable support, guidance and encouragement throughout the study. I would also like to thank* ***Dr. SHIVAPRASAD G SAVAGAVE,*** *Asst. prof., Department of Radiodiagnosis, Sri Devaraj Urs Medical College for his wholehearted support and guidance.*

I would like to thank ***Dr. A. NABAKUMAR SINGH, Dr. ASHWATHNARAYANA, Dr. RAJESWARI, Dr. SRINIVASA BABU C. R., Dr. GOWTHAMI M., Dr. RAVINDRA, Dr. MADHUKAR, Dr. SWAROOP, Dr. RAHUL, Dr. DARSHAN, Dr. ANIL KUMAR T. R.*** *and all my teachers of Department of Radio diagnosis, Sri Devaraj Urs Medical College and Research Institute, Kolar, for their constant guidance and encouragement during the study period.*

I am extremely grateful to the patients who volunteered to this study, without them this study would just be a dream.

I am thankful to my fellow ***postgraduates, especially Dr. Athira P.M., Dr. Anshul Singh., Dr. Parameshwar Keerthi.****,* ***and Dr. Esakki Rajulu,*** *for having rendered all their co-operation and help to me during my study.*

My sincere thanks to ***Mrs. Shobha*** *along with rest of the computer operators.*

I am also thankful to ***Mr. Aleem, Mr. Mateen, Mr. Ravi,*** *and* ***Mr. Chandrasekhar*** *with other* ***technicians*** *of Department of Radiodiagnosis, R.L Jalappa Hospital & Research Centre, Tamaka, Kolar for their help.*

Dr. HITHISHINI H.

SDUAHER

Sri Devaraj Urs Academy of Higher Education and Research

Certificate of Plagiarism Check for Thesis/Dissertation

Author Name	Dr.Hithishini H
Course of Study	MD RADIODIAGNOSIS
Name of Supervisor	Dr. RACHEGOWDA N.
Department	RADIODIAGNOSIS
Acceptable Maximum Limit	
Submitted By	librarian@sduu.ac.in
Paper Title	COMPARATIVE STUDY OF ELASTOGRAPHY AND ULTRASONOGRAPHY IN DIFFERENTIATING BENIGN AND MALIGNANT THYROID LESIONS WITH PATHOLOGICAL CORRELATION
Similarity	04 %
Paper ID	191122101751
Submission Date	2019-11-22 10:17:51

* This report has been generated by DrillBit Anti-Plagiarism Software

Signature of Student	Signature of Supervisor
Head of the Department	
University Librarian 22/11/19	Director Of Post Graduate Studies 26/11/19

Professor & Head
Dept. of Radio-Diagnosis,

Senior Librarian
Library and Information Centre
Sri Devaraj Urs Medical College
Tamaka, KOLAR-563 101.

Director
P.G. STUDIES
Sri Devaraj Urs Medical College
Tamaka, KOLAR-563 101

LIST OF ABBREVIATIONS

ACR- TIRADS - American College of Radiology Thyroid Data System

ADC - Apparent diffusion coefficient

ARFI - Acoustic radiation force impulse

AUC - Area under the curve

CT - Computed tomography

DWI - Diffusion weighted imaging

ECI - Elasticity contrast index

FDG - Fluorodeoxyglucose

FNAB - Fine Needle Aspiration Biopsy

FNAC - Fine needle aspiration cytology

H & E - Hematoxylin and eosin

HPE - Histopathology examination

MEN - Multiple endocrine neoplasia

MRI - Magnetic resonance imaging

NPV - Negative predictive value

PET - Positron emission tomography

PPV - Positive predictive value

ROI - Region of Interest

SE - Strain Elastography

SWE - Shear Wave Elastography

SWS - Shear wave speed

TI-RADS - Thyroid imaging reporting and data system

TSI - Thyroid stiffness index

USG - Ultrasonography

ABSTRACT

Background: Incidence of thyroid lesions is as high as 50% in general population and with recent spurt of malignancies it is important to characterize the lesion as benign or malignant. Elastography evaluation of thyroid gland acts an adjunct to conventional ultrasonography and helps in characterising the lesion better for further management.

Objectives: The objective of this study were to compare the role of conventional B mode ultrasonography and elastography in differentiating benign from malignant thyroid lesions and to correlate the results obtained with pathological findings.

Material and methods: This was a prospective observational study conducted over a period of one and half years (January 2018 to June 2019) and was performed on 140 patients suspected to have thyroid lesion referred to the Department of Radio Diagnosis at R. L. Jalappa Hospital and Research Centre. B mode ultrasonography was performed followed by elastography using a 5–12 MHz linear array transducer (PHILIPS EPIQ 5G Ultrasound Machine). Their pathological findings were correlated.

Results: Amongst 140 patients 120 were females (85.7 %) and remaining 20 patients were males (14.3 %). Based on pathological diagnosis 116 lesions were benign (82.86 %) and 24 were malignant (17.14 %). Both TIRADS and ACR-TIRADS had a similar sensitivity, specificity, positive predictive value, negative predictive value and accuracy of 44.44%, 92.31%, 66.7%, 82.76% and 80 % respectively.

Asteria criteria had a higher sensitivity, specificity and accuracy (sensitivity ~ 86.96 %, specificity ~ 95.73 % and accuracy ~ 94.29 %) than Rago (Tsukuba) criteria (sensitivity ~ 72%, specificity ~ 95.65 % and accuracy ~ 91.43 %). Elastography had a higher sensitivity, specificity, PPV, NPV and accuracy (sensitivity ~ 91.67%, specificity ~ 99.14% PPV~ 95.65%, NPV ~ 98.29% and accuracy ~ 97.86 %) than conventional ultrasonography (sensitivity ~ 66.67 %, specificity ~ 90.52 %, PPV~ 59.26%, NPV ~ 92.92% and accuracy ~ 86.43 %). Combined sensitivity, specificity, PPV, NPV and accuracy of elastography and ultrasonography was 79.17%, 94.83%, 76.00%, 95.65% and 92.14% respectively.

Conclusion: It was concluded that elastography can aid in distinguishing benign from malignant thyroid nodules. When elastography features are used in conjunction to the conventional ultrasonography findings it helps in characterising the lesions better and also aids in selecting nodules that need to undergo FNAC.

TABLE OF CONTENTS

LIST OF TABLES

LIST OF TABLES

LIST OF FIGURES

LIST OF FIGURES

LIST OF FIGURES

INTRODUCTION

INTRODUCTION

Elastography being a newly developed dynamic technology helps in evaluating thyroid nodules better. Elastography is considered a superior method in differentiating benign from malignant thyroid nodules as compared to conventional B mode ultrasonography[4]. It is performed under direct visual guidance and it measures the stiffness of the tissue which helps in accurately determining the nature of the lesion[1].

A recent spurt in the incidence of thyroid malignancies was reported. However, the rate of pre-operative misdiagnosis of thyroid malignancies remains high at 40 to 70%[1]. Although ultrasound is effective in diagnosing thyroid lesions it does not have a high accuracy in differentiating benign from malignant nodules. Elastography can overcome this limitation and allow for more definite characterization of benign vs malignant lesions[2]. Elastography acquires the image information by displacement of tissue as a response to the pressure that is applied to the area of interest. Semi quantitative methods with compression elastography using strain index is calculated by the ratio of nodule strain value to the strain of adjacent normal thyroid tissue[1].

Although fine needle aspiration cytology (FNAC) is considered the next step in characterizing thyroid nodules, up to 20% of biopsy aspirations are reported as non-diagnostic and hence need to be repeated, causing significant patient discomfort[3]. Addition of sonoelastography to B-mode ultrasonography study is known to help in more accurate characterization of lesion and identifying the key problematic areas, from where FNACs can be targeted to provide better diagnostic yield.

This study has been planned to compare and evaluate if addition of sonoelastography will increase the diagnostic confidence of conventional B-mode ultrasonography and improve the overall diagnostic yield.

AIMS & OBJECTIVES

AIMS AND OBJECTIVES

The aims and objectives of the study were:

1. To compare the role of conventional B mode ultrasonography and elastography in differentiating benign from malignant thyroid lesions.
2. To correlate the results obtained with pathological findings.

REVIEW OF LITERATURE

REVIEW OF LITERATURE

EMBRYOLOGY OF THYROID GLAND

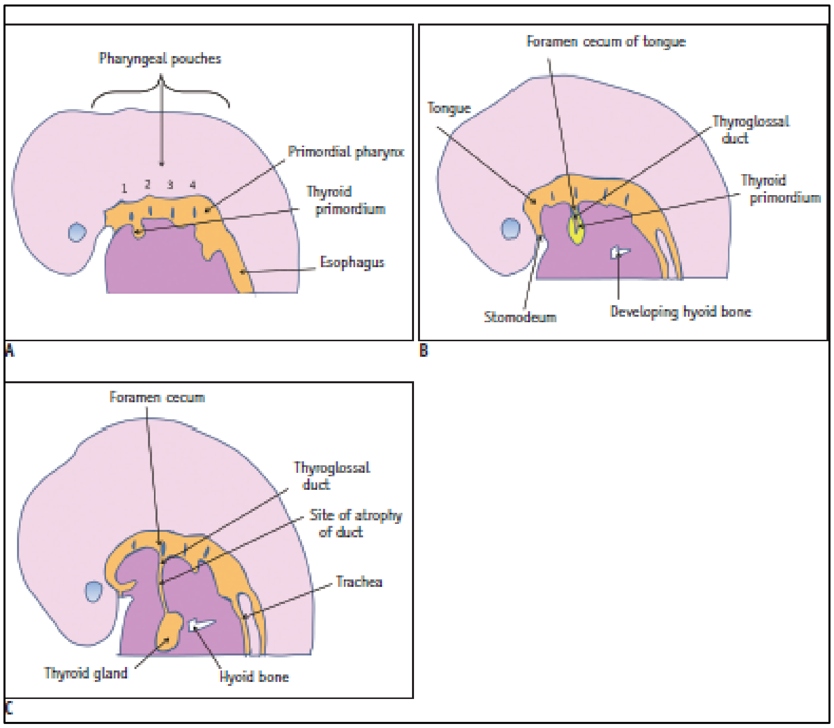

Figure 1 : Normal development of thyroid gland

Thyroid gland is formed by the paired lateral and median anlages. It is seen as an endodermal thickening in between the second and first pharyngeal arches. At 4^{th} to 5^{th} week of gestation the follicular cells are derived from the median anlage. Figure 1 demonstrates normal development of thyroid gland.

The primordium of thyroid is formed as small outward pouching, this elongates and becomes a diverticulum that is bilobed and descends down. Thyroglossal duct is seen as a small channel that temporarily connects caudal migration of thyroid primordium and tongue, which later involutes.

While thyroid descends it may get arrested anywhere from tongue down to lower neck. The thyroglossal duct disappears by seventh week.

Lateral thyroid anlages also called ultimobranchial bodies which arise from lateral aspect at 4^{th} and 5^{th} pharyngeal pouches at around fifth gestational week. Parafollicular cells are derived from lateral anlages. Median anlage merges with the lateral thyroid anlage after descent which leads to Parafollicular cells interspersed throughout the gland[15].

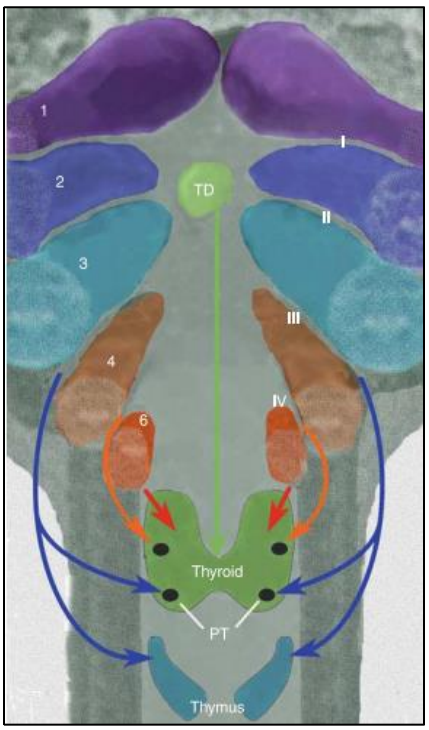

Figure 2 : Normal descent of thyroid gland

Primordial thyroid is seen as an endodermal invagination of tongue at foramen cecum which lies where midline intersects sulcus terminalis at the junction of posterior one third and anterior two thirds of tongue by fourth gestational week[7].

Initially thyroid diverticulum begins to descend through the tongue along with the thyroglossal duct as depicted in figure 2. Thyroid comes to lie anterior to larynx and hyoid bone.

At fifth week, degeneration involving superior part of duct is noted and thyroid has gained its rudimentary shape of two lobe and an isthmus connecting them.

By seventh week, thyroid gland descends to level of cricoid cartilage. There is degeneration of thyroglossal duct at distal portion which can sometimes be left behind as pyramidal lobe.

The cells from the fifth pharyngeal arch - ultimobranchial body which are of neural crest in origin differentiate into C cells and migrate into the thyroid. The C cells produce calcitonin.

Developmental anomalies of thyroid include –

Failure of thyroid to descend – which may lead to ectopic thyroid, anywhere along its path of descent.

The thyroglossal duct remnants may get hypertrophied and cystic.

Ovarian teratomas with thyroid tissue may be seen– known as struma ovarii[7].

ANATOMY OF THYROID GLAND

Anterior aspect of neck is where thyroid is placed, extending from fifth cervical to first thoracic vertebrae. It is highly vascular and appears brownish-red.

Thyroid gland comprises of left and right lobes connected by an isthmus. Pretracheal layer of deep cervical fascia encases the gland. Often a conical pyramidal lobe is seen ascending from either the isthmus or adjacent aspect of either lobe approaching hyoid bone.

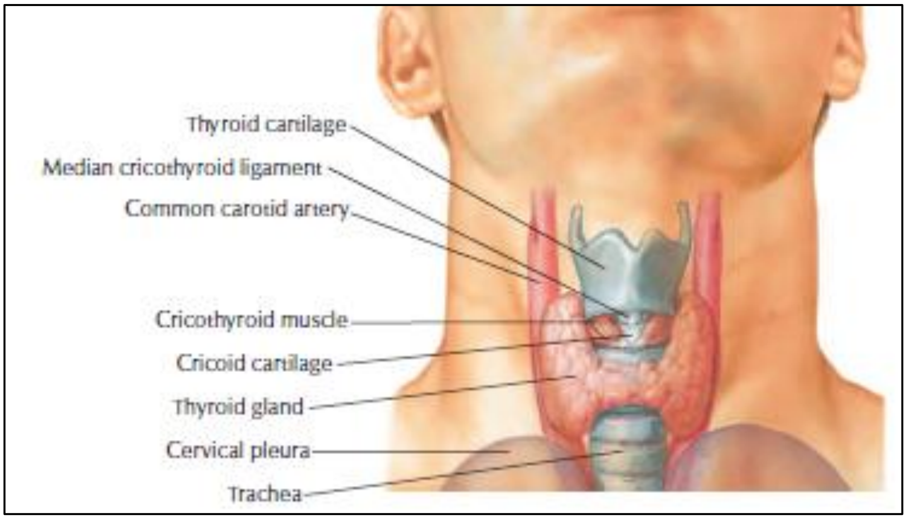

Figure 3: Anatomic relations of thyroid

Both left and right lobes are usually 5 cm in length, 2 cm in anteroposterior extent and 3 cm in its transverse diameter. Lateral ligament of thyroid attaches the posteromedial aspects of the lobes to the cricoid cartilage. Base of lobes are at fifth or fourth tracheal cartilage. Anatomic relations of thyroid are depicted in figure 3.

Isthmus connects the two lobes. It can be absent in some cases. It measures approximately 1.25 cm vertically as well as transversely. Seen at the level of 2^{nd} extending to 3^{rd} tracheal cartilages but may vary.

On an average the gland weighs 25 g. In females, the gland weighs a little more and also during menstruation and pregnancy[5].

VASCULAR SUPPLY AND LYMPHATIC DRAINAGE

Arteries

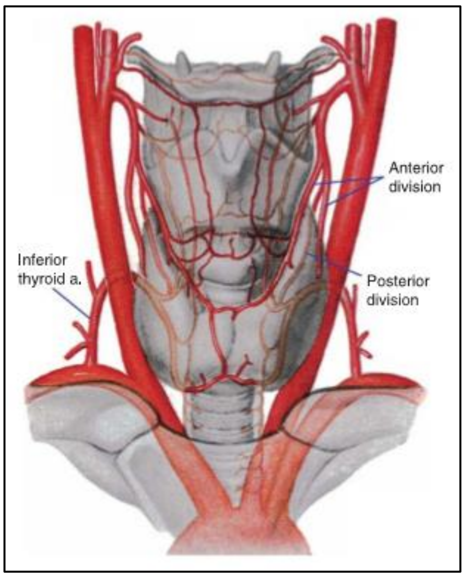

Figure 4 : Thyroid gland - Arterial supply

Blood supply is by the inferior and superior thyroid arteries as depicted in figure 4 and occasionally by thyorid ima artery from brachiocephalic trunk or aortic arch[5].

Superior thyroid artery arises as first branch from external carotid artery. It might also arise as a branch from common carotid artery[3].

Along with external laryngeal nerve, superior thyroid artery descends towards the superior pole. It divides to form 2 branches, the anterior and the posterior branches. Anterior surface is supplied by the anterior and posterior branches supply the medial and lateral surfaces[5].

Inferior thyroid artery normally seen at the base and divides into inferior and superior branches and supply the posterior and inferior portions[5]. The superior branch ascends to anastomose with superior thyroid artery (posterior branch) [7].

High variability in the relationship in between inferior thyroid artery and recurrent laryngeal nerve is seen. This has clinical importance owing to increased risk of iatrogenic injury to the nerve which can occur as a major complication of thyroid surgery[5].

Veins

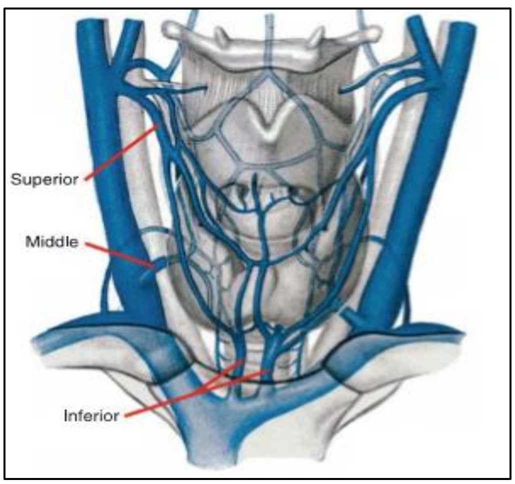

Figure 5: Thyroid gland - Venous drainage

The inferior, middle and superior thyroid veins drain the gland. The venous drainage of the gland is seen in figure 5.

Superior vein traverses along with superior thyroid artery. Middle thyroid artery drains the inferior part and exits from the gland along its lateral aspect. A venous plexus is present inside thyroid and inferior thyroid vein arises from this plexus and joins the middle and superior thyroid veins. Superior and middle thyroid veins drain into internal jugular veins on either side[5]. Inferior vein drains into brachiocephalic or it may drain into internal jugular vein[7].

Lymphatics

Superiorly, the medial portion of thyroid drains to digastric nodes and inferiorly to brachiocephalic and pretracheal nodes[7].

Lateral aspect of thyroid has lymphatic drainage along the arterial supply. They drain into jugular group of nodes either by ascending along with superior thyroid artery or descending along with the inferior thyroid artery[7].

Lymphatics sometimes communicates with tracheal plexus and then drain to prelaryngeal nodes and to pre and paratracheal nodes. Sometimes it also drains directly to the thoracic duct without draining into any nodes[5].

Innervation

Superior, middle and inferior cervical sympathetic ganglia contribute to innervation of the thyroid gland.

A plexus is formed by postganglionic fibres from inferior cervical ganglion along inferior thyroid artery. This is seen communicating with recurrent and external laryngeal nerves, and with plexus which is present around common carotid artery and superior cardiac nerve[5].

HISTOLOGY OF THYROID GLAND

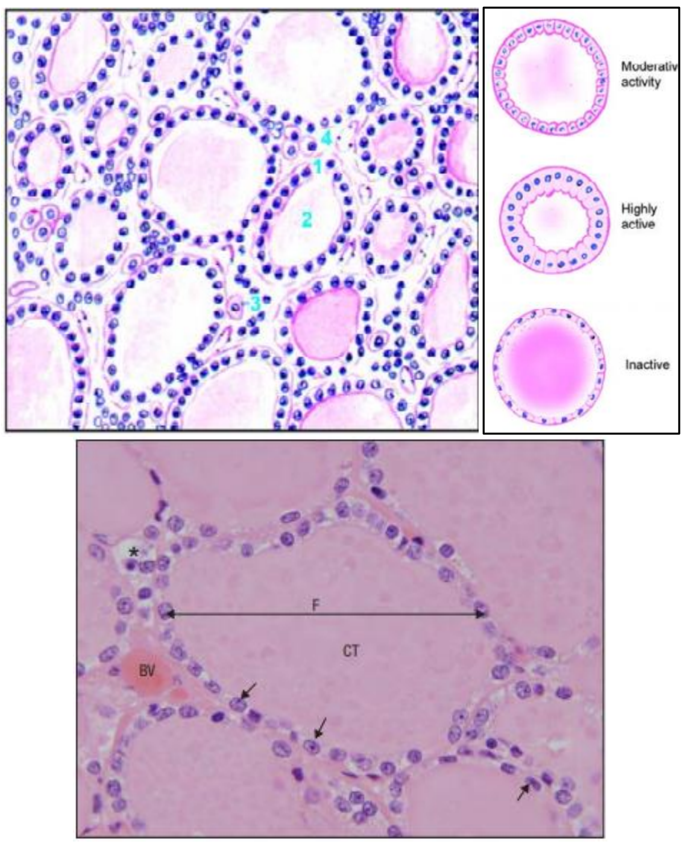

Figure 6 : Normal histology of thyroid gland

The gland is covered by fibrous septa from which the septa extend into it and form lobules. Multiple follicles together form a lobule. Follicular cells that lie on a basement membrane line the follicle.

A cavity with colloid which is noted as pink in hematoxylin and eosin stain is seen within the follicle. Connective tissue which contains dense lymphatics and capillary plexus and sympathetic nerves forms the stroma that lines the spaces in between the follicles as shown in figure 6.

Parafollicular cells or C- cells are also noted interspersed amongst the follicles[8].

USG ANATOMY OF THYROID

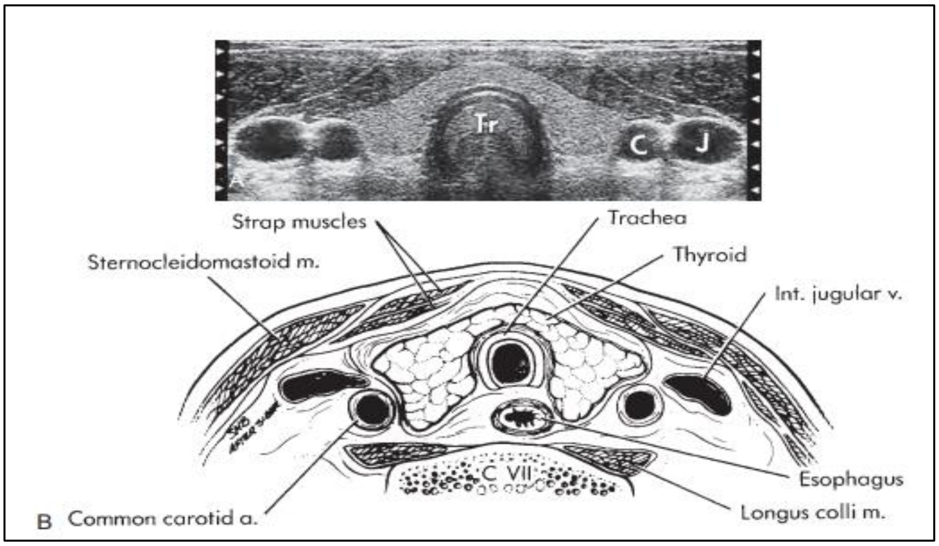

Figure 7 : Normal thyroid gland - USG anatomy

The gland is bilobed and present in the neck anteriorly, just anterior to trachea. On either side of trachea both left and right lobes are situated and are connected by an isthmus. Posterolaterally, the internal jugular veins and carotid arteries are seen. Strap muscles of the neck are located anterior to thyroid gland[12].

Normal USG appearance of gland parenchyma is homogenous echogenicity as demonstrated in figure 7. The capsule surround the lobes is seen as a thin hyperechoic line. The high vascularity is assessed using Doppler.

Along upper pole of either lobe, superior thyroid artery and vein are noted. The Inferior thyroid artery is seen posterior to lower third of both lobes and inferior thyroid veins are noted along lower poles.

Normally, the average mean diameter of thyroid arteries is 1 – 2 mm; and upto 8 mm in case of veins. Peak systolic velocity reaches upto 20 to 40 cm/sec in major arteries and around 15 to 30 cm/sec in intraparenchymal arteries[11].

The strap muscles, namely, the omohyoid and the sternohyoid appear as thin bands of hypoechogenicity present anteriorly. Bulkier and oval shaped band that is seen laterally is sternocleidomastoid. Another important region is posteriorly where the longus colli muscles are seen in close contact with the prevertebral space.

Esophagus is visualised lateral to thyroid gland commonly on left side and appears target shaped and when the patient swallows, peristalsis may be demonstrated. The artery (inferior thyroid) and nerve (recurrent laryngeal nerve) might be visualized between longus colli and thyroid gland on the right or between esophagus and thyroid gland on the left on longitudinal scans. The nerve (recurrent laryngeal nerve) and artery (inferior thyroid artery) pass through the angle between thyroid, trachea and esophagus[11].

DISEASES OF THYROID GLAND

Congenital thyroid abnormalities

Ectopia, varying degrees of hypoplasia and aplasia of one or both thyroid lobes constitute congenital abnormalities of thyroid gland. We can assess these conditions by Sonography. Congenital hypothyroidism can be assessed using the high frequency probe. This aids in determining the cause due to its importance in prognosis and therapy. It may help in initiation of therapy that prevents delayed bone development and mental retardation. Sonography is helpful to look for ectopic thyroid gland (eg. suprahyoid or lingual in position), however radionuclide scans are used more frequently for the same[11].

In most number of cases (~ 90 %) ectopic thyroid is visualised at base of the tongue. Usually functioning in only 75 % of such patients. Mostly located in close proximity to the hyoid bone. Seen as a round/oval area of uptake along midline. Scintigraphy is more sensitive than USG in assessing and diagnosing thyroid tissue that is ectopic[15].

Hemi-aplasia is usually an incidental finding. Function of thyroid gland may be reduced especially as puberty approaches as demand for these hormones is usually higher at puberty[15].

Inborn error of thyroxin synthesis is dyshormonogenesis in which thyroid peroxidase deficiency is a common defect and leads to failure of oxidization of iodide to form iodine. On ultrasound, a large orthotropic thyroid is seen due to elevated TSH levels. Both thyroid lobes develop a convex appearance laterally. On scintigraphy, increased uptake of isotope is noted in the enlarged gland present in normal location[15].

Thyroiditis

It constitutes a large group of conditions which are characterized by some form of thyroid inflammation. It consists of disorders that cause severe thyroid pain in acute illness (eg. granulomatous thyroiditis, infectious thyroiditis) and conditions with minimal inflammation and is primarily seen as thyroid dysfunction (Subacute thyroiditis/painless and Reidel's (fibrotic thyroiditis))[16].

Chronic Lymphocytic (Hashimoto) Thyroiditis

Areas where iodine levels are sufficient Hasthimoto's thyroiditis is seen to cause hypothyroidism. An autoimmune disease of the thyroid gland. Most commonly noted in middle aged women between 45 and 65 years. It is also noted in children[16].

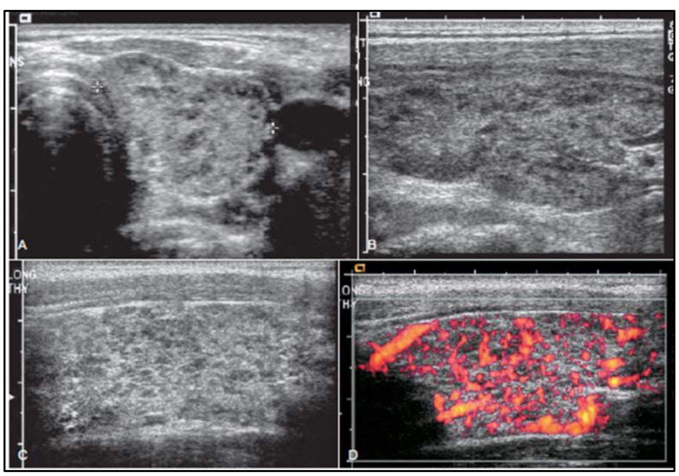

Figure 8: USG image of Hashimoto's thyroiditis.

There is development of antibodies to thyroglobulin and thyroid peroxidase.

On ultrasonography, the gland appears enlarged with altered, coarse parenchymal echotexture and usually reduced echogenicity as compared to the normal gland.

Nodules measuring ~ 1 to 6 mm that are discrete and multiple can imply chronic thyroiditis and is called micronodulation that has a PPV of 94.7 %.

Vascularity might appear normal or reduced on CDI and sometimes increased similar in appearance to the thyroid inferno noted in Graves' disease as shown in figure 8. The gland may appear atrophied in the end stage, where the gland appears small with ill-defined margins and altered heterogeneous echotexture due to fibrosis with severely reduced blood flow. Cervical lymphadenopathy may be noted[11].

Histology - Lobules of thyroid parenchyma that have been infiltrated by plasma cells and lymphocytes is represented by micronodules. Multiple fibrous septations surround the lobules and this produces a pseudo-lobulated appearance. Malignant and benign nodules may co-exist. There is increased risk of B-cell malignant lymphoma noted in these cases[11].

Subacute Granulomatous (de Quervain) Thyroiditis

It is commonly noted in age group ranging from 30 to 50 years and is prevalent in women than in men. The etiology considered is viral infection or inflammation that is secondary to viral infection. Most patients give a history of upper respiratory tract infection just before the onset of thyroiditis. As opposed to an autoimmune disease of thyroid gland this disease process is self limiting[16].

On USG it appears hypoechoic and bulky. On Colour Doppler imaging vascularity may be reduced or normal. CDI is useful in assessing de Quervain's after medical treatment[11].

Subacute Lymphocytic Thyroiditis

It is also called painless or silent thyroiditis. If it is noted after pregnancy it is known as postpartum thyroiditis. Antithyroid antibodies are noted in majority, therefore it is thought to have an autoimmune etiology. This usually presents as painless mass along the neck anteriorly and is commonly noted in middle aged women. Thyrotoxicosis is noted in the initial stages and euthyroid may be seen following this. Very few develop hypothyroidism[16].Progression to hypothyroidism is noted in postpartum thyroiditis.

On ultrasonography, there is inhomogeneity and micronodularity like in Hashimoto's thyroiditis[11].

Histology – Hyperplastic germinal centres and areas of lymphocytic infiltration interspersed in the thyroid parenchyma may be noted[16].

Riedel Thyroiditis

Is also called invasive fibrous thyroiditis. It constitutes extensive fibrosis which involves the entire gland and structures surrounding it. On examination appears as a hard and fixed mass mimicking a neoplasm. It is sometimes associated with retroperitoneal fibrosis or sclerosing cholangitis. Antithyroid antibodies is noted in some patients indicating an autoimmune etiology[16].

On ultrasonography, the gland appeared inhomogeneous and bulky. The main indication for sonographic evaluation is to assess the extrathyroid extension with encasement of surrounding vessels. This helps in planning for surgery. It needs to be differentiated from anaplastic carcinoma of thyroid as sonographically they may appear similar and therefore necessitate open biopsy[11].

Nodular thyroid disease –

USG assessment of nodule is required to:

1) To determine the location of the nodule/mass (thyroid or extrathyroid)
2) Detect nodules in head and neck in patients undergoing irradiation or MEN II syndromes
3) To assess and establish extension of malignancy.
4) To assess residual, recurrent or metastatic carcinoma.
5) To aid guided FNAC of mass/nodule or cervical lymph node[11].

Hyperplasia and Goiter

Goiter leads to overall increase in gland volume because of hyperplasia. Usually caused by deficiency of iodine, dyshormonogenesis or poor uptake of iodine in cases of intake of certain medications. Female predominance is noted and the age range is between 35 to 50 years.

On ultrasonography, most of the nodules appear isoechoic to the gland. However, they may appear hyperechoic. Occasionally, presence of hypoechoic nodules having honeycomb or spongiform pattern as depicted in figure 9.

Perinodular blood vessels and mild edema of the adjacent tissue form a hypoechoic halo around the nodule. Perinodular vascularity is detected on Doppler Sonography. Sometimes vascularity within the nodule may also be noted.

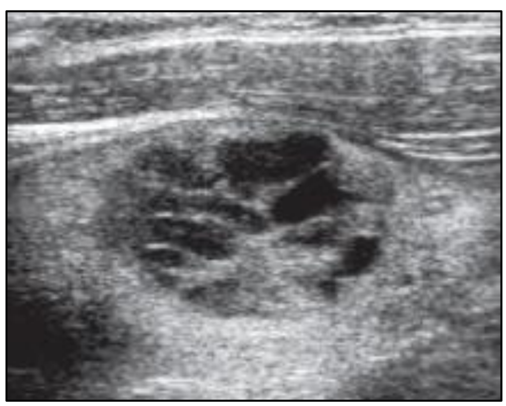

Figure 9: Spongiform appearance of nodule

The nodules seen in goiter tend to undergo degenerative changes. It may include hemorrhage, colloid degeneration, calcifications etc. Colloid or serous fluid is noted in completely anechoic cysts. If hemorrhage occurs, fluid- fluid levels noted. Colloid substance aggregates or microcrystals lead to hyperechoic foci with comet tail artifacts. Strands of tissue which appear completely avascular on Doppler Sonography are seen as thin internal septations.

Degeneration is noted in the form of calcifications. These may appear as highly reflective foci which are coarse with acoustic shadowing or as thin, peripheral eggshell calcification. Figure 10 demonstrates peripheral eggshell calcification.

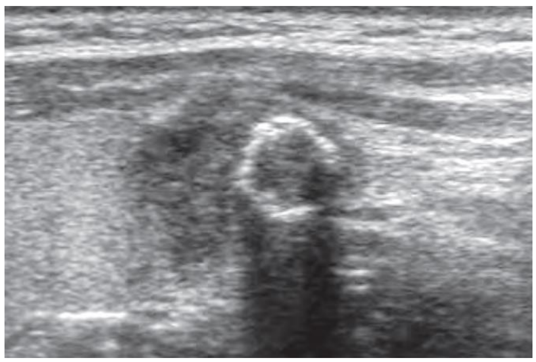

Figure 10: Peripheral eggshell calcification

Infrequently, solid projections or papillae may be seen within the cyst, similar to that of cystic papillary thyroid carcinoma.

On histology, cellular hyperplasia is in the beginning following which there is micronodule and macronodule formation. When blood, serous fluid and colloid accumulates the nodules undergo liquefactive degeneration. True epithelial lined cysts are rare. Calcifications which are frequently Perinodular and coarse may be noted. The patients may present in hyperthyroid, hypothyroid or euthyroid state[11].

Adenoma

Adenomas constitute ~ 5 to 10 % of nodular diseases. It is more prevalent in women than in men. Less than 10 % of them develop hyperfunction and may lead to thyrotoxicosis.

Fibrous encapsulation and compression of tissue in vicinity is visualised in benign follicular adenoma. The subtypes of follicular adenoma include embryonal adenoma, Hurthle cell adenoma and fetal adenoma.

The features of follicular adenomas on cytology are indistinguishable from follicular carcinomas. Capsular and vascular invasion is pathognomonic of follicular carcinoma which may be appreciated on histopathological examination. These tumors should be surgically excised and subjected to histopathological examination as needle biopsies are unreliable.

On ultrasonography, they may have a variable appearance – hypoechoic, isoechoic or hyperechoic. They appear as solid margins that have a smooth halo in the periphery that is hypoechoic which is formed by fibrous capsule and blood vessels that are identified in Doppler imaging. Occasionally, a “spoke and wheel “appearance may be noted. This is formed by vessels passing from the periphery to the center[11].

Carcinoma

Majority of the primary carcinomas are epithelial in origin. These are either derived from Parafollicular or follicular cells. Tumors arising from mesenchymal origin are extremely rare. Majority of tumors that originate from thyroid gland are well defined.

Papillary carcinoma constitutes the majority by contributing to 75% to 90 % of all thyroid malignancies. Anaplastic, follicular and medullary carcinomas together represent only 10% to 25 %[11].

Papillary Carcinoma of Thyroid

Papillary carcinoma peaks in third and seventh decade of life. Female predominance is noted. The route of dissemination is by lymphatics to nearby cervical lymph nodes. Incidence of distant metastasis is rare (2% to 3 %) and may be seen in lung or mediastinum.

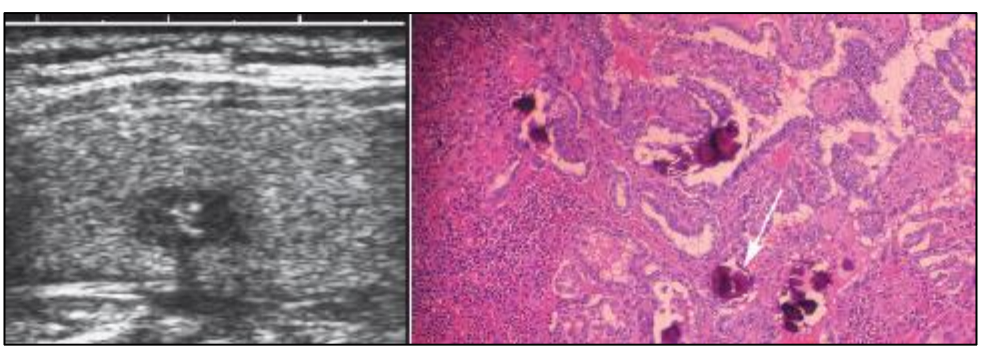

Figure 11: USG image of papillary carcinoma along with a microscopic image demonstrating "psammoma bodies" (arrow) (H & E stain, magnification x100)

On histology, microcalcifications and fibrous capsule are seen and on cytology, indentations of nuclear membrane, cytoplasmic inclusions in nucleus and ground glass nuclei is seen. Microcalcifications are also visualised, which are calcium salts that are deposited in the psammoma bodies as shown in figure 11. These psammoma bodies can be noted in both primary tumor and the cervical lymph node metastases.

On ultrasonography, papillary carcinoma may have a varied appearance. Closely packed cell content and minimal colloid content appears hypoechogenic in approximately 90 % of cases.

Multiple, tiny punctate calcifications which appear as hyperechoic foci with acoustic shadows are because of microcalcifications. This sometimes is the only finding of neoplasm on B-mode ultrasonography visualised in an unusual aggressive form of papillary carcinoma of the child hood in which no nodular lesion is noted.

Papillary carcinoma may also appear cystic due to extensive degeneration. Very rarely there may be infiltration of the adjacent muscles. Follicular variant of papillary carcinoma constitutes around ~ 10 % of all the cases. Papillary microcarcinoma is a very rare entity in which a non-encapsulated sclerosing tumor measuring < 1 cm is noted. On ultrasonography, they may appear as a hyperechoic patch under the capsule or as a minute hypoechoic nodule which has irregular blurred outline. Usually microcalcifications are not noted. Increased vascularity noted in these lesions is usually disorganized and is noted in approximately 90 % well encapsulated lesions.

Metastases involving cervical lymph nodes are common, as route of dissemination is via lymphatics. They may appear as microcalcifications in the involved lymph nodes. In some cases, cystic changes may be noted in them due to extensive degeneration. On Doppler imaging these metastatic nodes show increased vascularity. The vessels appear tortuous and sometimes arteriovenous shunts may be present. Also noted, high vascular resistance (RI > 0.8)[11].

Follicular Carcinoma

Follicular carcinoma is also a well differentiated subtype comprising 5% to 15 % of malignancies. As in other conditions of the thyroid, female predominance is noted.

Two variants are present, minimally invasive and widely invasive follicular variants. In minimally invasive carcinomas, there is histologic features of focal invasion of blood vessels of the fibrous capsule. In widely invasive carcinomas, which are not well differentiated, the invasion of adjacent thyroid and vessels are easy to identify.

Both the types have hematogenous spread rather than lymphatic spread. Distant metastases to brain, lung bones and liver is noted.

On B-mode ultrasonography, it poses a challenge in distinguishing between follicular carcinoma and follicular adenoma. The appearance may vary, usually they appear as well-defined homogenous masses with increased vascularity on Doppler imaging which appear as thick irregular halo due to tortuous vessels.

Fine needle aspiration is also not reliable in differentiating follicular carcinoma from adenoma. Only histological demonstration of invasion of capsule and vascular invasion helps make the diagnosis. This necessitates the follicles to be surgically removed for pathological diagnosis[11].

Medullary Carcinoma

Amongst all malignant thyroid diseases, medullary carcinoma accounts for approximately 5 %. Seen originating from C cells or Parafollicular cells. The lesion secretes calcitonin hormone. This hormone is helpful as a serum marker. Medullary carcinoma is frequently familial in ~ 20 % and is associated with multiple endocrine neoplasia (MEN) type II syndromes. In about 90% of familial cases, usually it might be bilateral and/or multicentric. Metastases is commonly noted in cervical lymph nodes. Prognosis is worse than papillary carcinoma.

On ultrasonography, medullary carcinoma resembles papillary carcinoma which appears like a hypoechoic mass. Coarse calcifications unlike microcalcifications in papillary carcinoma are noted. In some cases, calcifications occur in lymph node metastases and metastatic lesions of the liver.

On histology the tumors have an admixture of cell types. The nuclei appear moderately pleomorphic with stippled chromatin, small nucleoli and rarely pseudo-inclusions. Amyloid deposits noted in 90% of the cases[19].

Anaplastic Thyroid Carcinoma

Anaplastic carcinomas are usually noted in elderly patients. Most lethal tumors with worst prognosis. It constitutes less than 2 % of all thyroid cancers. It has a high mortality rate which is more than 95 %. The tumor is usually inoperable at the time of diagnosis. Associated with papillary or follicular carcinomas. These tumors tend to have a more aggressive local infiltration to adjacent vessels and muscles as opposed to lymphatic spread. On ultrasonography, they appear as hypoechoic lesions that infiltrate the neck muscles and may encase the vessels. Assessment may be suboptimal on ultrasonography due to their large size. In such conditions MRI or CT of neck is considered more useful in demonstrating extension of disease[11].

On histology, giant pleomorphic cells that have hyperchromatic nuclei growing in sheets is noted. Inflammation with necrosis is common in these tumors[17].

Lymphoma

Of all the malignancies of thyroid gland, lymphoma accounts for ~ 4 % of all the tumors. More common amongst older women and more commonly the non-Hodgkin's type. It may present as a rapidly growing mass that may cause obstructive symptoms like dyspnoea and dysphagia. In approximately 70 % to 80 % of lymphoma cases it is seen arising from a pre-existing Hashimoto's thyroiditis (chronic lymphocytic thyroiditis). They usually present with hypothyroidism. In early stages the five-year survival rate is almost 90 %, whereas in advanced and disseminated stages it is less than 5 %[11].

On B mode ultrasonography, primary thyroid lymphoma is classified into the following three types based on its morphology:

- Diffuse mass type – May involve both the lobes and is extremely hypoechoic, it may have a pseudocystic appearance.
- Multiple nodular type – Multiple hypoechoic nodules may be noted with well-defined borders.
- Mixed type – This has features of both the diffuse and multinodular variant and resembles adenomatous goiter. Adjacent cervical lymph nodes may be involved[18].

The adjacent thyroid parenchyma may appear heterogeneous because of associated chronic thyroiditis[11]. On histology, there is mild effacement of thyroid parenchymal architecture caused by multiple oval to round lymphoid cells that have large pleomorphic nuclei, coarse nuclear chromatin and scant cytoplasm. Sometimes infiltration of follicular epithelium creating lymphoepithelial lesions may be present. The adjacent thyroid parenchyma may show extensive coexisting chronic lymphocytic thyroiditis (Hashimoto's) [21].

Thyroid Metastases

Thyroid gland metastases are extremely rare. It is disseminated via hematogenous spread or less commonly via lymphatic route. Metastases usually noted are from renal cell (10%), breast (21%) and melanoma (39%).

On ultrasonography, they may appear as hypoechoic solitary/multifocal nodules and well circumscribed or may diffusely involve the gland. They usually do not show calcifications[11].

Thyroid Gland: Clinical assessment

History

In girls who are nearing puberty simple goiter is a common condition noted. Simple goiter is also noted in endemic regions that are deficient in iodide. Dyshormonogenesis and goitrogens are the main causes that lead to simple goiter. Amongst ages of 20 – 30 years colloid goiter, multinodular goiter and solid nodular goiters are common. Papillary carcinoma is noted in younger age group. Whereas follicular carcinoma is noted in older age group. Anaplastic carcinoma occurs exclusively in elderly age group. Primary toxic goiter is noted in younger patients, however, Hashimoto's disease is usually noted in middle aged population.

Females are commonly affected by goitre as compared to males. Many studies have shown that thyrotoxicosis occurs frequently in females than males by 8 times and malignancies are 3 times more frequently in females as compared to males.

Patients with thyroid disorder usually present with swelling along anterior aspect of neck. Pain may be the presentation in cases of inflammatory conditions. In malignancies, pain occurs much later. Amongst the malignancies, anaplastic carcinoma is known for its extensive infiltration to adjacent structures and this may lead development of pain.

Symptoms

In case of primary thyrotoxicosis, weight loss inspite of healthy appetite is a main symptom. Others include, intolerance to heat, excessive sweating, irritability, insomnia, tremors, weakness of muscles. Another symptom is amenorrhea. Cardiovascular manifestations like dyspnoea, tachycardia, ectopic beats and palpitations are more prevalent in secondary thyrotoxicosis. Congestive cardiac failure might be noted in much later stages.

Eye manifestations like exophthalmos, difficulty in closing eyes, double vision, diplopia, ophtalmoplegia (muscle weakness). Swelling/oedema of the conjunctiva also known as chemosis. Other eye signs include lid retraction, Von Graefe's sign (lid lag on down gaze), Joffroy's sign (loss of forehead corrugation while looking up), Stellwag's sign (incomplete and infrequent blinking), Moebius sign (poor convergence) and Dalrymple's sign (lid retraction).

In cases of hypothyroidism, usually weight gain is noted even though appetite is poor. Intolerance to heat, loss of eyebrows especially the lateral $2/3^{rd}$, muscle fatigue, lethargy and dryness of the skin is seen. Another symptom that may be present is oligomenorrhea.

When thyroid gland gets enlarged pressure effects noted are dyspnoea, owing to compression on trachea, dysphagia because of compression on esophagus and hoarseness of voice in cases of anaplastic carcinoma which leads to infiltration of the nerve.

Local examination

It is a point of importance that a thyroid swelling is seen to move superiorly on deglutition. This may because of its attachment to larynx. In cases of malignancy or inflammation it may get fixed and this movement may be restricted.

On palpation the following techniques are performed: -

Pizzillo’s technique – in this method the enlargement of gland is assessed with patients hand behind the head, following which patient is asked to push against the clasped hands on the occiput.

Lahey's method - Palpation of both the lobe is best carried out by pushing the gland to one side to assess margins.

Crile's method – with thumb on the gland patient is asked to swallow to look for any nodularity.

Kocher’s test – In this method a slight push on the lateral lobes will cause stridor, if so it indicates an obstructed trachea.

Pemberton’s sign – When patient is asked to lift their arms above the head and the arms touch the ears, if there is engorgement of neck veins it indicates obstruction to major veins in the thorax[30].

RADIOLOGICAL ASSESSMENT OF THYROID GLAND:

Radiograph

Conventional radiology has a limited diagnostic role in assessing thyroid pathologies. It can be useful in case of large thyroid lesions to assess the retrosternal extension. It has also been used to evaluate the calcifications in the lesion or metastasis to the lungs and bones from thyroid malignancies.

USG

Historic background

The beginning of the evolution of ultrasound dates back to 1700s. The principle has a theoretic explanation for bat aviation. In early 1900s it was used as a tool for medical imaging and was developed into a crucial imaging tool for both diagnostic and therapeutic purposes in modern medicine.

An Italian physiologist and priest Lazzaro Spallanzani (1729–1799), conducted a series of experiments and was able to explain how bats were able to fly during the night. This was the beginning of evolution of ultrasound. He observed that if a bat was blinded, the bat had the ability to fly appropriately abut if the bat were to be made deaf even in one ear, the bat was not able to fly properly. He inferred that the bat relied not on their vision but on sound to fly. Multiple other experiments were conducted by various other physicists who concluded that speed of sound in water was 1435m/sec, which is very similar to the modern-day standard of 1482m/sec which is used currently.

An Austrian physicist Christian Doppler postulated the Doppler effect/shift in 1842. He explained the concept of how changes in the frequency of light waves caused variation of visible colours of the stars. This concept was used to conduct experiments on sound waves in 1845 by Dutch mathematician C. H.D. Buys Ballot.

Piezoelectricity, Greek word piezen means to squeeze or press, was initially discovered by Pierre and Jacques Curie who were brothers. It was noted that crystals of Rochelle salt, cane sugar, quartz, topaz and tourmaline could produce electricity under pressure. It was observed that when voltage was applied to such crystalline materials, there was production of pressure waves. The ability of such crystals to produce and receive the pressure waves which is quantified in megahertz frequencies is used in technology to develop modern day transducers[28].

ULTRASOUND FEATURES:

A diffusely bulky gland consisting of multiple nodules, uniform halo surrounding the nodule, predominantly cystic composition and avascularity suggest benignity.

Features on ultrasound that raise a suspicion for malignancy include extension beyond the thyroid margin, metastasis to cervical lymph nodes, microcalicifications, nodules that appear hypoechogenic and taller than wider shape and increased intranodular vascularity[12].

Earlier TI-RADS was utilised for stratification of risk and determining the management as described in figure 12.

Ultrasound criteria according to TI-RADS classification (23) to determine risk of malignancy of thyroid nodules

Category	Ultrasound features*	Malignancy risk
1	Negative, no nodule	<0.1%
2	Benign nodule	<0.1%
3	Probably benign, no suspicious features on US	1.7%
4a	Low suspicion of malignancy with 1 suspicious feature on US	3.3%
4b	Intermediate suspicion of malignancy with 2 suspicious features on US	9.2%
4c	Moderate suspicion with 3 or 4 suspicious features on US	44.2–72.4%
5	Highly suggestive of malignancy with 5 suspicious features on US	87.5%

Figure 12: TIRADS risk stratification

ACR- TIRADS (American College of Radiology Thyroid Data System) aims to provide an easier to apply method for risk stratification and management planning[27] as depicted in figure 13.

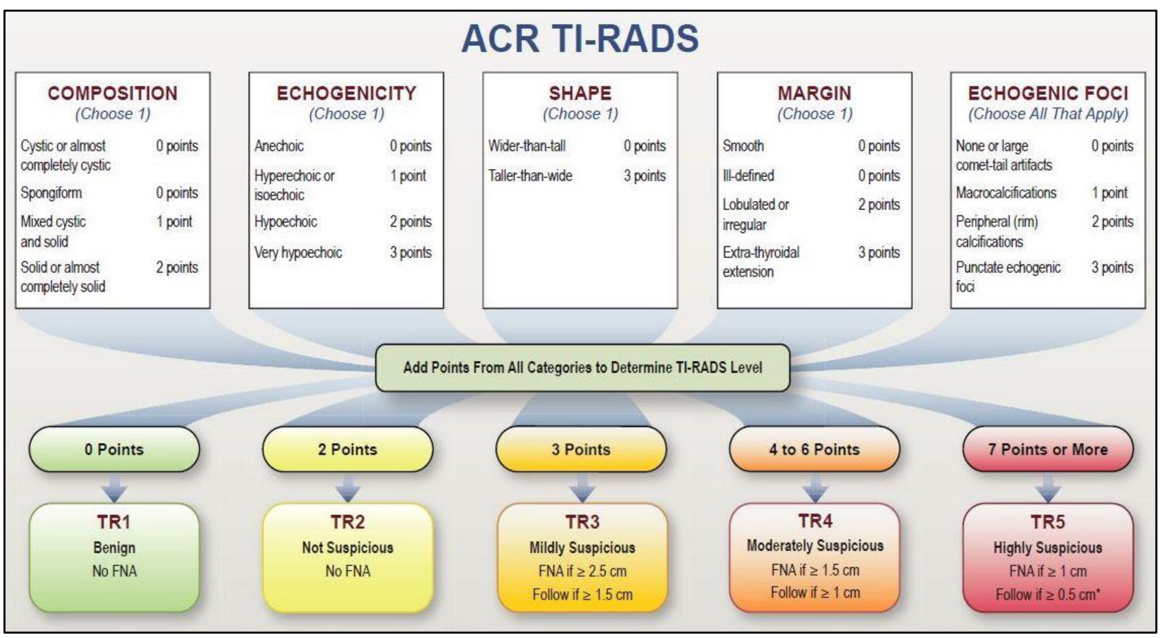

Figure 13: ACR-TIRADS risk stratification

Elastography

Historic background

Assessing the stiffness of tissues using ultrasound evolved from tissue motion studies which was performed in 1980s in England. Around 1988, a system that utilized colour Doppler to track movement of the tissue and produce tissue stiffness-based images were created by the researchers at the University of Rochester[10]. Elastography was introduced after 1990 and came into clinical setting in 1997[9].

Sono-elasticity had the ability to determine stiffness of lesions present in various organs as dark areas with a green background of moving tissue. In vibrational Doppler imaging the lesion is seen dark against a background of tissue that's vibrating. However, with this technique the image that is obtained is of relatively low resolution and required an inconvenient external vibratory device that induces motion within the tissue.

Local shear wave velocity and stiffness of the tissues can be assessed by using a newer application of a second vibration that operates at a different frequency and is seen producing a shifting interference pattern known as "crawling waves"[10].

Elastography is the first successful method of imaging the elasticity of tissue. It is known as strain elastography reported in 1991 by Cespedes and Ophir.

This is an imaging modality where the local tissue strains is calculated directly in strain ratio/Young Modulus or indirectly in shear wave velocity following the application of an external stress either static or dynamic used to compress or perturb the tissue [9].

Principle :

Elastography evaluation comprises of two major methods – strain elastography (SE) and shear wave elastography (SWE). These rely upon method of excitation, namely, internal force, external force and acoustic radiation force as shown in figure 15.

Strain Elastography

The ratio of stress (σ) to strain (ε) which is also called Young modulus (E) was utilized to assess the relationship between strain and compression.

E was measured using the following equation: -

$$E = \frac{\sigma}{\varepsilon},$$

The tissue is axially displaced caused by mechanical stress in strain elastography. Deformation of the tissue caused by stress is measured and is visualized on the monitor. There are two main types, firstly a visual scoring system, Tsukuba (5 point) and Asteria (4 point) and then secondly two ROIs (region of interest) which are drawn over the adjacent normal tissue first following which it is drawn in the nodule/affected area respectively. Following this the strain ratio is calculated automatically.

SE with external force

Free hand compression is applied by the transducer on the neck following which decompression is exercised. This method is utilized to obtain elastographic images. Spectrum of colours are utilized to assess the stiffness of the tissue, red for soft or less stiff lesions, green for medium stiffness lesions and blue for hard or very stiff lesions. In some machines the colour scale might also be applied inversely. A numerical scale or a curve that is sinusoid shaped is used to assess the quality of pressure which is applied by the operator in real- time mode.

Qualitative assessment:

5 – point Rago or 4 – point Asteria criteria was employed in Elastography scoring based on the pattern of colours obtained as shown in figure 14. Scores 3 and 4 on Asteria and scores 4 and 5 on Rago scale (Tsukuba) point towards malignancy and utilised for differentiating malignant from benign lesions.

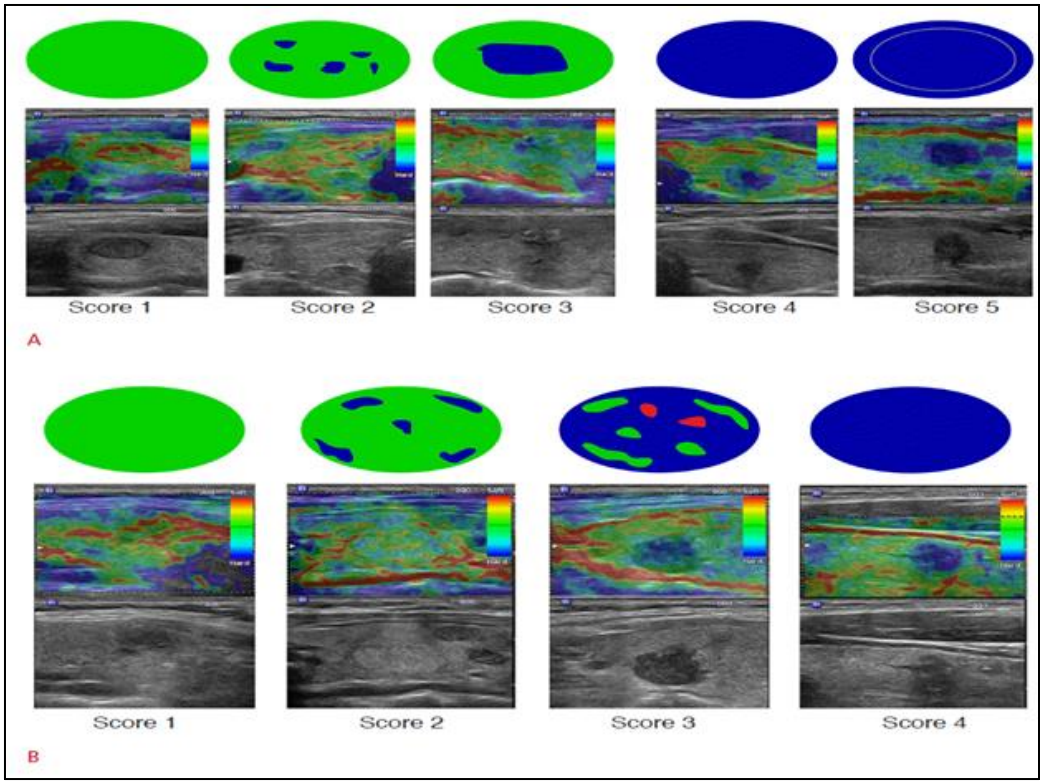

Figure 14: A- 5-point Rago (Tsukuba criteria) and B- 4-point Asteria colour scoring criteria

Semi-quantitative assessment: Strain ratio

Parenchyma/muscle to nodule ratio can be displayed on second generation SE devices. In cases where the surrounding normal thyroid is absent the ROI may be placed in the muscle. However, this is not representation of elasticity values due to difficulty in measuring the actual amount of stress that is applied.

SE : carotid artery pulsation

Carotid artery pulsation is used as the compression while the probe is motionless and held by the operator in this method. The strain images are obtained as the signals that are produced, pre and the post compression are tracked. Elasticity contrast index (ECI) and Thyroid stiffness index (TSI) are used to express the hardness.

Semi-quantitative assessment: TSI

On transverse scans, in a section where carotid artery and thyroid are visualised, ROI of 2 x 2 mm is used. The highest strain area which is near the carotid artery is divided by the strain obtained from the nodule in the thyroid (the lowest strain area). A high index value is noted in a stiff nodule.

Semi-quantitative assessment: ECI

Co-occurrence matrix is applied a strain oscillation map is acquired. Using this approach, the ECI is calculated. Benign thyroid nodules have very low or no contrast and the malignant thyroid nodules display a high contrast.

SE with Acoustic radiation force impulse (ARFI)

Focused US beams can image tissue deformation by applying ARFI. When focused ARF “push” pulses are administered, the imaging pulses after and before the application might be utilised to screen displacement of tissue in the area of pressure.

The following equation calculates ARF:

$$F = \frac{2\alpha I}{c},$$

F is ARF, acoustic absorption is α and average acoustic beam temporal intensity is denoted by I and speed of sound is by c. The changes in strain are obtained as a grey-scale image. Darker hue indicates a stiff tissue whereas a lighter hue indicates a less stiff lesion.

Qualitative assessment: ES

Based on the colour pattern that is predominant for the lesion a 6-point scale has been developed by Xu et al. The discrimination of a malignant nodule from a benign nodule is done by a cut off value between 3 and 4.

Semi-quantitative assessment with area ratio

The thyroid nodule area on ARFI divided by the area measured on conventional ultrasound is the definition of area ratio. Hypothesis that in malignant thyroid lesions there might be infiltrative margins is the concept what area ratio is based upon.

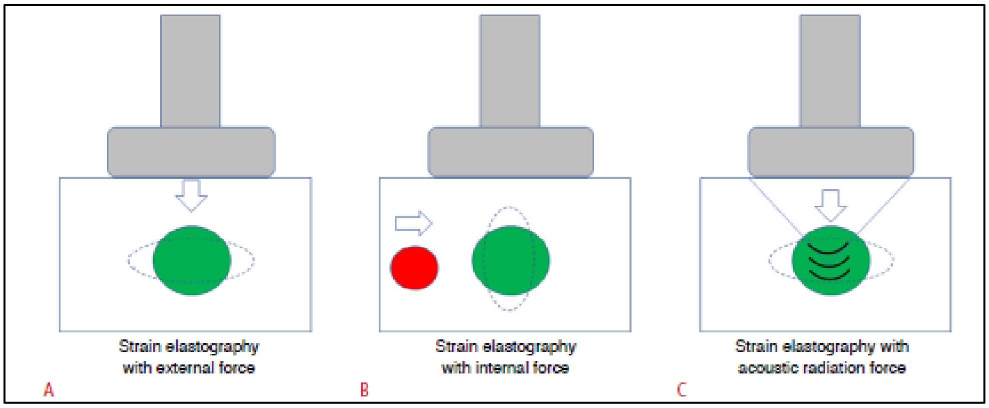

Figure 15: Depicts the various excitation methods used in strain elastography

Shear-Wave Elastography

Shear wave is created by the acoustic pulses that are produced by the probe and these stimulate the target tissue and travelling perpendicular to conventional ultrasound waves. These waves are transverse components as shown in figure 16 that are produced by particle displacement and are attenuated by the tissue rapidly (1-10 m/sec). This transverse element is trailed and is calculated into a numerical value corresponding to SWS (shear wave speed). It has close association with Young's modulus. In this the tissue elasticity is measured from propagation of SW.

SWS is calculated as follows:

$$E \approx 3\mu, \quad \mu = \rho c^2, \quad E = 3\rho c^2,$$

Young's modulus is denoted, shear modulus by μ , tissue density by ρ and SWS by c. It is quantitative, operator dependent and reproducible.

Two methods used are:

1. point SWE (pSWE)
2. 2 – dimensional (2-D) SWE techniques.

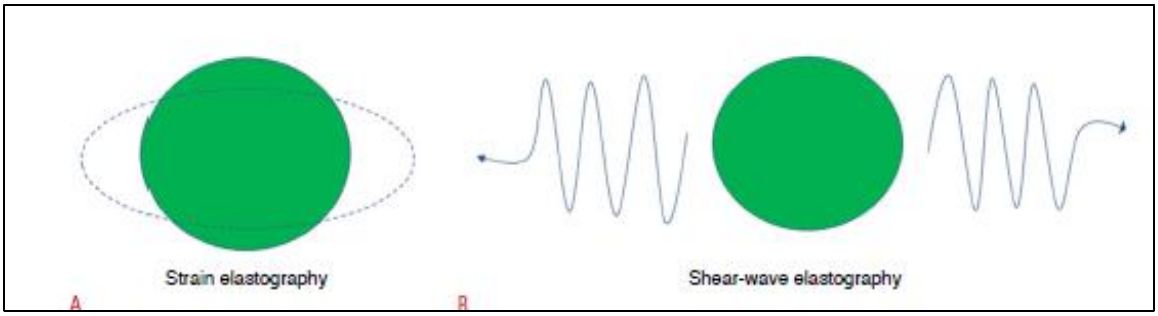

Figure 16: Image depicts principles of strain and shear wave elastography

Practical Clinical Applications

Diagnostic Performance -Thyroid Malignancy

Even though ultrasonography has a high sensitivity in detecting and characterizing thyroid nodules, there is no isolated or combination of features that can diagnose thyroid malignancy reliably.

Diagnostic performance of combination of elastography and conventional US and isolated elastography

It was noted in a meta-analysis including 639 patients that strain elastography was useful in evaluating malignancy with a mean specificity of 90 % and mean sensitivity of 92 %. In another meta-analysis of the strain ratio method showed poor specificity and sensitivity of 80% and 85 %, respectively. It was inferred that strain elastography was an adjunct to ultrasonography and improved efficacy of B-mode ultrasonography in evaluation of thyroid nodules that was conducted as a prospective multicenter study, DEGUM which consisted of 657 patients (90 malignant, 567 benign). A total of 1,867 thyroid nodules demonstrated a mean specificity of 88.4 % and sensitivity 84.3 % respectively for SWE noted in meta-analysis of 15 studies. Contrary to the above-mentioned studies, a retrospective study challenged the above-mentioned studies, which included a total of 703 lesions that showed sensitivity of SE measurements (65.4 % for 4-point Asteria criteria and 15.7 % for 5-point Rago criteria) that were comparatively lesser than B-mode ultrasonography features. In modern clinical practice, elastography is generally not performed independently but used in conjunction to B-mode ultrasonography.

A study conducted by Trimboli et al, noted addition of elastography to ultrasonography resulted in a negative predictive value (NPV) of 97 % and sensitivity of 97 % which was much higher than ultrasonography and elastography individually. However, positive predictive value, specificity, and accuracy were much lesser than that of B-mode ultrasonography alone.

Moon et al. noted that neither combination of both grey-scale ultrasonography and elastography nor elastography alone was better than Conventional ultrasonography in characterizing malignant from benign thyroid nodules. Hence, utilization of US elastography in clinical application should be done depending on the experience of the operator in regards to both conventional ultrasonography and elastography for thyroid.

Assessment of papillary thyroid microcarcinoma

It was observed in some studies that strain elastography may help in distinguishing malignant thyroid micronodules from benign. Ma et al., conducted a study to predict papillary microcarcinoma of thyroid gland using multiparametric ultrasonography, it was concurred that along with conventional ultrasonography, addition of both strain elastography and contrast enhances ultrasonography improves the diagnostic efficacy. pSWE had a superior specificity as compared to conventional ultrasonography in diagnosing malignant lesions in a study by Zhang et al.

Differentiation of nodules in Hashimoto Thyroiditis

It is a matter of debate whether the inflammation that occurs in Hashimoto's thyroiditis is a hindrance in assessing nodules as it possesses higher stiffness. SWE could accurately measure the elasticity of nodules even in cases with co-existent Hashimoto's thyroiditis. Strain elastography has a specificity of 95 %, sensitivity of 92.9 %, a NPV of 86.7 %, PPV of 97.4 % and an accuracy of 94.4 % in differentiating pseudo-nodules from true nodules. This was relatively superior to the values obtained in conventional ultrasonographic and Doppler assessment. As compared to elastographic scoring, strain ratio proved to be far superior.

Liu et al. studied that as compared to SE, ARFI was better in predicting malignancy in Hashimoto's thyroiditis.

Reducing Unnecessary FNAs - Role of US Elastography

Ultrasound elastography has a crucial role in assessing which nodule needs to be followed up by avoiding FNACs and had a high NPV. This helps in reducing unnecessary FNACs. Zhao et al. observed that out of 37 nodules with very little suspicion on conventional US, 2-D SWE was able to prevent unnecessary FNACs in about 77.1 % of benign lesions and 3-D SWE had a higher percentage (88.6 %).

Recommendations for Surgery

In all meta-analyses conducted, it was noted that SWE and SE is used as an adjunct in diagnosing thyroid gland malignancies. They also help in selecting patients accurately for surgery.

Diagnostic Utility - TNs with Indeterminate Cytology or Nondiagnostic Cytology

Following ultrasonography, relatively noninvasive FNAC is the further mode of investigation and is known to have excellent performance. However, FNA cytology has its own set of limitations in eliminating diagnosing malignancy in indeterminate cases or non-diagnostic cytology. Molecular testing, intraoperative frozen sections and repeated FNAs. But the repeat FNAs and molecular testing require extra expenditure. Mixed results regarding the use of elastography in indeterminate/ non-diagnostic cytology were noted.

Nondiagnostic cytology - Diagnostic utility

Conventional ultrasound has displayed a good diagnostic performance in non-diagnostic cytology cases. It was proposed by Lin et al. that elastography may be effective in such case. Park et al. noted that if there is absence of other suspicious features only observation is suggested in solid thyroid nodules.

Indeterminate cytology - Diagnostic utility

In a meta-analysis that consisted of 8 studies and 486 nodules with indeterminate cytology, SE had a specificity, sensitivity and accuracy of 75 %, 69 % and 73 %. As reported by Samir at al. A higher Young modulus median from a plane that is transverse in SWE was associated with thyroid malignancy. Area under the curve (AUC) of 0.81 in predicting malignant nodule about 35 patients with indeterminate follicular thyroid lesions was present. Similar SWE parameters were noted in both malignant and benign lesions, thus making it ineffective in assessing indeterminate thyroid lesions. A total of ~ 10 – 75 % of indeterminate lesions are follicular lesions. SWE might be effective in assessing the extension of thyroidectomy that may be required in thyroid neoplasms.

Assessment of lymph nodal metastases of papillary carcinoma

Thyroidectomy with complete lymph node dissection of the cervical region had a higher risk of hypothyroidism and injury involving recurrent laryngeal nerve (maybe permanent). This necessitates optimal evaluation of cervical region. It is noted that elastography aids in assessing lymph nodes metastases. Park et al., observed after analysing 363 patients diagnosed to have papillary carcinoma thyroid that using SWE that E mean and E max was associated with metastasis to central lymph nodes and E min was associated with metastases to the lateral lymph nodes.

Comparisons between various SE Evaluation Methods

Multiple studies showed that SR had a diagnostic accuracy higher than ES (0.88 vs. 0.79).

Influencing Factors

Nodule Features

Nodules with cystic changes and calcifications

It is difficult to perform elastography on lesions with peripheral calcifications as it is difficult for sound waves to penetrate. In case of presence of intralesional calcifications, it may lead to increased stiffness on strain elastography.

Any cystic lesion or necrotic degeneration in malignant nodules tend to demonstrate a classic BGR (blue, green and red) artifact on colour scoring. These lesions have a less elastography index value and malignancies with necrotic/ cystic degeneration might be underdiagnosed as malignant. Hence, selective utilisation of elastography in these lesions with cystic changes or calcifications should be done.

Nodule position

Near field artifact is noted in superficially located nodules. Deep seated nodules are affected by ARFI pulse decay phenomenon or by stress. It is difficult to evaluate isthmic nodules since they are compressed in between the stiff trachea and the skin.

Nodule size

In nodules larger than 3 cm, inadequate compression is noted by external compression due to deeper extension.

Experience of the Operator

It has been investigated and observed that reproducibility of SWE is marginally superior to SE. Operator dependent variations are noted in manual external compression. Even though SWE is less operator dependent, the pressure exerted externally affects SW propagation and this type fallacy is a common source of artifacts. Hence, it is recommended that US elastography be performed by operators who are experienced and using parameters that are objective with a quality indicator.

Carotid artery Pulsation - Motion Artifacts

Pulsations of the carotid artery generates compressive and decompressive movements that interfere with evaluation done by elastography. On longitudinal scans these effects are not present and hence is a better option for elastographic evaluation. But in case of scans wherein SE with carotid artery needs to be performed, transverse scans need to be used.

Thyroid Malignancy : Pathological Type

Few studied have shown that few non-papillary malignancies like medullary carcinomas and follicular malignancies are soft and are hard to differentiate from benign nodules.

Summary & Future Directions

In many high – end systems, ultrasound elastography is integrated into B-mode ultrasonography. No separate preparation for the patient, requires few additional minutes and is completely painless. It helps has an adjunct to conventional ultrasonography. It is non-invasive and has a potential to help differentiate malignant from benign nodules. Elastography is useful in providing information regarding which nodules need to be followed up, avoiding unnecessary FNA or surgery because of its high Negative predictive value. Elastography may have utility in Indeterminate or nondiagnostic FNAC. In nodules which are negative for malignancy, elastography can be helpful for follow up.

Multiple authors have debated that the modulus estimates for thyroid may be incorrect. The varied results available can be because of bias – selection bias (depending on number of malignancies) less cohort size and standardization technique that is non-uniform (scoring systems and stiffness indices.

Many different cut-off values have been proposed, but there have been no multicentric studies or meta-analysis to arrive at an average. The usefulness of elastography in evaluating indeterminate lesions is inconsistent. The role of elastography in avoiding and reducing unnecessary FNA. More research needs to done in establishing the definitive data regarding diffuse thyroid disease and thyroiditis.

As an upcoming technology it is still under development. It is yet to acquire widespread application in modern clinical practice and requires further validation based on studies conducted on large cohorts in a multicentric background. Further investigation on how characteristic of nodules on conventional ultrasonography can be integrated with elastography in characterizing malignant and benign thyroid nodules better is needed.

The role of elastography in treatment monitoring following microwave, laser ablation or radiofrequency warrants further research. Utility of elastography- guided FNA of thyroid lesions is yet to be evaluated. Computer aided diagnosis has been introduced to utilize the various features and machine algorithms for classification. Diagnostic are prevented and the whole process is made simple with easy formulation and standardization[29].

Computed Tomography (CT)

Thyroid lesions have a varied and non-specific appearance on CT scans. Most common findings on CT include glandular enlargement, nodules and calcifications. Additional information regarding local extension of any malignancy, lymphadenopathy, recurrence and mass effect can be acquired. CT has a pivotal role preoperative surgical planning and evaluation[22].

Magnetic resonance Imaging (MRI)

Thyroid disorders can be evaluated better owing to MRI signal intensity characteristics on various sequences. This helps in characterizing the lesions better and in efficient clinical management. Diffusion weighted Imaging (DWI) is used as an important diagnostic tool in evaluating thyroid diseases, including Hashimoto's thyroiditis, Graves and subacute thyroiditis. Tezuka et al., noted that the Apparent diffusion coefficient (ADC) values in subacute thyroiditis or Hashimoto's thyroiditis was significantly lower than that in Grave's disease[25].DWI is useful in differentiating malignant from benign thyroid lesions[24].

Thyroid malignancies are observed to demonstrate significantly lower ADC values in comparison to benign thyroid nodules[23].

Nuclear medicine

Homogenous tracer uptake is noted in normal thyroid. Scintigraphy has pivotal role in evaluating patients with reduced levels of serum thyroid stimulating hormone. To identify a hyperfunctioning or "hot" nodule scintigraphy is performed with I-123 and these nodules demonstrate a greater radiotracer uptake in comparison to the normal adjacent thyroid tissue. Cytological analysis not recommended for "hot" nodules because they are very rarely malignant. In case of an iso-functioning or "warm" nodule, uptake of radiotracer is equal to adjacent normal thyroid tissue. Radiotracer uptake in a hypofunctioning or "cold" nodule is much less than that of the adjacent normal thyroid tissue. These nodules warrant further evaluation.

Iodine-131 is used widely as both an imaging radionuclide and as a therapeutic agent. Whole body scan is done using I-131 to diagnose metastatic disease and as a follow up tool in post radioiodine ablation. Ablation of residual thyroid tissue, detection of any distant metastases and lymph nodes and ablation of tumor foci can be done with high doses of I-131 in post thyroidectomy for malignancy.

On Positron emission tomography, assessment of thyroid gland, low level diffuse homogenous FDG uptake is noted. This FDG uptake is comparable to the uptake noted in the normal musculature. In about 1 – 2 % incidental focal uptake is noted with 11 – 14 %

reported malignancy. In view of such a high risk, the AACE (American Association of Clinical Endocrinologists) and ACR (American College of Radiology) have recommended sonographic evaluation and FNA. However, ATA (American Thyroid Association) recommends evaluation of FDG avid nodules both clinically and sonographically and in case of nodule measuring > 1 cm, FNA is suggested. No standard uptake value has been established that can differentiate malignant from benign thyroid nodules. In 2 % patients there is diffusely increased radiotracer uptake. This is observed in inflammatory conditions like Hashimoto's disease and other types of thyroiditis[13].

Bethesda was revised in 2007. It comprises a 6-tiered system that classifies cytology reporting shown in image 17.

Grade-I: Nondiagnostic or Unsatisfactory
Cyst fluid only
Virtually acellular specimen
Other (obscuring blood, clotting artifact, etc.)
Grade-II: Benign
Consistent with a benign follicular nodule
(includes adenomatoid nodule, colloid nodule, etc.)
Consistent with lymphocytic (Hashimoto) thyroiditis in the proper clinical context
Consistent with granulomatous (subacute) thyroiditis
Other
Grade-III: Atypia of undetermined significance or follicular lesion of undetermined significance
Grade-IV: Follicular neoplasm or suspicious for a follicular neoplasm
Specify if Hürthle cell (oncocytic) type
Grade-V: Suspicious for malignancy
Suspicious for papillary carcinoma
Suspicious for medullary carcinoma
Suspicious for metastatic carcinoma
Suspicious for lymphoma
Other
Grade-VI: Malignant
Papillary thyroid carcinoma
Poorly differentiated carcinoma
Medullary thyroid carcinoma
Undifferentiated (anaplastic) carcinoma
Squamous cell carcinoma with mixed features (specify)
Metastatic carcinoma
Non-Hodgkin lymphoma

Figure 17: Classification based on Bethesda criteria

Indeterminate Result

The FNA specimens have atypia of undetermined significance (indeterminate) or Follicular nodules do not warrant them as suspicious but do consist of features that preclude them being labelled as benign. In about 3-6 % in which indeterminate results are seen, it does not mean that it is non-diagnostic. Repeat biopsy needs be performed 3 months later as there is 5 – 15 % chance of these lesions being malignant.

FNAB and Core Biopsy

In cases that are non-diagnostic or indeterminate FNAB, core biopsy can be performed in conjunction. A far superior diagnostic yield and accuracy is obtained with the combined approach. Measurement of proportion of true results (i.e., true negative and true positive) is accuracy. Accuracy for FNAB and combined FNAB and core biopsy is 82 % and 94 % respectively[12].

CLINICAL STUDIES

Recent increase in incidence of malignant thyroid lesions requires better characterization of nodules as the pre-operative misdiagnosis of thyroid malignancies remains high at 40 to 70%[31]. Ultrasound does not have high accuracy in differentiating malignant from benign lesions[2].

Compression elastography acquires information of displacement of tissue because of pressure applied to area of interest. Semi quantitative method using strain index is calculated as ratio of nodule strain value to strain of normal thyroid tissue in the vicinty[4,31,70]. It measures tissue elasticity and differentiates between malignant and benign nodule on the basis of consistency of nodule. Non-invasive technique to differentiate benign from malignant lesions[2].Allows for more definite characterization of malignant and benign lesions[32].

Sonoelastography helps in more accurate characterization of lesion and identifying areas, from where FNACs can be targeted for better diagnostic yield[3].

High diagnostic performance yield compared to conventional sonography. High accuracy in differentiating malignant and benign nodules even in small thyroid nodules (sizes ranging from 3 to 10 mm). Sensitivity and specificity rates of 0.91 and 0.89 respectively[33].

In a meta-analysis by Dudea S et al, strain index was taken as nodule strain divided by the strain obtained in the adjacent normal tissue and expressed as a ratio. A strain ratio of > 2.905 produced a higher sensitivity and negative predictive value in comparison to conventional ultrasonography. It was recommended that such nodules need to be biopsied irrespective of whether some of them turn out benign on pathological analysis. It was observed that combination of elastography and conventional ultrasonography can help identify nodules that need to be biopsied and may prevent unnecessary biopsies in lesions that have benign features on both the modalities. However, elastography is like an extension of ultrasonography and the results that are obtained on elastography need to be combined with conventional ultrasonography features[34].

In a study conducted by Moraes P et al., it was noted that in the lesions that in some malignant may not differ in echogenicity making it difficult to diagnose, in these cases elasticity needs to be measured. Elastography helps us in obtaining additional information on elasticity of the lesions and in characterizing malignant and benign nodules[38].

Yang J et al., compared efficacy of B-mode ultrasonography and elastography in distinguishing malignant from benign thyroid nodules. A total of 123 patients who underwent elastography. 150 thyroid nodules were noted in total. It was noted that in 86% of benign nodules low elasticity (grade I/II) was noted with a mean strain ratio of 2.30±1.01. Contrary to this, high elasticity (grade III/IV) was observed in 90% of malignant lesions with mean strain ratio of 6.39±2.50. They concluded that strain ratio and elastography can be helpful as an adjunct to conventional ultrasound in distinguishing malignant from benign thyroid lesions[35].

Kyariakidou G et al., made a comparison of various elastography methods, which are 2D-Shear Wave Elastography (2D-SWE), Strain Elastography (SE) and Point Shear-Wave Elastography (pSWE) using Acoustic Radiation Force Impulse (ARFI)-Imaging in the same sample of thyroid nodules. Total of 62 patients and 84 nodules amongst which 11 were malignant and 73 were benign were examined. The specificity, sensitivity and NPV of 2D-SWE and ARFI were 67%, 73% and 94 % and 79%, 90% and 98 %. Specificity, sensitivity and NPV for SE were 70%, 73% and 94%. The cut off used for 2D-SWE was 2.65m/s (21.07kPa) and for ARFI it was 1.98m/s. The AUROC of 2D-SWE, SE and ARFI in characterizing malignant lesions were 71 %, 52 % and 86%. It was noted that significant variation existed in AUROC in case of ARFI and SE (p=0.008). However, no significant difference between SWE and ARFI (p=0.31) or SE and SWE (p = 0.26) was present[36].

Monpeyssen H et al., noted that as most of the thyroid malignancies are hard, therefore assessment of elasticity of lesions is important. Based on this study, tumour strain ratio > 3.7 and stiffness greater than 65kPa as compared to adjacent normal tissue should raise a suspicion of malignancy. Lymph nodal metastases leads to higher strain index of lymph node involved[37]. They also help in selecting nodules that need to be biopsied[3,34,37].

Bojunga J et al., noted that Fine-needle aspiration (FNA) was easily available and cost-effective method to assess and select patients who need to undergo surgery with specificity 60%-96% and sensitivity 54 – 90% in diagnosing malignant nodules. Elastography helps in assessing elasticity of nodules and helps in characterising malignant lesions. In a meta-analysis conducted including eight studies, total of 639 lesions that were evaluated. The mean specificity and sensitivity in diagnosing malignant lesions was 90 % confidence interval 85-95 and 92 % confidence interval 88-96, respectively. It was concluded that elastography has high specificity and sensitivity in assessing malignant thyroid lesions. In conjunction to conventional ultrasonography it may aid in FNA and in selecting patients who require surgery[39].

MATERIALS & METHODS

MATERIALS AND METHODS

Source of Data:

This observational study has been conducted over a course of 18 months from January 2018 to June 2019. Informed consent was obtained from the individuals included for their willingness to participate. The individuals have been included if they met the inclusion/exclusion criteria. Baseline data was secured from the patient with pertinent clinical history.

Ultrasonography and elastography both were performed on participating patients and character of the lesion was noted. Elastography findings were correlated with pathological findings (FNAC/HPE) which was considered the gold standard test.

Ultrasound and elastography was performed using 5–12 MHz linear array transducer (PHILIPS EPIQ 5G Ultrasound Machine).

Figure 18: PHILIPS EPIQ 5G Ultrasound Machine

This study is hospital-based study – an observational study and was conducted over a period of eighteen months including minimum of 58 patients. Patients who had thyroid nodule visualised on conventional B-mode ultrasonography underwent elastography.

Elastography findings were compared with pathological findings, which is the gold standard test for thyroid lesions.

Sample Size Calculation

Sample size will be estimated by using the proportion of subjects with malignant and benign lesions detected by ultrasonography, elastography and pathology from the study by Chaudhary et al, using the formula,

P = 81.5 or 0.81

q = 18.5 or 0.18

d = 10 % or 0.1

$$\text{Sample size} = \frac{Z_{1-\alpha/2}{}^{2}\, p(1-p)}{d^2}$$

Considering 10% Nonresponse a sample size of 52 + 5.2 ≈ 58 subjects will be included in the study.

Methods of collection of data:

Baseline data was secured from patients along with pertinent clinical history, relevant lab investigations and pathological report. Individuals with clinically suspicious thyroid pathology underwent ultrasonography and elastography.

Ultrasonography was done first using a 5–12 MHz linear array transducer (PHILIPS EPIQ 5G Ultrasound Machine). Each scan was interpreted and morphological changes were recorded and categorized as benign or malignant based on TIRADS and ACR-TIRADS.

Using the same 5–12 MHz linear array transducer (PHILIPS EPIQ 5G Ultrasound Machine), elastography is performed. The technique used was application of free hand compression and decompression on the neck. Colouring scoring criterias which have been based on colour spectrum in which red for soft or less stiff lesions, green for medium stiffness lesions and blue for very hard or stiff lesions was utilized. This colour spectrum may be calibrated inversely in some machines. Qualitative assessment is done by colour scoring wherein, a range 4 and 5 on Rago scale (Tsukuba) and scores of 3 and 4 on Asteria was suspicious for thyroid malignancy and used for differentiating malignant from benign lesions. A numerical scale has been utilised to assess the quality of the pressure applied in real time mode.

Semi- quantitative assessment is done using strain ratio. In this method normal parenchyma or strap muscle to lesion ratio was calculated. The ROI (region of interest) was first placed in adjacent normal thyroid tissue, however in case of absent normal thyroid tissue it was placed in adjacent strap muscles following which second ROI of same area is placed within nodule.

Based on the features observed with elastography, scoring has been obtained, according to strain ratio and colour scoring systems (Rago criteria and Asteria criteria).

The cut off used for benign lesions was < 2.905 and for malignant lesions was > 2.905[34]. Lesions with higher scores were considered as hard and have more suspicion for malignancy. Lesions with stiffness similar to adjacent tissue were considered as benign lesion.

Elastography and conventional ultrasonography findings were correlated with pathological findings.

Data Analysis

Statistical Methods

Analysed using SPSS 22 version software.

Categorical data represented in frequencies and proportions.

Chi-square was used as test of significance.

Continuous data represented as mean and standard deviation

Independent t test was used as test of significance.

Inclusion criteria:

All patients with clinically suspected thyroid nodule.

Exclusion criteria:

Patients who have undergone recent FNAC of thyroid lesion (< 6 weeks)

Study Design – Schematic Representation

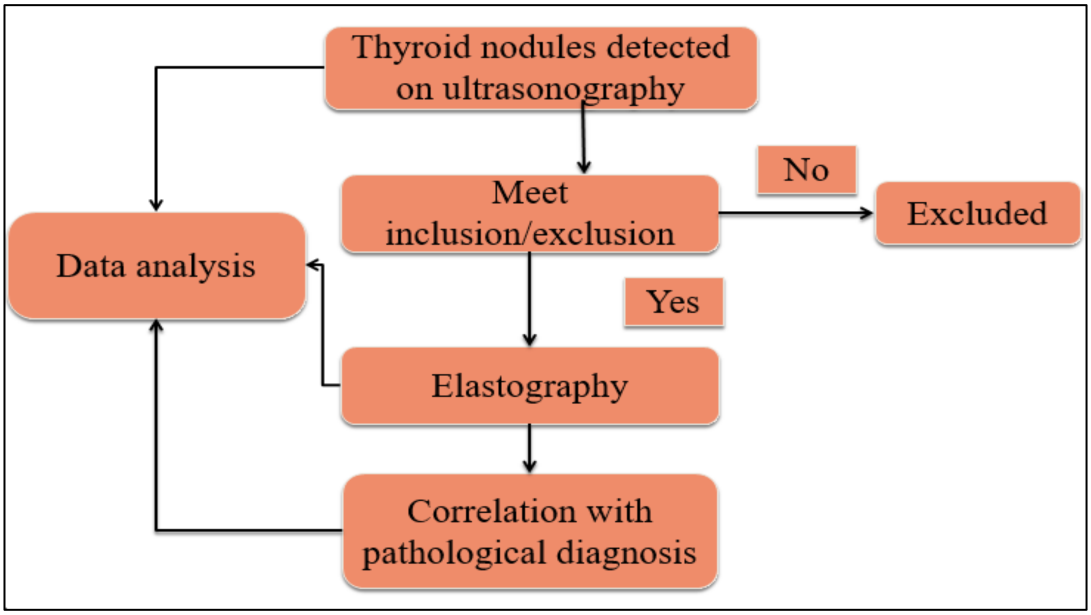

Figure 19: Schematic representation of study design

RESULTS

RESULTS

Demographics

In this study 140 patients with thyroid lesions were observed.

Gender wise distribution:

Out of 140 patients 120 (85.7%) were females and 20 (14.3%) were males (Figure :20; Table:1).

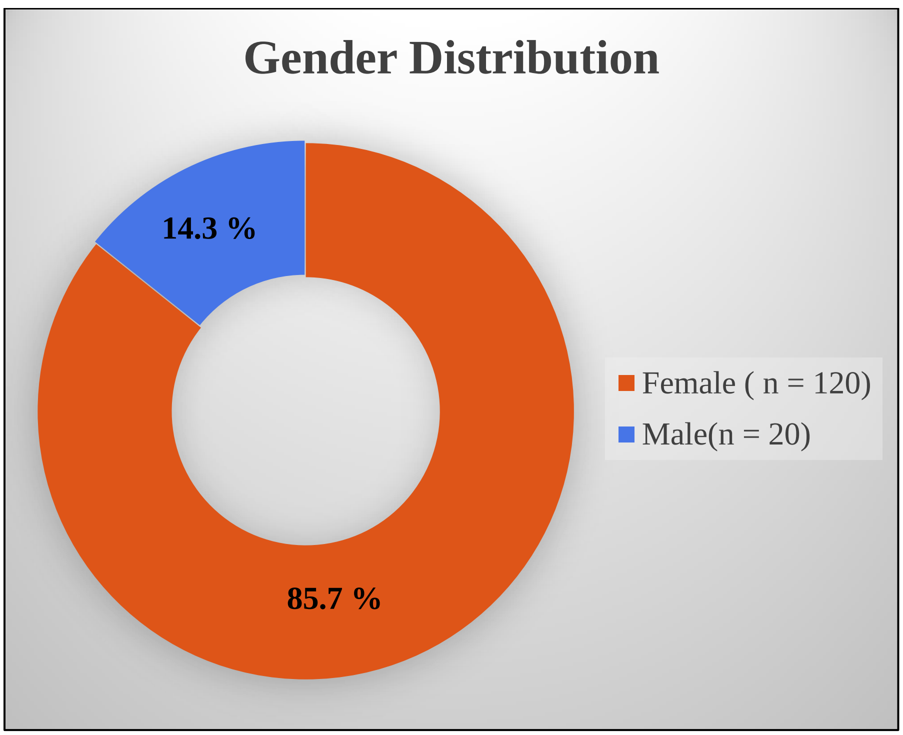

Figure 20: Gender-wise distribution

Table 1: Gender distribution of patients studied

Gender	No. of patients	%
Female	120	85.7
Male	20	14.3
Total	140	100.0

There were 140 patients with thyroid lesions who were included in the final analysis. In our study 120 (85.7%) were females and 20 (14.3%) were males. Gender-wise distribution of patients is mentioned in Table 1.

Age group distribution

Most common age group in our study was < 40 years (54 %), followed by 41-60 years (36 %) (Figure 21, Table 2)

Table 2: Age Group Distribution.

Age in years	No. of patients	%
<40	76	54
41-60	50	36
>60	14	10
Total	140	100

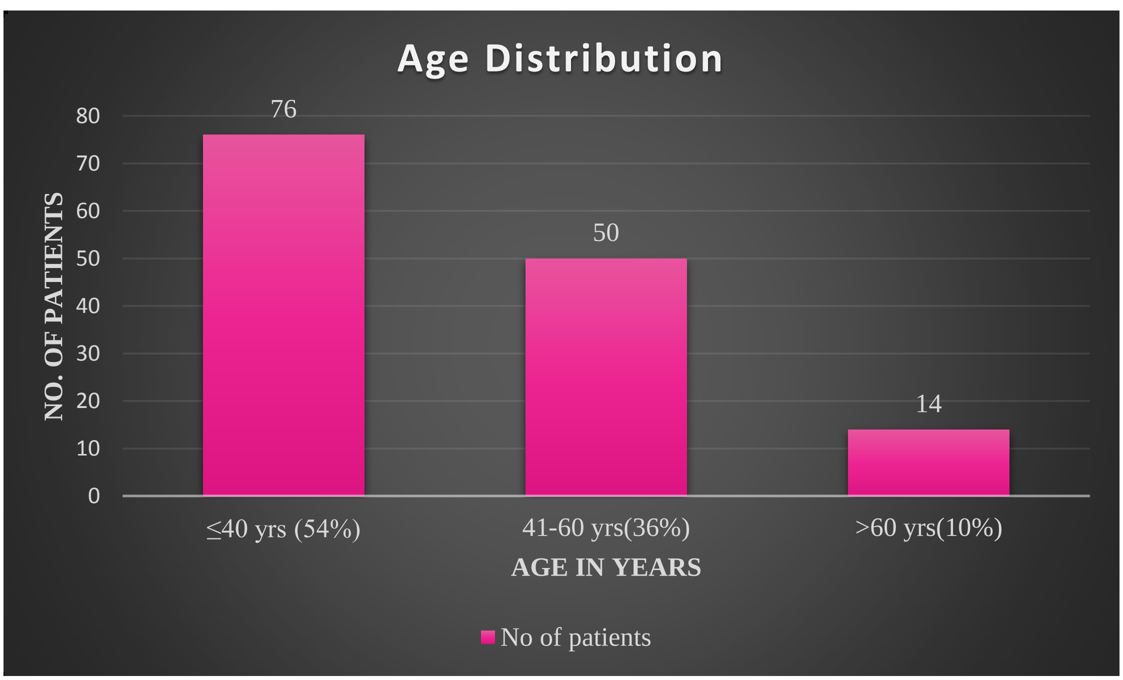

Figure 21: Age group distribution

The commonest age groups belonged to patients of age < 40 years (n = 76; 54 %) followed by 41 to 60 years (n = 50 ; 36 %), and lastly age group of > 60 years (n = 14 ; 10 %) as depicted in figure 21.

Table 3: Association of age with Final diagnosis of patients studied

Age in years	Final Diagnosis		Total (n=140)	*p* value
	Benign (n=117)	Malignant (n=23)		
• <40	63 (45%)	13 (9.28%)	69 (49.3%)	0.441505
• 41-60	43 (30.7%)	7 (5%)	57 (40.7%)	
• >60	10 (7.14%)	4 (2.85%)	14 (10%)	

The *p* value calculated for age distribution was 0.441505 (table: 3). No significant difference was derived in occurrence of disease in any particular age group. The association noted was not statistically significant.

Distribution of lesions based on morphological features on Conventional ultrasonography

Based on the morphological features on conventional ultrasonography, the lesions were categorized based on TIRADS and ACR-TIRADS scoring systems.

Table 4: Distribution of lesions based on TIRADS

TIRADS	No. of patients	%
1	9	6.4
2	60	42.9
3	35	25.0
4A	21	15.0
4B	6	4.3
5	5	3.6
6	4	2.9
Total	140	100.0

Majority of the lesions were benign 42.9 % (n = 60), 22.9 % were suspicious for malignancy (n = 33) and 2.9% were biopsy proven malignant lesions (n = 4) as shown in table 4.

Table 5 : Correlation between TIRADS & Pathological Diagnosis

TIRADS	Pathological Diagnosis	
	Benign	Malignant
1	9	0
2	54	6
3	33	2
4A	16	5
4B	3	3
5	1	4
6	0	4

On comparing TIRADS and pathological diagnosis amongst the 104 cases that were categorized as benign on TIRADS, 8 were malignant on pathological diagnosis. Amongst the 32 cases that were suspicious for malignancy 20 turned out to be benign. Apart from this there were 4 malignancy proven cases as shown in table 5.

Table 6: Distribution of lesions based on ACR - TIRADS

ACR TIRADS	No. of patients	%
1	7	5.0
2	34	24.3
3	63	45.0
4	22	15.7
5	14	10.0
Total	140	100.0

Majority of the lesions were benign 74.28 % (n = 104), 25.7 % were suspicious for malignancy (n = 36) as shown in table 6.

Table 7 :Correlation between ACR-TIRADS & Pathological Diagnosis

ACR-TIRADS	Pathological Diagnosis	
	Benign	Malignant
1	7	0
2	33	1
3	56	7
4	17	5
5	3	11

On comparing ACR- TIRADS and pathological diagnosis amongst the 104 cases that were categorized as benign on TIRADS 8 were malignant on pathological diagnosis. Amongst the 36 cases that were suspicious for malignancy 20 turned out to be benign as shown in table 7.

Both TIRADS and ACR-TIRADS had a similar sensitivity, specificity, positive predictive value, negative predictive value and accuracy of 44.44%, 92.31%, 66.7%, 82.76% and 80 % respectively.

Table 8: Diagnosis of lesions based on diagnosis on Conventional ultrasonography

USG Diagnosis	No. of patients	%
Benign	95	67.9
Probably Benign	11	7.9
Probably Malignant	27	19.3
Malignant	7	5.0
Total	140	100.0

Depending on characteristics of lesions of conventional ultrasonography the lesions were categorized as benign, probably benign, probably malignant and malignant. Features that were favouring malignant were- hypoechogenicity, taller than wider lesions, increased internal and peripheral vascularity, irregular margins and micro calcifications.

Majority of the lesions were benign n = 95 (67 %), whereas 36 were suspicious for malignancy (24.3 %) as shown in table 8.

Table 9 :Correlation between USG Diagnosis & Pathological diagnosis

USG Diagnosis	**Pathological Diagnosis**	
	Benign	Malignant
Benign	89	5
Probably Benign	8	3
Probably Malignant	18	9
Malignant	1	7

Conventional ultrasonography findings were correlated with pathological diagnosis and it was made note of that amongst 140 cases, 18 cases were overdiagnosed to be probably malignant and 1 as malignant depending on conventional ultrasonography findings. 8 cases were underdiagnosed as benign when compared to pathological findings, this is depicted in table 9.

Table 10: Relation between Conventional ultrasound findings and pathological findings

Pathological Diagnosis	N (%)	Conventional US finding				*p*-value
		B	**P B**	**P M**	**M**	
		N%	N%	N %	N%	
B	117 (83.58 %)	90 64.3%	8 5.71%	18 12.86%	1 0.71%	<0.00001*
M	23 (16.42 %)	4 2.86%	3 2.14%	9 6.43%	7 5%	
B- Benign, PB – Probably Benign, PM – Probably Malignant, M – Malignant						

The *p* value for Relation between conventional ultrasound findings and pathological findings was <0.00001 (table:10). The association noted was statistically significant.

Distribution of lesions based on Elastography Color scoring systems

The color systems used for elastography assessment of thyroid lesions were 5 – point Rago (Tsukuba) and 4 – point Asteria criteria.

A range of 4 and 5 on Rago scale (Tsukuba) and scores of 3 and 4 on Asteria and is suspicious for malignancy and used for differentiating malignant from benign lesions[29].

Table 11: RAGO (TSUKUBA) Score distribution of patients studied

RAGO (TSUKUBA) Score	No. of patients	%
1	32	22.85
2	44	31.42
3	40	28.57
4	14	10
5	10	7.14
Total	140	100.0

Majority of the lesions were benign 82.86 % (n = 116), 17.14 % were suspicious for malignancy (n = 24) as shown in table 11.

Table 12 :Correlation between RAGO (TSUKUBA) & Pathological Diagnosis

Tsukuba Scoring	Final Diagnosis	
	Benign	**Malignant**
Score 1	30	2
Score 2	43	1
Score 3	37	3
Score 4	5	9
Score 5	1	9

Based on 5 – point Rago colour scoring amongst the 116 cases that were categorized as benign, 6 were malignant on pathological diagnosis. Amongst the 24 cases that were suspicious for malignancy, 6 turned out to be benign as shown in table 12.

Table 13: Relation between Elastography colour score Rago (Tsukuba) criteria and pathological findings

Pathology	**Elastography colour score- Rago criteria (Tsukuba criteria)**					***p*-value**
	Score 1	**Score 2**	**Score 3**	**Score 4**	**Score 5**	<0.00001*
	N %	N %	N %	N %	N %	
B (n = 117)	30 21.4%	43 30.7%	37 26.4%	5 3.57%	1 0.71%	
M (n = 23)	2 1.42%	1 0.71%	3 2.14%	9 6.42%	9 6.42%	
N (%)	31 22.82%	44 31.5%	40 28.6%	15 10%	10 7.1%	
B – Benign, M – Malignant						

The *p* value for Relation between Elastography colour score Rago (Tsukuba) criteria and pathological findings was <0.00001 (table:13). The association noted was statistically significant.

Table 14 : ASTERIA Criteria distribution of patients studied

ASTERIA Criteria	No. of patients	%
1	22	15.7
2	94	67.1
3	12	8.57
4	12	8.57
Total	140	100.0

Majority of the lesions were benign 82.86 % (n = 116), 17.14 % were suspicious for malignancy (n = 24) as shown in table 14.

Table 15 : Correlation between ASTERIA & Pathological Diagnosis

Asteria Criteria	**Pathological Diagnosis**	
	Benign	**Malignant**
Score 1	21	1
Score 2	91	3
Score 3	3	9
Score 4	1	11

Based on 4 – point Asteria colour scoring amongst the 116 cases that were categorized as benign, 4 were malignant on pathological diagnosis. Amongst the 24 cases that were suspicious for malignancy, 4 turned out to be benign as shown in table 15.

Table 16 : Relation between Elastography colour score Asteria criteria and pathological findings

Pathology	**Elastography colour score- Asteria criteria**				***p*-value**
	Score 1	Score 2	Score 3	Score 4	
	N %	N %	N %	N %	
Benign (n = 117)	21 15%	91 65%	3 2.14%	1 0.71%	<0.00001*
Malignant (n = 23)	1 0.71%	3 2.14%	9 6.43%	11 7.86%	
N (%)	22 15.72%	93 67.14%	13 8.57%	12 8.57%	
B – Benign, M – Malignant					

The *p* value for Relation between Elastography colour score Asteria criteria and pathological findings was <0.00001 (table:16). The association noted was statistically significant.

Table 17 : Comparison of Rago and Asteria criteria

	Rago criteria	Asteria criteria
Sensitivity	72%	86.96%
Specificity	95.65%	95.73%
PPV	78.26%	80.00%
NPV	94.02%	97.39%
Accuracy	91.43%	94.29%

It is noted that Asteria criteria had a higher sensitivity, specificity and accuracy (sensitivity ~ 86.96 %, specificity ~ 95.73 % and accuracy ~ 94.29 %) than Rago (Tsukuba) criteria (sensitivity ~ 72%, specificity ~ 95.65 % and accuracy ~ 91.43 %) as shown in table 17.

Distribution of lesions based on Mean Elastography Index

The cut off of mean elastography index used for benign lesions was < 2.905 and for malignant lesions was > 2.905[34]. Based on this, 117 lesions (83.6 %) were benign and 23 lesions (16.4%) were malignant as shown in figure 22.

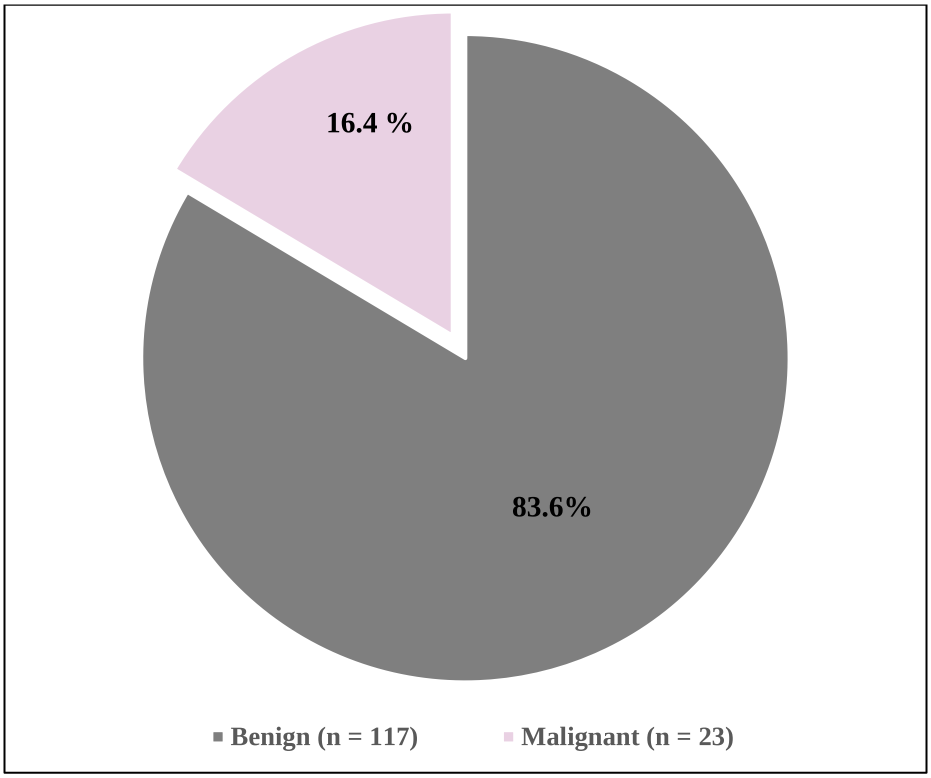

Figure 22: Distribution based on Mean elastography index

Table 18 :Correlation between Elastography & Pathological diagnosis

Elastography	Pathological Diagnosis	
	Benign	Malignant
Benign	115	2
Malignant	1	22

Mean elastography index was correlated with pathological findings. Strain elastography overdiagnosed one case as malignant and underdiagnosed 2 cases as benign and overdiagnosed 1 benign lesion as malignant as depicted in table 18.

Table 19 :Correlation between USG & Elastography

USG diagnosis	Elastography	
	Benign	Malignant
Benign	90	4
Probably Benign	8	3
Probably Malignant	18	9
Malignant	1	7

Amongst the 98 cases that were considered benign based on conventional ultrasonography features 7 of them had higher mean elastography index > 2.905 values. Out of the 35 lesions which were suspicious for thyroid malignancy 19 of them had lower mean elastography index < 2.905 values as seen in table 19.

Table 20: Relation between Mean Elastography Index and pathological findings

Mean Elastography Index	N (%)	Pathological Diagnosis		*p*-value
		B	**M**	<0.0000001*
Favoring **B** (EI mean < 2.905)	117 (83.57 %)	115 82.14 %	2 1.42%	
Favoring **M** (EI mean > 2.905)	23 (16.43 %)	1 0.71%	22 15.7%	
B – Benign, M – Malignant				

The *p* value for Relation between Mean Elastography Index and pathological findings was <0.0000001 (table:20). The association noted was statistically significant.

Table 21 : Mean elastography index for malignant and benign lesions with standard deviation

Type of lesion	Mean EI	
	Average	SD
Benign lesions	1.478966	0.626295
Malignant lesion	4.145417	0.545

Mean elastographic index for benign lesions were ~ 1.4 ±0.626 and malignant thyroid lesions were ~ 4.14 ± 0.545 respectively as shown in table 21.

Table 22: Relation between Mean Elastography Index (EI) and conventional US findings

Mean EI	N (%)	Conventional US finding				*p*-value
		B	**P B**	**P M**	**M**	<0.00001*
		N %	N %	N %	N %	
B (EI mean < 2.905)	117 (83.57%)	90 64.2%	8 5.71%	18 2.86%	1 0.71%	
M(EI mean > 2.905)	23 (16.43%)	4 2.86%	3 2.14%	9 6.43%	7 5%	
B- Benign, PB – Probably Benign, PM – Probably Malignant, M - Malignant						

The *p* value for Relation between Mean Elastography Index and conventional US findings <0.00001 (table: 22). The association noted was statistically significant.

Table 23: Comparison of USG, elastography and combined

	Ultrasound	Elastography	Combined
Sensitivity	66.67%	91.67 %	79.17%
Specificity	90.52%	99.14%	94.83%
Positive predictive value	59.26%	95.65%	76.00%
Negative predictive value	92.92%	98.29%	95.65%
Accuracy	86.43%	97.86%	92.14%

Elastography is having higher sensitivity, specificity, PPV, NPV and accuracy (sensitivity ~ 91.67%, specificity ~ 99.14% PPV~ 95.65%, NPV ~ 98.29% and accuracy ~ 97.86 %) than conventional ultrasonography (sensitivity ~ 66.67 %, specificity ~ 90.52 %, PPV~ 59.26%, NPV ~ 92.92% and accuracy ~ 86.43 %). Combined sensitivity, specificity, PPV, NPV and accuracy of elastography and ultrasonography was 79.17%, 94.83%, 76.00%, 95.65% and 92.14% respectively as depicted in table 23.

Distribution of lesions based on Pathological diagnosis

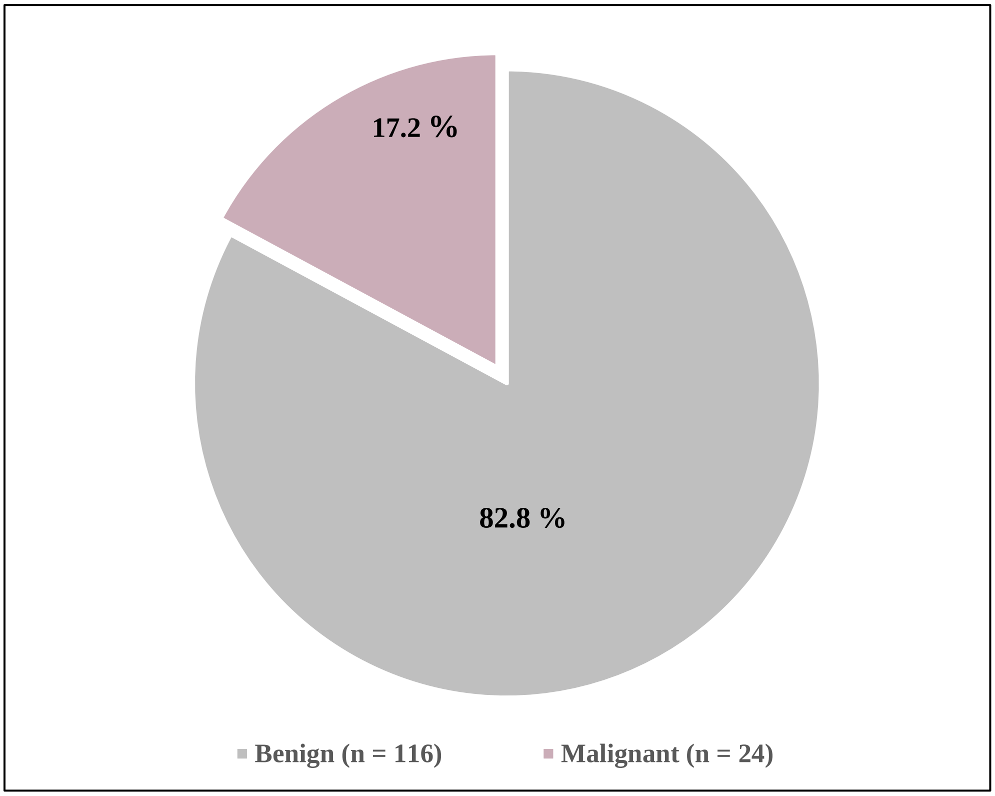

Figure 23: Distribution of lesions based on pathological diagnosis

Based on the pathological findings amongst 140 lesions majority 82.8 % (n = 116) were benign and 17.2 % (n = 24) lesions were malignant as shown in figure 23.

Table 24: Distribution of lesions based on pathological diagnosis

Pathological diagnosis	No. Of patients	%
Colloid cyst	3	2.14
Colloid goiter	20	14.28
Nodular goiter	35	25.00
Benign thyroid nodule	14	10.00
Lymphocytic thyroiditis	33	23.57
Hashimoto's thyroiditis	4	2.85
Autoimmune thyroiditis	5	3.57
Follicular adenoma	2	1.42
Papillary carcinoma thyroid - classic type	11	7.85
Papillary carcinoma (oncocytic variant)	1	0.71
Follicular variant of papillary carcinoma	10	7.14
Follicular carcinoma of thyroid	1	0.71
Medullary carcinoma	1	0.71
Total	140	100

Out of the 116 lesions that were benign based on pathological diagnosis, majority of them 25 % (n = 35) were cases on nodular goiter. Amongst the 24 malignant cases, majority of them 15.7 % (n = 22) were papillary carcinoma of thyroid as seen in table 24.

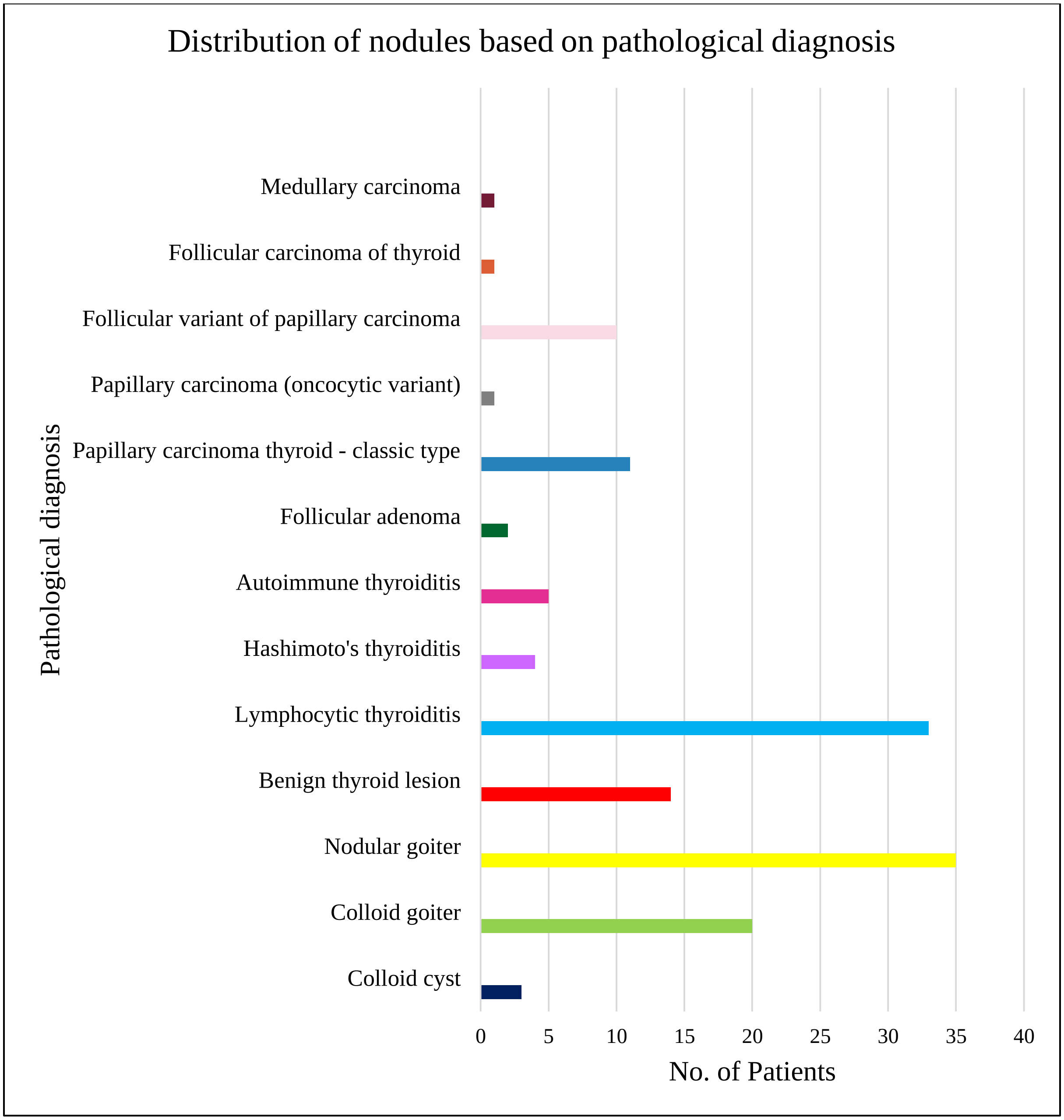

Figure 24: Distribution of nodules according to pathological diagnosis

IMAGES

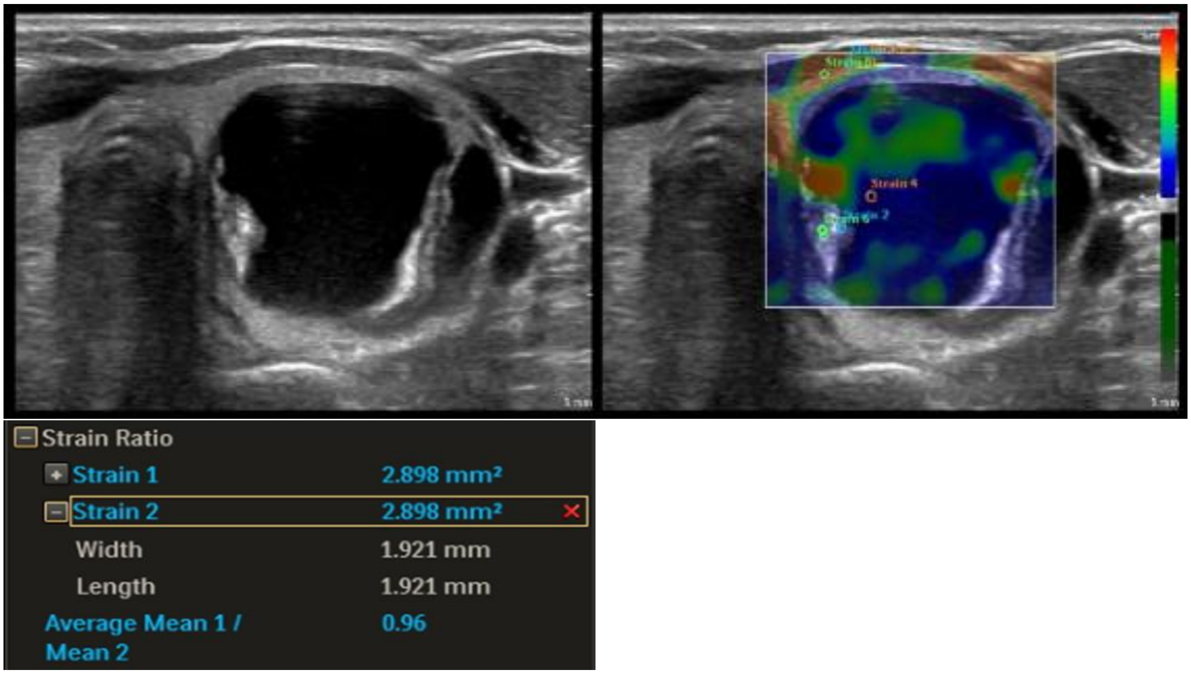

Figure 25 : Cystic lesion noted on greyscale images with a classic BGR (blue, green, red) artifact on elastography colour scoring, Mean elastography ~ 0.96, indicating a less stiff lesion.

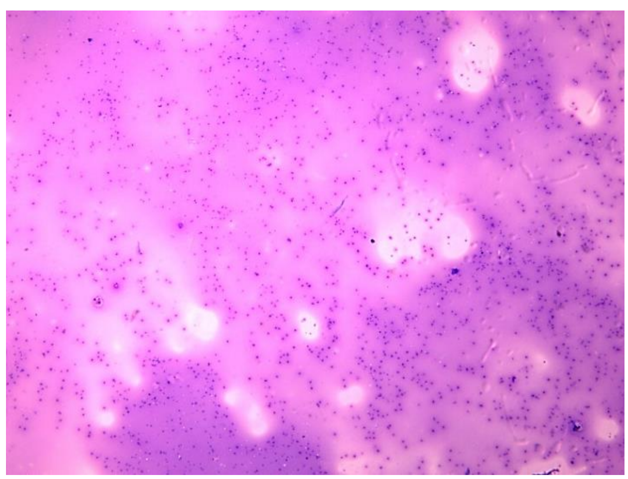

Figure 26 : Microphotograph of FNAC showing abundant colloid in the background (H & E stain, magnification x100)

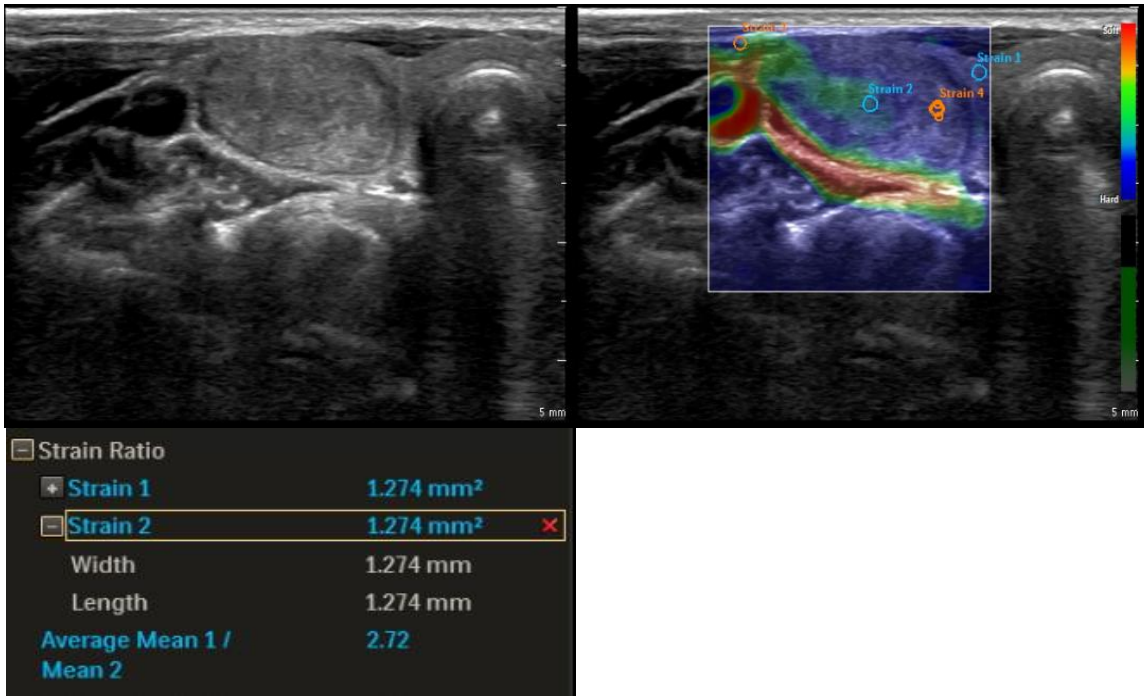

Figure 27: Follicular adenoma – Well defined hyperechoic lesion noted in right lobe on grey scale images demonstrating colour pattern indicating benignity on elastography colour scoring criteria with a mean elastography index ~ 2.72 indicating a lesion of benign etiology

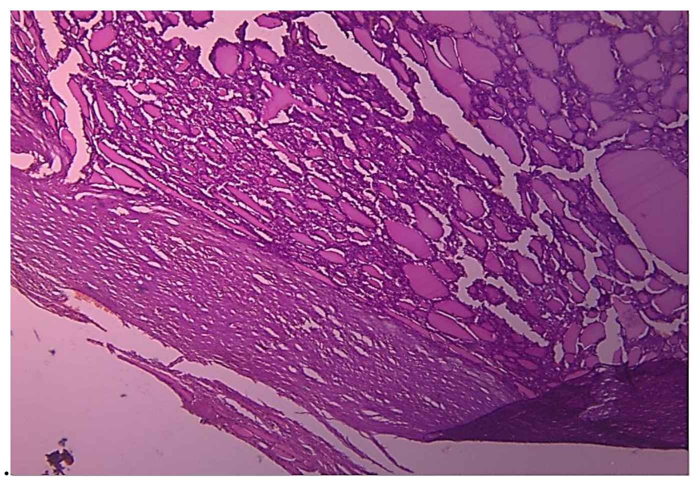

Figure 28: Microphotograph showing well encapsulated tissue with follicles of varying sizes. No vascular and/or capsular invasion noted – follicular adenoma – mixed pattern. (H & E stain, magnification x100)

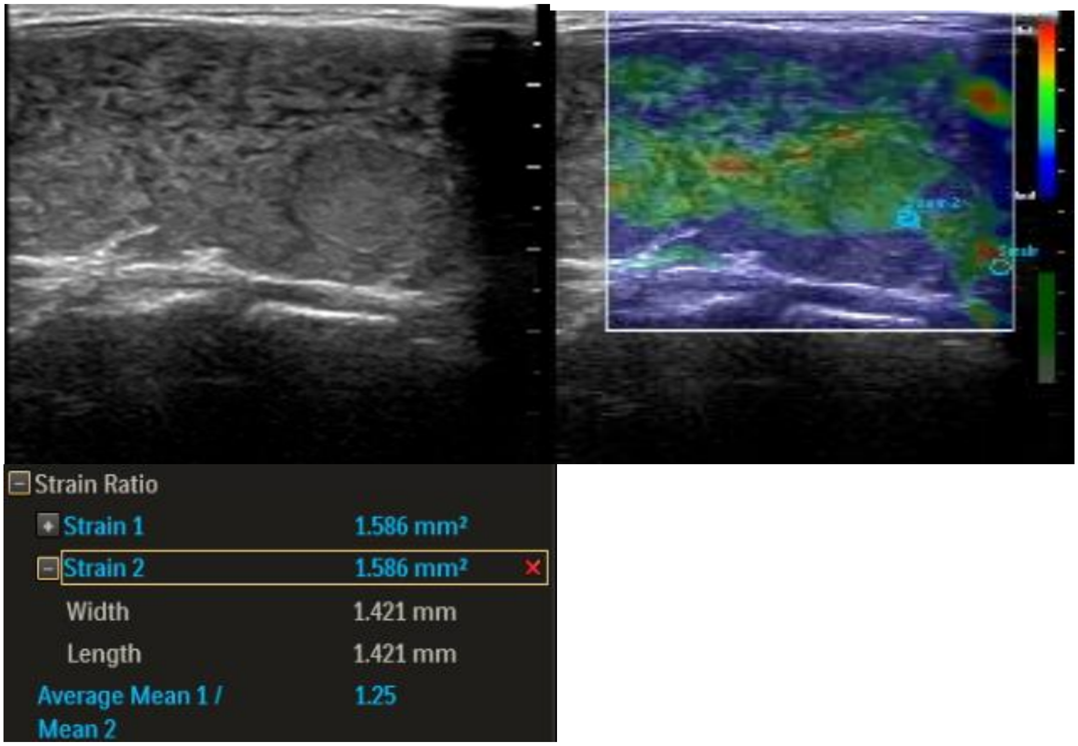

Figure 29 : Hashimoto's thyroiditis – Grey scale image shows diffuse heterogeneous echo texture with pseudo nodule formation, Mean elastography index ~ 1.25 on elastography indicating a benign etiology.

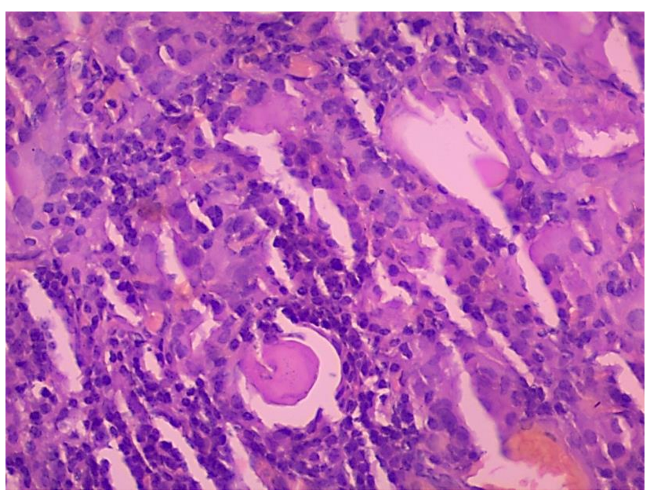

Figure 30 : Microphotograph of thyroid tissue showing variable sized thyroid follicles with occasion replacement by lymphocytes forming lymphoid follicles with reactive germinal centre. (H & E stain, magnification x400)

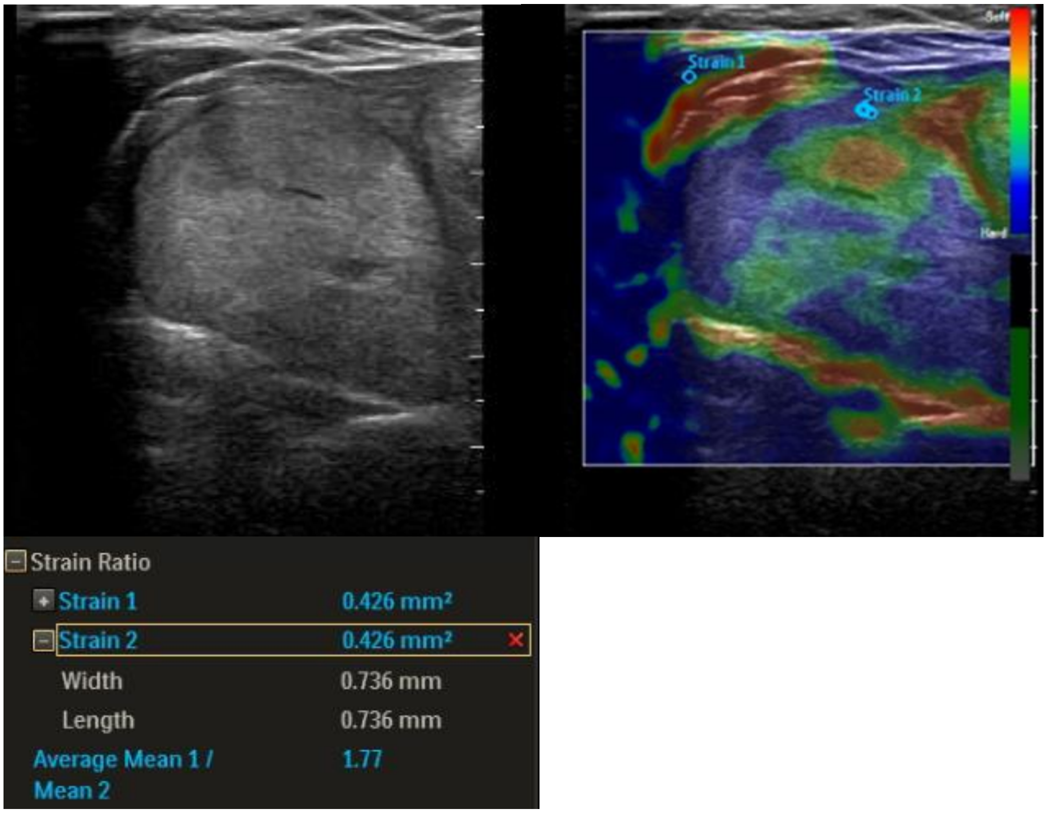

Figure 31: Nodular goitre – Greyscale image demonstrates bulky gland consisting multiple nodules of varying size with increased perinodular vascularity, Mean elastography index ~ 1.77 suggesting benignity of lesion.

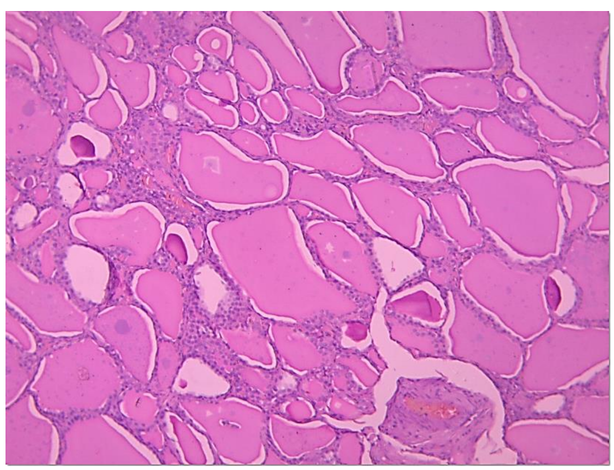

Figure 32: Microphotograph thyroid tissue showing follicles of different sizes lined by cuboidal or flat epithelial cells. The follicles are arranged within ill-defined nodular areas. (H & E stain, magnification x 400)

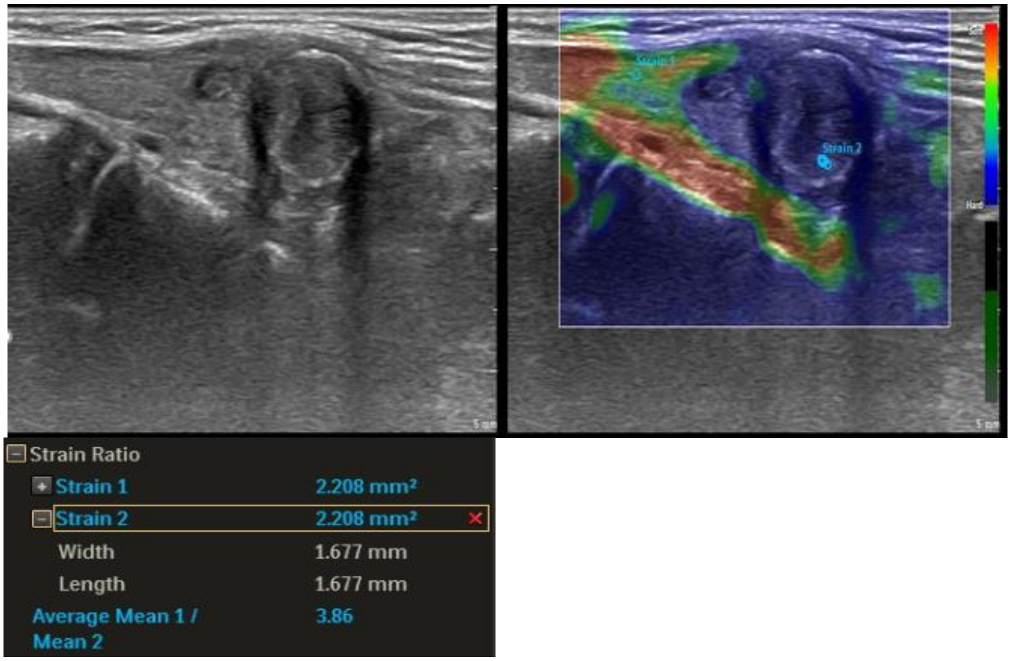

Figure 33 : Papillary carcinoma – Grey scale image demonstrates a well-defined lesion of heterogeneous echogenicity with areas of internal and peripheral calcifications, the area appeared blue on elastographic evaluation indicating a very stiff lesion, mean elastography index ~ 3.86 , suggesting a malignant etiology.

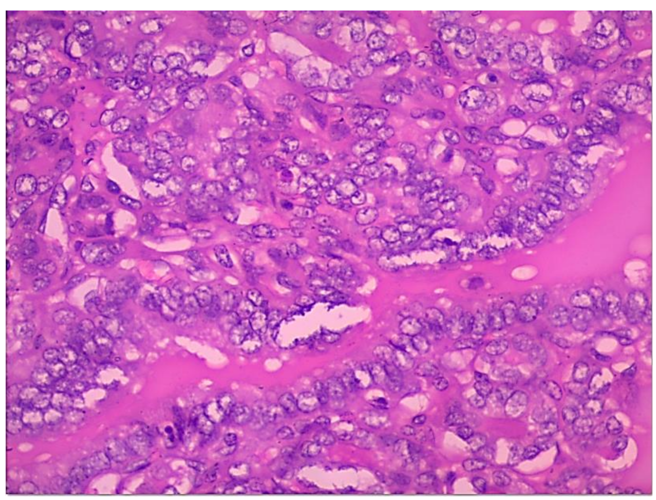

Figure 34: Microphotograph of thyroid tissue shows tumor cells arranged in follicular and occasional papillary pattern demonstrating overcrowding and overlapping. These cells show nucleomegaly and a few of them showing nuclear groove. Few cells show Hurthle cell change – Follicular variant of papillary carcinoma. (H & E stain, magnification x 400)

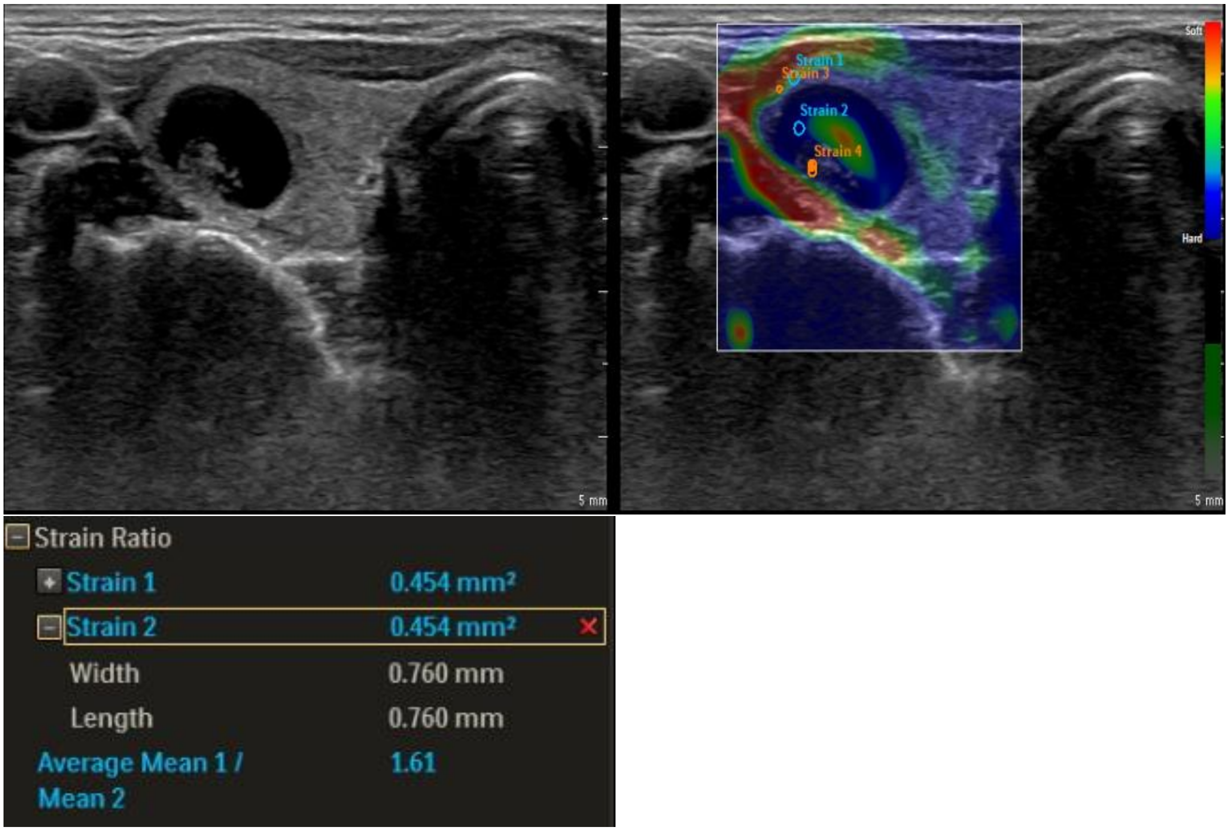

Figure 35: Grey scale image shows a well-defined solid cystic lesion, on elastography evaluation a classic BGR artifact was noted, a mean elastography index ~ 1.61 was obtained, suggesting a lesion of benign etiology. Histopathology report showed papillary carcinoma - oncocytic variant. As discussed earlier cystic/necrotic degeneration leads to reduced mean elastography index which can underdiagnose a malignant lesion as benign.

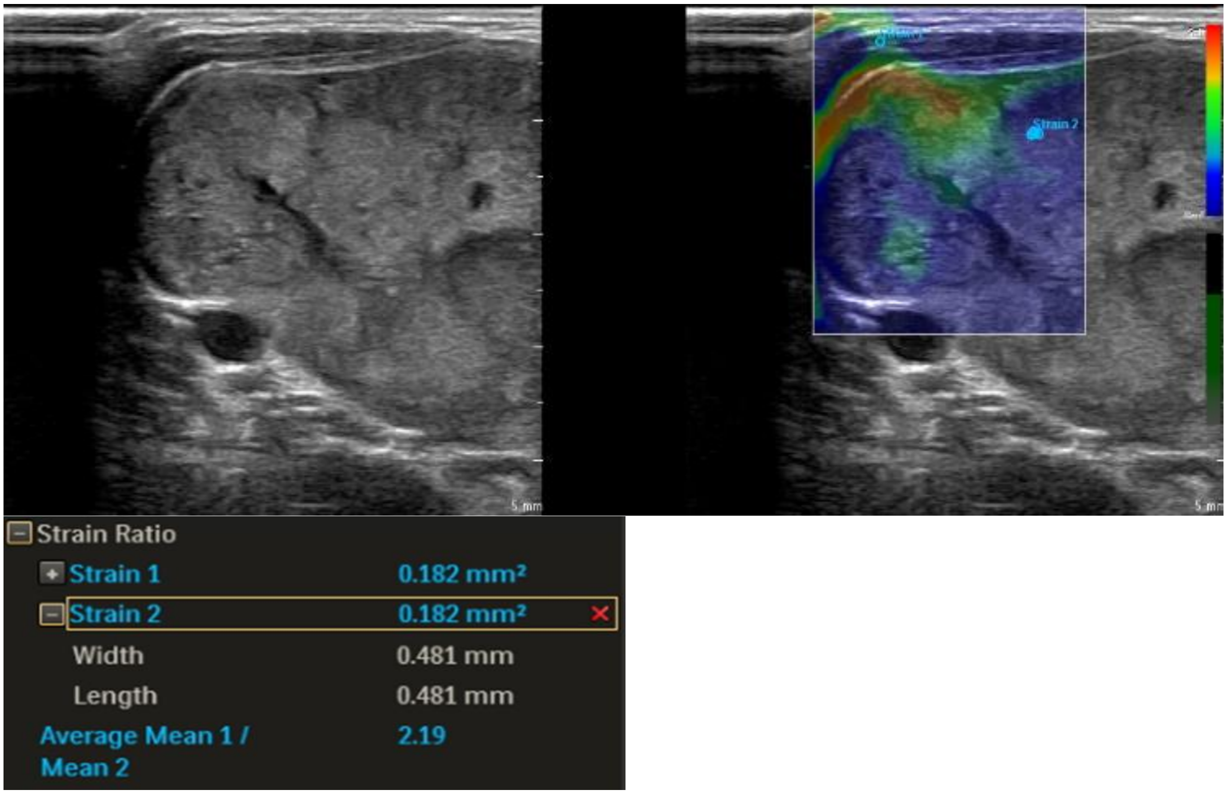

Figure 36: Greyscale image demonstrates a large lesion of heterogeneous echogenicity involving right lobe and isthmus displacing carotid artery laterally, mean elastography index obtained was ~ 2.19 indicating a less stiff benign lesion. On histopathology the lesion was diagnosed as papillary carcinoma – classic type. As discussed earlier, large nodules with deeper extensions tend to demonstrate a lower mean elastography value leading to underdiagnosis of a malignant lesion as benign.

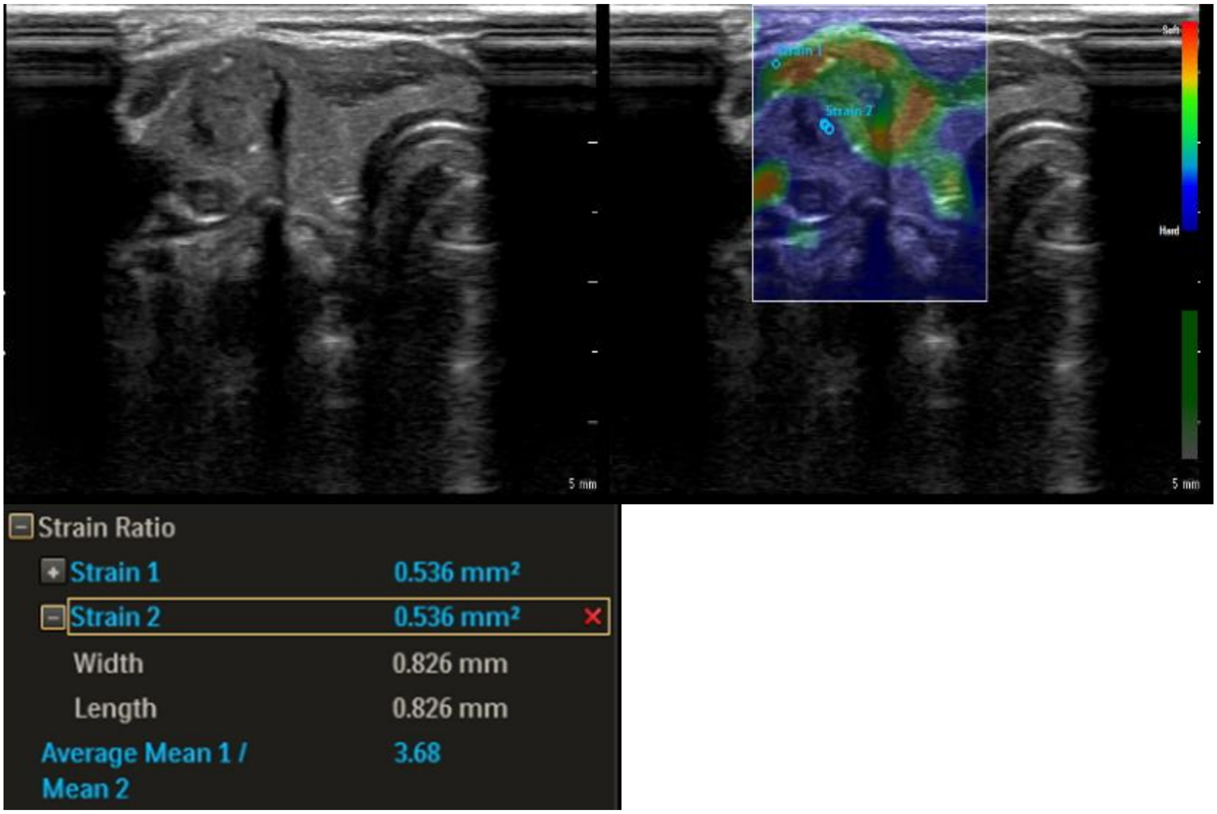

Figure 37: Grey scale image shows a well-defined lesion with few punctate peripheral calcifications in right lobe with a mean elastography index ~ 3.68 indicating malignant etiology. On histopathology, the lesion was diagnosed to be nodular goitre. As described earlier, presence of calcifications in lesion contributes to high mean elastography values leading to overdiagnosis of a nodular goitre lesion with calcifications as malignant.

DISCUSSION

DISCUSSION

In our prospective study, 140 patients underwent Conventional ultrasonography and Elastography for assessing various thyroid diseases. Out of 140 patients, 120 (85.7 %) were females and 20 (14.3 %) were males with a female: male ratio of 6:1. Comparable results was obtained by Kumar S et al., which had 160 patients and reported female to male ratio of 4:1[40].

Most common age group in our study was < 40 years (49.3%), followed by 41-60 years (57 %) with mean age of 41.52 ± 15.31 years (mean ± SD) (range 18 to 75 years). Kumar S et al., noted that thyroid disease was prevalent in the age group between 20-50 years of age[40]. The *p* value calculated for age distribution was 0.441505. No significant difference was derived in occurrence of disease in any particular age group.

Majority of lesions were benign, 83 % (n = 116) and 17 % were malignant (n = 24). Nodular goiter comprised majority of the benign lesions 25 % (n=35). However, amongst the malignancies, papillary carcinoma was seen more commonly, 15.7 % (n = 22). Similar results were derived by Zhuo J et al, wherein amongst the 191 cases studied, 122 were benign and 69 were malignant. There were 58 nodular goitres, which were the most commonly encountered benign lesion whereas papillary carcinoma of thyroid gland (n = 40) constituted a majority amongst the malignant lesions[31].

Our study observed that amongst 140 cases, 18 cases were overdiagnosed to be probably malignant and 1 case as malignant based on conventional ultrasonography findings. 8 cases were underdiagnosed as benign on pathological correlation.

The ultrasonography features that was characteristic of benign thyroid nodules were hyperechoic or iso-echoic lesions, surrounding hypoechoic halo, cystic nodules that contained colloid which had an appearance of cyst with hyperechoic foci within, ‘ring down’ or ‘comet tail’ artifact and some nodules that had honeycomb/spongiform appearance. Peripheral calcification (eggshell calcifications) are noted in few benign thyroid nodules. On Colour Doppler imaging of nodule, peripheral vascularity was noted in benign thyroid nodules[42,43].

Features that should point towards malignancy include hypogenicity, taller than wider in shape, intranodular calcifications, coarse calcifications are noted in medullary carcinoma (multinodular goitre as well) on USG and intranodular vascularity is noted in malignant lesions. Indeterminate lesions tend to demonstrate both intranodular and perinodular vascularity on CDI[42].

The *p* value for Relation between conventional ultrasound findings and pathological findings was <0.00001 in our study. The association noted was statistically significant.

Conventional ultrasonography had a sensitivty, specificity, NPV, PPV and accuracy of 66.67%, 90.52%, 92.92%, 59.26% and 86.43% respectively in our study.

Comparable results were obtained by Kim KM et al., wherein the sensitivity, specificty, NPV, PPV and accuracy were 66.0 %, 96.0%, 99.4 %, 47.7 % and 86.7 % respectively[43,51].

In our study both TIRADS and ACR-TIRADS were utilised for risk stratification based on conventional ultrasonography features of nodules. As per TIRADS lesions were divided into 6 categories. According to ACR-TIRADS points were given based on five ultrasonography features from TR1 to TR 5. Based on these scoes further management was recommended[46,47].

Both TIRADS and ACR-TIRADS had a similar sensitivity, specificity, NPV ,PPV and accuracy of 44.44%, 92.31%, 82.76%, 66.7%and 80 % respectively. Similarly a study conducted by Phuttharak W et al., demonstrated that for TIRADS sensitivity, specificity, NPV, PPV and accuracy were 41.7%, 89.3%, 83.5%, 43.5% and 80.6% and for ACR- TIRADS it was 58.3%, 79.2%, 89.1%, 34% and 90.4% respectively[44].

In our study both Rago (Tsukuba) and Asteria criterias were used for colour scoring of the thyroid lesions. Rago criteria is a 5-point colour scoring criteria and Asteria is a 4-point colour scoring criteria. These colour scoring criterias are qualitative elastography scores. According to Rago criteria, scare 1, 2 and 3 is given for a lesion with less stiffness and score 4 and 5 is for a very stiff lesion that is suspicious for malignancy. In Asteria criteria, 1 and 2 scores is given for less stiff nodules and scores of 3 and 4 is given for more stiff nodules [29,41,43].

In our study, The p value for Relation between Elastography colour score Rago (Tsukuba) and Asteria criteria and pathological findings was <0.00001. The association noted was statistically significant. It was also noted that Asteria criteria had a higher sensitivity, specificity and accuracy (sensitivity ~ 86.96 %, specificity ~ 95.73 %, PPV ~ 80%, NPV ~ 97.39% and accuracy ~ 94.29 %) than Rago (Tsukuba) criteria (sensitivity ~ 72%, specificity ~ 95.65 %, PPV ~78.26 %, NPV ~ 94.02 % and accuracy ~ 91.43 %). The results acquired were similar to a study by Afifi AH et.al, in which Rago criteria had a sensitivity, specificity, NPV, PPV and accuracy of 78.6 %, 78.9%, 73.3%, 83.3% and 78.8 % respectively[1,48,65].Moon WJ et al., conducted a retrospective study where Asteria criteria was better in characterising malignant and benign nodules as compared to Rago criteria, similar to our study[49].

The cut off used for Mean Elastography Index of benign lesions was < 2.905 and for malignant lesions was > 2.905 in our study[34].

Mean elastographic index for malignant and benign lesions are ~ 1.4 ±0.626 and 4.14 ± 0.545 respectively in our study. Malignant lesions had a much high elastography index of 4.14 ± 0.545 as compared to 2.905. Results similar to this were noted Lyshchik A et al., wherein a strain index > 4 was considered for the diagnosis of thyroid malignancy[50].

Mean elastography index was correlated with pathological findings and strain had elastography overdiagnosed one case as malignant and underdiagnosed 2 cases as benign and overdiagnosed 1 benign lesion as malignant. The *p* value for Relation between Mean Elastography Index and pathological findings was <0.0000001. The association noted was statistically significant. The *p* value for Relation between Mean Elastography Index and conventional US findings <0.00001. The association was also statistically significant.

Elastography has a sensitivity, specificity and accuracy (sensitivity ~ 91.67%, specificity ~ 99.14% PPV~ 95.65%, NPV ~ 98.29% and accuracy ~ 97.86 %). Afifi AH et al., obtained similar results wherein a mean elastography index of < 2.52 was considered to characterise benign or less stiff lesions and a mean elastography index of >2.52 was considered to diagnose or suspect malignant or very stiff thyroid lesions. Elastography index had a sensitivity ~85.7%, specificity~ 90,5 %, PPV ~ 85.7 %, NPV ~ 90.5 % and diagnostic accuracy ~ 88.6 %[48]. Similar results were observed by Garg M et al.,[51].

Amongst the 24 lesions that were malignant on pathological diagnosis, 2 lesions were underdiagnosed by elastography. One of these lesions had extensive necrotic degeneration. This led to lower mean elastography index values and BGR (blue, green and red) artifact on colour scoring criteria. Other lesion was larger, lower mean elastographic index obtained maybe attributable to inadequate compression owing to the deep location of lesion. One benign lesion was over-diagnosed as malignant lesion due to higher mean elastography index values which was attributable to the peripheral calcifications present in the nodule.

It was noted in multiple studies that that there few limitations to real time elastography. These comprise nodule position, size, cystic degeneration within the nodule, calcifications, compression intensity, carotid pulsations, presence of healthy thyroid tissue and observer experience [29,52,53,54].

If there is presence of calcifications especially in the periphery it is difficult for the sound waves to penetrate. Intranodular calcifications contribute to increased stiffness of lesion, also in case of rim calcifications higher mean elastography index values are obtained as it leads to increased stiffness[,52,53,58,59,60,60,61].

Contrary to this, there are few studies that have shown that elastography is a helpful tool in categorizing calcified thyroid nodules[55].

In multiple studies conducted for assessment of thyroid lesions using real time elastography, cystic lesions and malignant lesions with cystic/necrotic degeneration demonstrate classic (blue, green and red) BGR artifact. These lesions have a much lesser mean elastography index values and the malignant lesions with extensive cystic/necrotic degeneration are usually underdiagnosed as benign[29,52].

Size of nodule affects the elastography values. Nodules more than 3 cm tend to underestimate the nodule stiffness and compression is not adequate because of deeper/retrosternal extension [29,56].

Contrarily Cantisani V et al., concluded that nodule size does not affect the diagnostic quality of ultrasonography[57].

Position of nodule also affects the elastography values. Profound nodules are difficult to assessed by strain elastography. In deep seated lesions because of increased distance the stress transmission is less, this leads to hardening of lesion which give a false positive results. Nodules located in anterior thyroid should always be compared with surrounding thyroid tissue and not the surrounding muscles because of false impression as soft lesion and a false negative result is obtained[34,52,56,59,63,77,79,80].

Compression alters the nodule appearance. Experience of operator is crucial factor that strain elastography is dependent upon. Compression should be both reproducible and reliable. A reliable and stable result is produced after several cycles of compression[39,52,58,64]. Palpation or precompression before elastography evaluation should be avoided as it can cause false increase of stiffness[52,59].

To compare the lesion with normal thyroid parenchyma, atleast more than half should be green in colour. Diffuse fibrosis or thyroid atrophy may alter the relative stiffness[34,52].

Carotid pulsations are utilised to assess the stiffness of lesions by internal compression. Conditions like tachycardia alters stiffness of nodules. Hence, diagnostic accuracy of elastography assessment of nodules which are in close proximity to the carotid artery is hindered[53,54,78].

An integral part of performing this elastography examination is observer experience. It requires assessing right amount of compression and dimension and position of ROI[52,62].

In a meta-analysis by Tian w et al., they compared both techniques of elastography evaluation, that is real time elastography and shear wave elastography. Both methods of elastography were useful in distinguishing benign from malignant lesions. Sensitivity for shear wave elastography was 78.4 % and for real time elastography it was 82.9 %. Specificity for shear wave elastography was 82.4 % and 82.8 % for real time elastography. It was observed that real time elastography was marginally better than shear wave elastography in distinguishing malignant from benign nodules. It was concluded that real time elastography can identify malignancies better due to lesser negative likelihood in comparison to shear wave elastography. The capacity of real time elastography to predict malignancy was reported as specificity of 96 % and sensitivity of 82 %. Real time elastography had a high diagnostic performance with specificity and sensitivity nearing 85 – 95 % and 88-90 % respectively. One of the drawbacks of real time elastography is its inability to adequately assess follicular neoplasms and multinodular goiters. Some follicular neoplasms are less stiff as compared to other malignancies[2,39,67,68,69,72].

Shear wave elastography is superior to real time elastography in characterising nodules in the background of thyroiditis. Since real time elastography requires adjacent normal thyroid tissue for measuring stiffness of lesion, however, absent normal thyroid tissues in diffuse thyroid disease is a confounding factor[2].

Xing P et al., observed a overall specificity ~ 85.7%, sensitivity ~ 97.8 %, NPV ~ 97.8 % and PPV ~ 88.0 %, respectively for strain ratio[66].

Elastography had higher sensitivity, specificity, PPV, NPV and accuracy (sensitivity ~ 91.67%, specificity ~ 99.14% PPV~ 95.65%, NPV ~ 98.29% and accuracy ~ 97.86 %) than conventional ultrasonography (sensitivity ~ 66.67 %, specificity ~ 90.52 %, PPV~ 59.26%, NPV ~ 92.92% and accuracy ~ 86.43 %) and combined sensitivity, specificity, PPV, NPV and accuracy of elastography and ultrasonography was 79.17%, 94.83%, 76.00%, 95.65% and 92.14% respectively.

Afifi AH et al., observed that combination of both elastography and conventional ultrasonography are useful in distinguishing solitary nodules. Apart from suspicious features on grey mode ultrasonography, elastographic colour scoring and high strain ratios help in diagnosing malignant lesions and assess that necessity for further pathological evaluation. On convention ultrasonography, lobulated/irregular margins, micro-calcifications, hypoechogenicity and a shape that is taller rather than wider should raise a suspicion of malignancy. Rago’s colour score of 4 and 5 and Asteria - 3 and 4 and a high strain elastography index should point towards a malignancy. A cut off of 2.52

was used to differentiate malignant and benign nodules. It was concluded that when sono-elastography was combined with convention ultrasonography it yielded better results with a specificity ~ 95 %, sensitivity ~ 92 %, NPV ~ 92 %, PPV ~ 89 % and accuracy ~ 96 %[48].

Trimboli P et al., observed that based on conventional ultrasonography, sensitivity and NPV were 85 % and 91 % respectively, whereas with real time elastography the specificity and sensitivity were 62 % and 81 % respectively. However, when both were combined and if conventional ultrasonography had even one features suspicious for malignancy the NPV and sensitivity were 97 % and 97 % respectively[75].

In many studies, it was seen that elastography is also an operator dependent method of examination, however it is easier than conventional ultrasonography and its reproducibility is high. Elastography can be used in conjunction to conventional ultrasonography. It aids in selecting nodules for further FNAC evaluation. It has superiority identification of benignity. Elastography can be employed to select nodules for FNAC and also helps in preventing unnecessary FNACs in lesions with lower elasticity and colour scores. It can also be utilised in indeterminate or non-diagnostic FNACs. Further multicentre studies are encouraged to be performed in this regard before establishing efficacy of elastography a supplement to conventional ultrasonography[1,37,51,73,74,76].

A major advantage of sono-elastography is that same transducer is utilised to perform both conventional ultrasonography and elastography in many high - end systems.

Since it is a non-invasive procedure and hardly requires a few extra minutes, no inconvenience is encountered. It is like an extension of conventional ultrasonography. No additional patient preparation is required. It basically offers additional non-invasive information and helps distinguishing benign from malignant lesions. Considering its high NPV, elastography can be useful in follow up of lesions without FNAC or surgery. Evaluation of Indeterminate or non-diagnostic thyroid lesions on FNAC by elastography may prove helpful [29].

On correlation with final pathological diagnosis, in it was noted that most lesions were benign, n = 116 (83 %) and only few were malignant n = 24 (17 %). Majority of the lesions were nodular goitre n = 35 (25 %), followed by thyroiditis n = 33 (23.5 %). Amongst 24 malignant lesions 22 were papillary carcinoma (15.7 %) and its variants, 1 lesion was medullary carcinoma (0.71 %) and 1 was follicular carcinoma (0.71 %). Histopathological diagnosis was available for the malignant lesions and cytological diagnosis for the benign lesions and wherever histopathological diagnosis was available for the benign lesions it was included. Two cases of follicular neoplasms on cytology underwent histopathological evaluation and were diagnosed to be follicular adenoma. Bethesda criteria was employed to categorise the lesions into benign or malignant lesions. Zhuo J et al., studied 191 cases, out of which 122 were benign and 69 were malignant. Amongst the 122 benign lesions, 58 lesions were nodular goitres, which were the most commonly encountered benign lesion. Out of the 69 malignant cases 40 lesions were papillary carcinoma[31].

CONCLUSION

CONCLUSION

It was concluded that elastography can aid in distinguishing benign from malignant thyroid nodules. It was observed that elastography had a higher sensitivity, specificity, NPV, diagnostic accuracy and PPV in characterising and distinguishing malignant from benign thyroid nodules in comparison to conventional ultrasonography or combined elastography and conventional ultrasonography.

As elastography is integrated with conventional ultrasonography in high end systems and is non-invasive technique it is performed with ease within few extra minutes. It is especially useful to follow up lesions in view of its high NPV without resorting to FNAC or surgery. When elastography features are used in conjunction to the conventional ultrasonography findings it helps in characterising the lesions better and also aids in selecting nodules that need to undergo FNAC.

However, few limitations like cystic degeneration of nodules, calcifications, intensity of compression, nodule size and position, presence of normal thyroid tissue in the vicinity and observer experience. More studies regarding future advances in its usefulness in clinical application need to be conducted.

SUMMARY

SUMMARY

Incidence of thyroid lesions is as high as 50% in population. This highlights importance of accurate diagnosis of thyroid nodules. A recent increase in incidence of malignancies in thyroid was reported. All thyroid nodules need to undergo extensive evaluation to rule out malignancy. Elastography is a non-invasive technique differentiate benign from malignant lesions. Acquires information by displacement of tissue caused by pressure applied to area of interest. Measures tissue elasticity and differentiates between malignant and benign nodule depending on consistency of lesion. Semi quantitative method using strain index is calculated as ratio of nodule strain value to strain of adjacent normal thyroid tissue. Allows for more definite characterization of malignant and benign lesions. Multiple studies have demonstrated that elastography has a high diagnostic performance yield compared to conventional ultrasonography. It also has a high accuracy in differentiating benign and malignant nodules even in small thyroid nodules

This was a prospective observational study performed on 140 patients suspected to have thyroid lesion referred to Department of Radio Diagnosis at R. L. Jalappa Hospital and Research Centre affiliated to Sri Devaraj Urs medical college, Kolar. Study was performed over a course of one and half years (Jan 2018 - June 2019). All patients with clinically suspected thyroid lesion, who were referred to our department for ultrasound and elastography of thyroid gland for evaluation of lesion and whose pathological diagnosis were available participated in the study. B-mode ultrasonography and elastography was performed using 5–12 MHz linear array transducer (PHILIPS EPIQ 5G Ultrasound Machine). Findings on conventional ultrasonography and elastography were correlated with pathological findings.

Out of 140 patients in this study majority of them were females (n = 120) and maximum number of patients were below the age group of 40 years.

All patients underwent B-mode ultrasonography and subsequently they underwent elastography. On B- mode ultrasonography, TIRADS and ACR- TIRADS were used to categorize the lesions as benign and malignant. Using the same transducer elastography was performed. For elastography evaluation of the lesion, two colour scoring criterias were used, 5-point Rago (Tsukuba) criteria and a 4-point Asteria criteria were used to categorise lesions into benign and malignant. A score of 4 and 5 in Rago criteria and a score of 3 and 4 in Asteria criteria was considered malignant. A semi-quantitative method was employed to assess the elasticity of the lesion. A mean elastography index of <2.905 was considered benign, whereas a mean elastography index of > 2.905 was considered malignant.

Findings on conventional B-mode ultrasonography and elastography were then correlated with pathological findings. Bethesda criteria was utilised to categorise the lesions into benign and malignant. Amongst the 140 cases that were evaluated 116 (83 %) and 24 (17 %) were malignant. Most common lesion among the benign lesions was nodular goiter 25 % (n=35) followed by thyroiditis 23.5 % (n = 33). Amongst the malignancies, papillary carcinoma of thyroid gland was seen more commonly, 15.7 % (n = 22) followed by medullary carcinoma (0.71 %) (n =1) and follicular carcinoma (0.71 %) (n =1). Sensitivity, specificity, PPV, NPV and accuracy was higher than ultrasonography alone and combined elastography and ultrasonography.

Elastography helps in more accurate characterization of lesion and identifying areas, from where FNACs can be targeted for better diagnostic yield. It is utilised as an adjunctive diagnostic technique to conventional ultrasonography and helps increasing the diagnostic performance. Elastography could be used as an ancillary tool in evaluating thyroid lesions and risk stratification.

BIBLIOGRAPHY

BIBLIOGRAPHY

1. Rago T, Santini F, Scutari M, Pinchera A, Vitti P. Elastography: new developments in ultrasound for predicting malignancy in thyroid nodules. J Clin Endocrinol Metab 2007;92:2917-22.
2. Tian W, Hao S, Gao B, Jiang Y, Zhang S, Guo L, et al. Comparison of diagnostic accuracy of real-time elastography and shear wave elastography in differentiation malignant from benign thyroid nodules. Medicine (Baltimore) 2015;94:1-9.
3. Menzilcioglu MS, Duymus M, Avcu S. Sonographic Elastography of the Thyroid Gland. Polish J Radiol 2016;81:152-6.
4. Zhuo J, Ma Z, Fu W-J, Liu S-P. Differentiation of benign from malignant thyroid nodules with acoustic radiation force impulse technique. Br J Radiol 2014;87:20130263.
5. Thyroid gland. Head and Neck. In: Standring S editor. Gray's Anatomy: The anatomical basis of clinical practice. 40thedition.Chapter 25. Spain: Churchill Livingstone Elsevier 2008. p 462-4.
6. Netter FH, Colacino S. Atlas of human anatomy. Ciba-Geigy Corporation 1989; 87-8.
7. B. Stewart, William & Rizzolo, Lawrence. Embryology and Surgical Anatomy of the Thyroid and Parathyroid Glands. Surgery of the Thyroid and Parathyroid Glands 2011; 15-23.
8. Vasudeva N, Mishra S. Inderbir Singh's Textbook of Human Histology (With Color Atlas and Practical Guide). Jaypee 2016; 325-7.

9. Faruk, Tasnuva & Islam, Md. Kafiul & Arefin, Sams & Zahurul Haq, Md. The Journey of Elastography: Background, Current Status and Future Possibilities in Breast Cancer Diagnosis. Clinical Breast Cancer 2015; 313-24.
10. Garra, Brian. Elastography: history, principles, and technique comparison. Abdominal imaging 2015; 305-8.
11. Solbiati L, William C, Reading C, James M and Hay I. The Thyroid Gland. In: Rumack CM, Wilson SR, Charbonneau JW, Levine D, editors. Diagnostic ultrasound. 4thedition. Chapter 18. Philadelphia: Elsevier Mosby 2011. p 708-49.
12. Nachiappan AC, Metwalli ZA, Hailey BS, Patel RA, Ostrowski ML, Wynne DM. The thyroid: review of imaging features and biopsy techniques with radiologic-pathologic correlation. Radiographics 2014 Mar;34:276-93.
13. Brito JP, Gionfriddo MR, Al Nofal A, et al. The accuracy of thyroid nodule ultrasound to predict thyroid cancer: systematic review and meta-analysis. J Clin Endocrinol Metab 2014;99:1253-63.
14. Sabih D, Rahim K. Thyroid Nodule Imaging, Status and Limitations. Asia Oceania J Nucl Med Biol 2015; 50-57.
15. Hong, H., Lee, E., Jeong, S., Park, J., & Lee, H. Ultrasonography of Various Thyroid Diseases in Children and Adolescents: A Pictorial Essay. Korean J Radiol 2015; 419-29.
16. Kumar V, Abbas AK, Fausto N, Aster JC. Robbins and Cotran pathologic basis of disease, professional edition e-book. Elsevier health sciences; 2014.

17. Ahmed S, Ghazarian MP, Cabanillas ME, Zafereo ME, Williams MD, Vu T, Schomer DF, Debnam JM. Imaging of anaplastic thyroid carcinoma. Am J of Neuroradiol 2018;39:547-51.
18. Wei X, Li Y, Zhang S, Li X, Gao M1. Evaluation of primary thyroid lymphoma by ultrasonography combined with contrast-enhanced ultrasonography: A pilot study. Indian J Cancer 2015;546-50.
19. DeLellis RA, Mangray S. Medullary thyroid carcinoma: a contemporary perspective. AJSP: Reviews & Reports 2017;22:196-208.
20. Abdullah N, Hajeer M, Abudalu L, Sughayer M. Correlation study of thyroid nodule cytopathology and histopathology at two institutions in Jordan CytoJournal. 2018;15.
21. Peixoto R, Pinto JC, Soares V, Koch P, Gomes AT. Primary thyroid lymphoma: A case report and review of the literature. Annals of Medicine and Surgery 2017;13:29-33.
22. Saeedan MB, Aljohani IM, Khushaim AO, Bukhari SQ, Elnaas ST. Thyroid computed tomography imaging: pictorial review of variable pathologies. Insights into imaging 2016;7:601-17.
23. Noda Y, Kanematsu M, Goshima S, Kondo H, Watanabe H, Kawada H, Bae KT. MRI of the thyroid for differential diagnosis of benign thyroid nodules and papillary carcinomas. Am J of Roentgenol 2015;204:W332-5.
24. Bozgeyik Z, Coskun S, Dagli AF, Ozkan Y, Sahpaz F, Ogur E. Diffusion-weighted MR imaging of thyroid nodules. Neuroradiol 2009;51:193-8.

25. Tezuka M, Murata Y, Ishida R, Ohashi I, Hirata Y, Shibuya H. MR imaging of the thyroid: correlation between apparent diffusion coefficient and thyroid gland scintigraphy J Magn Reson Imaging 2003; 17:163–9
26. Soelberg KK, Bonnema SJ, Brix TH, et al. Risk of malignancy in thyroid incidentalomas detected by 18F-fluorodeoxyglucose positron emission tomography: a systematic review. Thyroid 2012;22:918-25.
27. Tessler FN, Middleton WD, Grant EG. Thyroid imaging reporting and data system (TI-RADS): a user's guide. Radiol 2018;287:29-36.
28. Kaproth-Joslin K, Nicola R, Dogra V. The History of US: From Bats and Boats to the Bedside and Beyond:RSNA Centennial Article. RadioGraphics 2015;35:960-970.
29. Zhao C, Xu H. Ultrasound elastography of the thyroid: principles and current status. Ultrasonography 2019;38:106-124.
30. Lahey FH. A Method of Palpating the Lobes of the Thyroid. J of the Am Med Association 1926;86:813-4.
31. Hamidi C, Göya C, Hattapoğlu S, Uslukaya Ö, Teke M, Durmaz MS, Yavuz MS, Hamidi A, Tekbaş G. Acoustic Radiation Force Impulse (ARFI) imaging for the distinction between benign and malignant thyroid nodules. La radiologia medica 2015 ;120:579-83.
32. Chaudhary V, Bano S. Imaging of the thyroid: Recent advances. Indian J of Endocrinoland Metabol 2012;16:371-376.

33. Cappelli C, Pirola I, Gandossi E, Agosti B, Cimino E, Casella C, et al. Real-time elastography: a useful tool for predicting malignancy in thyroid nodules with nondiagnostic cytologic findings. J Ultrasound Med 2012;31:1777-82.
34. Dudea S, Botar Jid C. Ultrasound elastography in thyroid disease. Medical Ultrasonography 2015;17:74 - 96.
35. Yang J, Song Y, Wei W, Ruan L, Ai H. Comparison of the effectiveness of ultrasound elastography with that of conventional ultrasound for differential diagnosis of thyroid lesions with suspicious ultrasound features. Oncology Letters 2017;14:3515-21.
36. Kyriakidou G, Friedrich-Rust M, Bon D, Sircar I, Schrecker C, Bogdanou D, Herrmann E, Bojunga J. Comparison of strain elastography, point shear wave elastography using acoustic radiation force impulse imaging and 2D-shear wave elastography for the differentiation of thyroid nodules. PloS one 2018;13(9):e0204095.
37. Monpeyssen H, Tramalloni J, Poirée S, Hélénon O, Correas J. Elastography of the thyroid. Diagnostic and Interventional Imaging 2013;94:535-44.
38. Moraes P, Sigrist R, Takahashi M, Schelini M, Chammas M. Ultrasound elastography in the evaluation of thyroid nodules: evolution of a promising diagnostic tool for predicting the risk of malignancy. Radiol Brasileira 2019;52:247-53.
39. Bojunga J, Herrmann E, Meyer G, Weber S, Zeuzem S, Friedrich-Rust M. Real-Time Elastography for the Differentiation of Benign and Malignant Thyroid Nodules: A Meta-Analysis. Thyroid 2010; 20:1145-50.

40. Kumar S, Jain V, Gupta A, Netam S, Gupta N. Elastography evaluation of normal thyroid gland and its comparison with diffuse non nodular enlarged thyroid gland using strain ultrasound elastography. International J of Research in Medical Sciences 2019;7:1435-40.
41. Sigrist R, Liau J, Kaffas A, Chammas M, Willmann J. Ultrasound Elastography: Rview of Techniques and Clinical Applications. Theranostics 2017;7:1303-29.
42. Xie C, Cox P, Taylor N, LaPorte S. Ultrasonography of thyroid nodules: a pictorial review. Insights into imaging 2016 ;7:77-86.
43. Moon WJ, Jung SL, Lee JH, Na DG, Baek JH, Lee YH, et al. Benign and malignant thyroid nodules: US differentiation--multicenter retrospective study. Radiol 2008;247:762–70.
44. Kim KM, Park JB, Kang SJ, Bae KS. Ultrasonographic guideline for thyroid nodules cytology: single institute experience. J of the Korean Surgical Society 2013 ;84:73-9.
45. Phuttharak W, Boonrod A, Klungboonkrong V, Witsawapaisan T. Interrater Reliability of Various Thyroid Imaging Reporting and Data System (TIRADS) Classifications for Differentiating Benign from Malignant Thyroid Nodules. Asian Pacific J of Cancer Prevention 2019;20:1283-8.
46. Zhuang Y, Li C, Hua Z, Chen K, Lin JL. A novel TIRADS of US classification. Biomedical engineering online 2018 Dec;17:82.
47. Tessler FN, Middleton WD, Grant EG. Thyroid imaging reporting and data system (TI-RADS): a user's guide. Radiol 2018;287:29-36.

48. Afifi AH, Alwafa WA, Aly WM, Alhammadi HA. Diagnostic accuracy of the combined use of conventional sonography and sonoelastography in differentiating benign and malignant solitary thyroid nodules. Alexandria J of Medicine 2017;53:21-30.

49. Moon HJ, Sung JM, Kim EK, Yoon JH, Youk JH, Kwak JY. Diagnostic performance of gray-scale US and elastography in solid thyroid nodules. Radiol 2012;262:1002-13.

50. Lyshchik A, Higashi T, Asato R, Tanaka S, Ito J, Mai JJ, Pellot-Barakat C, Insana MF, Brill AB, Saga T, Hiraoka M. Thyroid gland tumor diagnosis at US elastography. Radiology 2005 ;237:202-11.

51. Garg M, Khandelwal D, Aggarwal V, Raja KB, Kalra S, Agarwal B, Dutta D. Ultrasound elastography is a useful adjunct to conventional ultrasonography and needle aspiration in preoperative prediction of malignancy in thyroid nodules: A Northern India perspective. Indian J of endocrinol and metabol 2018;22:589-99.

52. Stoian D, Bogdan T, Craina M, Craciunescu M, Timar R, Schiller A. Elastography: a new ultrasound technique in nodular thyroid pathology. Thyroid Cancer 2016:87-110.

53. Oliver C, Vaillant-Lombard J, Albarel F, Berbis J, Veyrières JB, Sebag F, Petit P. What is the contribution of elastography to thyroid nodules evaluation?. In Annales d'endocrinologie 2011 Apr 1 (Vol. 72, No. 2, pp. 120-124). Elsevier Masson.

54. Dietrich C, Bamber J. Editorial on the Special Issue of Applied Sciences on the Topic of Elastography. Applied Sciences 2018;8:1232 - 40.

55. Kim MH, Luo S, KO SH, Lim DJ, Lim Y. Elastography can effective decrease the number of fine-needle aspiration biopsies in patients with calcified thyroid nodules. Ultrasound Med Biol 2014; 40:2329–35.

56. Bathia KS, Rasalkar DP, Lee YP, et al. Cystic changes in thyroid nodules. A cofounding factor for real-time qualitative thyroid ultrasound elastography. Clin Radiol 2011; 66:799–807.

57. Cantisani V, Grazhdan H, Ricii P, Mortele K, Di Segni M, D'Andrea V, et al. Q elastography of solid thyroid nodules: assessment of diagnostic efficacy and interobserver variability in large patient cohort. Eur Radiol 2014; 24:143–150.

58. Rago T, Scutari M, Santini F, et al. Real time elastography: use fool tool for redefining the presurgical diagnosis in thyroid nodules with intermediate or nondiagnostic cytology. JCEM 2010;95 :5274–80.

59. Havre RF, Waage JR, Gilja OH, Ødegaard S, Nesje LB. Real-time elastography: strain ratio measurements are influenced by the position of the reference area. Ultraschall in der Medizin-European J of Ultrasound. 2011.

60. Andrioli M, Persani L. Elastographic techniques of thyroid gland: current status. Endocrine 2014;46:455-61.

61. Kim JK, Baek JH, Lee JH, Kim JL, Ha EJ, Kim TY, Kim WB, Shong YK. Ultrasound elastography for thyroid nodules: a reliable study?. Ultrasound in med & biol 2012;38:1508-13.

62. Calvete AC, Rodriquez JM, de Dios Berna-Mestre J, Rios A, Abellan-Rivero D, Reus M. Interobserver agreement for thyroid elastography: value of quality factor, J Ultrasound Med 2013;32:495–504.

63. Hong Y, Liu X, Li Z, Zhang X, Chen M, Luo Z. Real- time ultrasound elastography in the differential diagnosis of benign and malignant thyroid nodules. J of Ultrasound in Med 2009;28:861-7.

64. Park SH, Kim SJ, Kim EK, Kim MJ, Son EJ, Kwak JY. Interobserver agreement in assessing the sonographic and elastographic features of malignant thyroid nodules. Am J of Roentgenol 2009 ;193:W416-23.

65. Mansor M, Okasha H, Esmat S, Hashem AM, Attia KA, Hussein HE. Role of ultrasound elastography in prediction of malignancy in thyroid nodules. Endocrine research 2012 ;37:67-77.

66. Xing P, Wu L, Zhang C, Li S, Liu C, Wu C. Differentiation of benign from malignant thyroid lesions: calculation of the strain ratio on thyroid sonoelastography. J of ultrasound in med 2011 ;30:663-9.

67. Sun J, Cai J, Wang X. Real-time ultrasound elastography for differentiation of benign and malignant thyroid nodules: a meta-analysis. J Ultrasound Med 2014; 33:495–502.

68. Magri F, Chytiris S, Zerbini F, et al. The maximal stiffness evaluation by real time ultrasound elastography, an improved tool for the differential diagnosis of thyroid nodules. Endocr Pract 2015; 21:474–481.

69. Mehrotra P, McQueen A, Kolla S, et al. Does elastography reduce the need for thyroid FNAs? Clin Endocrinol (Oxf) 2013; 78:942–949.

70. Ophir J, Cespedes I, Ponnekanti H, et al. Elastography: a quantitative method for imaging the elasticity of biological tissues. Ultrason Imaging 1991; 13:111–34.

71. Ragazzoni F, Deandrea M, Mormile A, et al. High diagnostic accuracy and interobserver reliability of real-time elastography in the evaluation of thyroid nodules. Ultrasound Med Biol 2012; 38:1154–62.

72. Liu BX, Xie XY, Liang JY, et al. Shear wave elastography versus real-time elastography on evaluation thyroid nodules: a preliminary study. Eur J Radiol 2014; 83:1135–43.

73. Hong Y, Liu X, Li Z, Zhang X, Chen M, Luo Z. Real-time ultrasound elastography in the differential diagnosis of benign and malignant thyroid nodules. J Ultrasound Med 2009;28:861-7.

74. Asteria C, Giovanardi A, Pizzocaro A, Cozzaglio L, Morabito A, Somalvico F, et al. US-elastography in the differential diagnosis of benign and malignant thyroid nodules. Thyroid 2008;18:523-31.

75. Trimboli P, Guglielmi R, Monti S, Misischi I, Graziano F, Nasrollah N, Amendola S, Morgante SN, Deiana MG, Valabrega S, Toscano V. Ultrasound sensitivity for thyroid malignancy is increased by real-time elastography: a prospective multicenter study. The J of Clinical Endocrinol & Metabol 2012 ;97:4524-30.

76. Habib LA, Abdrabou AM, Geneidi EA, Sultan YM. Role of ultrasound elastography in assessment of indeterminate thyroid nodules. The Egyptian J of Radiol and Nuclear Med 2016 ;47:141-7.

77. Tranquart F , Bleuzen A , Pierre-Renoult P , Chabrolle C , Sam Giao M , Lecomte P. Elastosonography of thyroid lesions. J Radiol 2008; 89:35–39.

78. Dighe M , Bae U , Richardson ML , Dubinsky TJ , Minoshima S , Kim Y. Differential diagnosis of thyroid nodules with US elastography using carotid artery pulsation. Radiol 2008; 248:662–9.

79. Friedrich-Rust M, Sperber A, Holzer K, Diener J, Grünwald F, Badenhoop K, Weber S, Kriener S, Herrmann E, Bechstein WO, Zeuzem S. Real-time elastography and contrast-enhanced ultrasound for the assessment of thyroid nodules. Experimental and clinical endocrinol & diabetes 2010;118:602-9.

80. Kagoya R, Monobe H, Tojima H. Utility of elastography for differential diagnosis of benign and malignant thyroid nodules. Otolaryngology—Head and Neck Surgery 2010;143:230-4.

ANNEXURES

ANNEXURE I

"COMPARATIVE STUDY OF ELASTOGRAPHY AND ULTRASONOGRAPHY IN DIFFERENTIATING BENIGN AND MALIGNANT THYROID LESIONS WITH PATHOLOGICAL CORRELATION"

PATIENT PROFORMA

Demographic details:

Name:

Clinical History:

Local Examination:

USG Findings:

TIRADS –

ACR-TIRADS-

Elastography Findings:

Rago colour score-

Asteria colour score-

Mean elastography index-

Final diagnosis:

Pathological Diagnosis:

ANNEXURE II

INFORMED CONSENT FORM

STUDY TITLE: **COMPARATIVE STUDY OF ELASTOGRAPHY AND ULTRASONOGRAPHY IN DIFFERENTIATING BENIGN AND MALIGNANT THYROID LESIONS WITH PATHOLOGICAL CORRELATION**

CHIEF RESEARCHER/ PG GUIDE'S NAME: Dr. N. RACHEGOWDA

PRINCIPAL INVESTIGATOR: Dr. HITHISHINI H.

NAME OF THE SUBJECT:

AGE :

GENDER :

a. I have been informed in my own language that this study involves CT and use of contrast material as part of procedure. I have been explained thoroughly and understand its complication and possible side effects.

b. I understand that the medical information produced by this study will become part of institutional record and will be kept confidential by the said institute.

c. I understand that my participation is voluntary and may refuse to participate or may withdraw my consent and discontinue participation at any time without prejudice to my present or future care at this institution.
d. I agree not to restrict the use of any data or results that arise from this study provided such a use is only for scientific purpose(s).
e. I confirm that ___________________ (chief researcher/ name of PG guide) has explained to me the purpose of research and the study procedure that I will undergo and the possible risks and discomforts that i may experience, in my own language. I hereby agree to give valid consent to participate as a subject in this research project.

Participant's signature/thumb impression

Signature of the witness: Date:

1)

2)

I have explained to ___________________________ (subject) the purpose of the research, the possible risk and benefits to the best of my ability.

Chief Researcher/ Guide signature Date:

ANNEXURE II

COMPARATIVE STUDY OF ELASTOGRAPHY AND ULTRASONOGRAPHY IN DIFFERENTIATING BENIGN AND MALIGNANT THYROID LESIONS WITH PATHOLOGICAL CORRELATION

Patient Information Sheet

Principal Investigator: Dr. Hithishini H. / Dr. N. Rachegowda

I, Dr. Hithishini. H, post-graduate student in Department of Radio-Diagnosis at Sri Devaraj Urs Medical College. I will be conducting a study titled "Comparative study of elastography and ultrasonography in differentiating benign and malignant thyroid lesions with pathological correlation." for my dissertation under the guidance of Dr. Rachegowda, Professor, Department of Radio-Diagnosis. In this study, we will assess the role of Elastography In this study, we will assess the diagnostic value of Conventional ultrasonography and elastography sequence in evaluation of thyroid lesions. You would have undergone ultrasonography before entering the study. You will not be paid any financial compensation for participating in this research project. You will not be paid any financial compensation for participating in this research project.

All of your personal data will be kept confidential and will be used only for research purpose by this institution. You are free to participate in the study. You can also withdraw from the study at any point of time without giving any reasons whatsoever. Your refusal to participate will not prejudice you to any present or future care at this institution

Name and Signature of the Principal Investigator

Date

ANNEXURE III

KEY TO MASTER CHART

ACR TIRADS - American College of Radiology Thyroid Data System

B - Benign

EI - Elastography Index

F - Female

M - Male

M - Probably Malignant

MNG - Multinodular Goitre

PB - Probably Benign

PM - Probably Malignant

TIRADS - Thyroid imaging reporting and data system

USG - Ultrasonography

s.no	UHID NO	Age	Gender	Clinical Diagnosis	USG diagnosis	USG Diagnosis	Side of lesion	TIRADS	ACR -TIRADS	ASTERIA CRITERIA	RAGO CRITERIA	EI -Mean	Pathological diagnosis	B/M	BETHESDA Scoring
1	542297	57	F	MNG	Cystic lesion - ? Neoplastic	PM	Left	4A	4	1	1	1.36	Colloid cyst	B	II
2	544286	59	F	MNG	MNG	B	Right	2	2	1	2	1.01	Lymphocytic thyroiditis	B	II
3	542957	18	F	? Thyroid swelling	Benign cystic lesion with septations	B	Bilateral	2	2	1	2	1.86	Nodular goitre	B	II
4	527688	34	F	?MNG	Colloid nodule with solid component	PB	Right	2	3	1	1	1.83	Nodular goitre	B	II
5	561449	50	F	?Papillary carcinoma	Likely neoplastic lesion	M	Right	5	5	4	5	5.03	Follicular variant of papilary carcinoma	M	VI
6	576392	60	F	Swelling on lt side of neck	MNG	B	Bilateral	2	3	1	2	1.23	Nodular goitre	B	II
7	585842	30	F	?MNG	MNG	B	Bilateral	2	3	2	2	2.02	Nodular goitre	B	II
8	594484	45	F	?Thyroglossal cyst	MNG	B	Bilateral	3	3	2	1	0.39	Nodular goitre	B	II
9	600552	50	F	Hypothyroidism	Thyroiditis	B	Bilateral	2	2	2	3	1.8	Lymphocytic thyroiditis	B	II
10	326644	18	F	?MNG	Thyroiditis	B	Bilateral	2	3	2	2	2.41	Lymphocytic thyroiditis	B	II
11	530967	65	F	?MNG	Likely neoplastic lesion (with calcifications)	PM	Right	4A	4	4	3	3.94	Follicular variant of papilary carcinoma	M	VI
12	605308	28	F	?MNG	MNG	B	Bilateral	2	3	2	3	1.86	Nodular goitre	B	II
13	605905	60	F	H/o swelling in the neck	MNG	B	Bilateral	2	2	2	3	2.72	Nodular goitre	B	II
14	601446	60	F	H/o swelling in the neck	Thyroiditis	B	Bilateral	2	3	2	2	2.46	Lymphocytic thyroiditis	B	II

s.no	UHID NO	Age	Gender	Clinical Diagnosis	USG diagnosis	USG Diagnosis	Side of lesion	TIRADS	ACR -TIRADS	ASTERIA CRITERIA	RAGO CRITERIA	EI -Mean	Pathological diagnosis	B/M	BETHESDA Scoring
15	602786	35	F	? MNG	MNG	B	Bilateral	2	2	1	3	0.87	Lymphocytic thyroiditis	B	II
16	604476	18	M	?MNG	Thyroiditis	B	Bilateral	2	3	2	2	1.45	Lymphocytic thyroiditis	B	II
17	596855	57	F	?MNG	MNG	B	Bilateral	3	3	2	1	2.17	Lymphocytic thyroiditis	B	II
18	560554	64	F	? Solitary nodule	MNG	B	Bilateral	2	3	2	4	0.83	Lymphocytic thyroiditis	B	II
19	608458	29	F	?MNG	Thyroiditis	B	Bilateral	3	3	1	2	1.75	Lymphocytic thyroiditis	B	II
20	608801	40	F	? Thyroid swelling	MNG	B	Bilateral	2	3	2	3	0.89	Lymphocytic thyroiditis	B	II
21	415227	70	F	Thyroid swelling	Likely neoplastic	M	Left	5	5	4	5	4.41	Follicular variant of papilary carcinoma	M	VI
22	610527	27	F	Solitary thyroid nodule	MNG	B	Bilateral	2	3	1	1	1.37	Colloid goitre	B	II
23	608904	11	F	Swelling in the neck	Thyroiditis	B	Bilateral	2	2	2	2	1.52	Colloid goitre	B	II
24	610665	35	F	? MNG	MNG	B	Bilateral	3	3	2	2	1.6	Nodular goitre	B	II
25	613953	30	F	? Goitre	MNG	B	Bilateral	3	2	2	4	1.05	Hashimoto's thyroiditis	B	II
26	605905	60	F	Swelling in the neck	MNG	B	Left	2	3	2	2	2.16	Nodular goitre	B	II
27	615747	18	F	? Thyroid swlling	Grade III spongiform nodule	B	Left	3	2	1	1	1.04	Nodular goitre	B	II
28	622300	34	F	Thyroid swelling	Thyroiditis	B	Bilateral	3	3	2	2	1.4	Autoimmune thyroiditis	B	II

s.no	UHID NO	Age	Gender	Clinical Diagnosis	USG diagnosis	USG Diagnosis	Side of lesion	TIRADS	ACR -TIRADS	ASTERIA CRITERIA	RAGO CRITERIA	EI -Mean	Pathological diagnosis	B/M	BETHESDA Scoring
29	616101	65	F	? MNG	MNG	B	Bilateral	2	3	2	1	1.14	Colloid goitre	B	II
30	621811	20	F	? Thyroid swelling	Thyroiditis	B	Bilateral	3	3	2	2	1.09	Lymphocytic thyroiditis	B	II
31	624292	75	M	K/c/o Ca supraglottis	Neoplastic	M	Right	6	5	4	5	4.54	Follicular variant of papilary carcinoma	M	VI
32	629900	35	F	Hyperthyroidism	Thyroiditis	B	Bilateral	3	4	2	1	1.4	Autoimmune thyroiditis	B	II
33	283539	15	F	? Thyroid swelling	MNG	B	Right	3	3	1	2	1.04	Nodular goitre	B	II
34	629525	32	F	? Neoplastic	? Neoplastic	PM	Left	4A	5	2	3	2.33	Lymphocytic thyroiditis	B	II
35	629899	30	F	? Thyroid swelling	? Neoplastic	PM	Right	4A	5	4	5	5.33	Papillary carcinoma thyroid classic type	M	VI
36	633088	40	F	? Thyroid swelling	? Neoplastic	PM	Left	4B	5	3	3	4.3	Follicular variant of papilary carcinoma	M	VI
37	633118	30	M	? Thyroid swelling	? Neoplastic	PM	Right	4A	4	4	4	4.4	Follicular variant of papilary carcinoma	M	VI
38	632163	30	F	? Thyroid swelling	MNG	B	Bilateral	3	3	2	3	1.8	Nodular goitre	B	II
39	642176	55	F	Dyspahgia for evaluation	MNG	B	Bilateral	2	4	2	2	1.36	Lymphocytic thyroiditis	B	II
40	643806	34	M	MNG	? Neoplastic	PM	Right	4A	3	2	3	1.77	Nodular goitre	B	II
41	629019	50	F	Thyroid swelling	MNG	B	Bilateral	2	2	2	2	1.3	Lymphocytic thyroiditis	B	II
42	645665	53	F	Thyroid nodule	? Neoplastic	PM	Left	4A	4	2	4	2.5	Benign thyroid lesion	B	II
43	645669	29	F	MNG	Thyroiditis	B	Bilateral	3	3	2	3	2.48	Lymphocytic thyroiditis	B	II
44	641499	48	M	Thyroid swelling	MNG	B	Bilateral	2	2	2	1	1.47	Colloid goitre	B	II

s.no	UHID NO	Age	Gender	Clinical Diagnosis	USG diagnosis	USG Diagnosis	Side of lesion	TIRADS	ACR -TIRADS	ASTERIA CRITERIA	RAGO CRITERIA	EI -Mean	Pathological diagnosis	B/M	BETHESDA Scoring
45	640575	45	F	Solitary thyroid nodule	MNG	B	Right	3	3	2	4	4.4	Papillary carcinoma thyroid classic type	M	VI
46	620514	30	F	Solitary thyroid nodule	Nodule with colloid degeneration	B	Right	1	1	2	1	2.5	Colloid goitre	B	II
47	610665	35	F	MNG	Hashimoto's thyroiditis	B	Bilateral	3	3	2	2	1.2	Hashimoto's thyroiditis	B	II
48	640269	40	M	? Thyroid malignancy	Thyroid malignancy with metastatic lymphadenopathy	M	Right	6	5	4	5	5.8	Papillary carcinoma thyroid classic type	M	VI
49	647204	35	M	? Cervical lymphadenopathy	Thyroiditis	B	Bilateral	3	3	2	4	2.5	Lymphocytic thyroiditis	B	II
50	648041	55	F	? Thyroid swelling	MNG/Thyroiditis	B	Bilateral	2	3	2	3	1.02	Colloid goitre	B	II
51	643259	57	F	? Thyroid malignancy	Likely neoplastic	PM	Right	5	4	3	4	6.02	Papillary carcinoma thyroid classic type	M	VI
52	652394	30	F	MNG	Benign nodules	B	Bilateral	2	2	2	3	0.81	Benign thyroid lesion	B	II
53	658306	21	F	? Thyroid swelling	Benign thyroid lesion	B	Left	2	3	3	4	3.93	Follicular variant of papilary carcinoma	M	VI
54	661494	20	F	Solitary thyroid nodule	Likely neoplastic	PM	Left	4A	4	2	2	1.57	Benign thyroid lesion	B	II
55	661976	67	F	Swelling in the neck	Benign lesion with cystic degeneration	B	Bilateral	2	2	1	2	1.06	Nodular goitre	B	II
56	662716	32	M	Solitary thyroid nodule	Likely neoplastic	PM	Left	4A	5	3	4	4.52	Papillary carcinoma thyroid classic type	M	VI
57	655377	54	M	Solitary thyroid nodule	Cystic thyroid nodule	B	Left	2	2	2	2	1.96	Benign thyroid lesion	B	I
58	655772	28	F	Solitary thyroid nodule	Liklely benign	PB	Right	2	3	3	4	4.56	Papillary carcinoma thyroid classic type	M	VI

s.no	UHID NO	Age	Gender	Clinical Diagnosis	USG diagnosis	USG Diagnosis	Side of lesion	TIRADS	ACR -TIRADS	ASTERIA CRITERIA	RAGO CRITERIA	EI -Mean	Pathological diagnosis	B/M	BETHESDA Scoring
59	663097	40	F	?MNG	Thyroiditis (likely hasimotos)	B	Bilateral	3	3	2	2	1.01	Nodular goitre	B	II
60	598302	38	F	Swelling in the neck	Benign thyroid lesion	B	Bilateral	2	2	3	4	2.99	Follicular variant of papilary carcinoma	M	VI
61	666010	45	M	Solitary thyroid nodule	Likely neoplastic	PM	Right	5	5	2	2	1.63	Colloid goitre	B	II
62	670888	40	F	? Thyroid swelling	Benign thyroid lesion	B	Left	2	2	2	1	0.8	Colloid goitre	B	II
63	670747	48	F	?MNG	? Neoplastic	PM	Right	4B	4	2	3	2.69	Nodular goitre	B	II
64	670909	30	F	?MNG	Hashimoto's thyroiditis	B	Bilateral	3	3	2	2	0.8	Lymphocytic thyroiditis	B	II
65	673541	30	M	K/c/o Ca thyroid (papillary)- post hemithyroidectomy	Likely recurrence	M	Right	6	5	4	5	5.1	Medullary carcinoma thyroid	M	VI
66	676642	40	F	? Thyroid swelling	? Neoplastic	PM	Bilateral	4A	4	2	3	1.3	Nodular goitre	B	II
67	676887	41	M	Solitary thyroid nodule	? Neoplastic	PM	Left	4A	4	2	3	2.3	Nodular goitre	B	II
68	677521	58	M	? MNG	Cystic thyroid nodule	B	Right	4A	4	1	2	1.2	Nodular goitre	B	II
69	679675	25	F	Thyroid swelling	Thyroiditis	B	Bilateral	3	3	2	2	0.9	Lymphocytic thyroiditis	B	II
70	679934	42	F	Swelling in the neck	? Neoplastic	PM	Right	4B	4	2	3	2.96	Papillary carcinoma thyroid classic type	M	VI
71	687300	55	F	Hemorrhagic cyst	Hemorrhagic cyst	B	Left	2	2	2	2	1.12	Benign thyroid lesion	B	I
72	681563	55	F	?MNG	? Neoplastic	PM	Bilateral	4A	4	2	3	1.99	Nodular goitre	B	II

s.no	UHID NO	Age	Gender	Clinical Diagnosis	USG diagnosis	USG Diagnosis	Side of lesion	TIRADS	ACR -TIRADS	ASTERIA CRITERIA	RAGO CRITERIA	EI -Mean	Pathological diagnosis	B/M	BETHESDA Scoring
73	682191	42	M	Swelling in the neck	Likely benign	PB	Bilateral	2	2	2	1	1.03	Colloid goitre	B	I
74	682413	46	F	Thyroid swelling	Solitary thyroid nodule	PM	Right	4A	3	2	2	2.7	Nodular goitre	B	II
75	682550	25	F	Thyroid swelling	Benign	M	Bilateral	3	3	2	3	2.62	Nodular goitre	B	II
76	683492	55	F	?MNG	? Neoplastic	PM	Left	4A	4	2	3	2.56	Nodular goitre	B	II
77	683485	18	F	Thyroid swelling	Thyroiditis	B	Bilateral	3	3	1	2	0.9	Lymphocytic thyroiditis	B	II
78	685278	20	M	? Thyroglossal cyst	Ectopic thyroid with cystic changes	B	Ectopic gland	1	2	1	1	0.72	Colloid goitre	B	I
79	685122	75	F	Swelling in the neck	? Neoplastic	PM	Bilateral	4A	4	2	3	1.22	Hashimoto's thyroiditis	B	II
80	686831	32	F	Thyroid swelling	Thyroiditis	B	Bilateral	3	3	2	3	0.84	Lymphocytic thyroiditis	B	II
81	689686	32	F	Swelling in the neck	MNG with suspiciou nodule	PM	Left	4A	4	2	1	2.4	Lymphocytic thyroiditis	B	II
82	689887	35	F	MNG	MNG with suspicious nodule	PM	Right	4B	4	2	2	2.87	Follicular adenoma	B	II
83	680620	60	F	Swelling in the neck	Benign thyroid nodule	B	Left	2	2	2	2	1	Follicular adenoma	B	II
84	682643	70	F	MNG	MNG	B	Bilateral	2	3	2	5	2.5	Nodular goitre	B	II
85	690326	35	M	Hypothyroidism	Thyroiditis	B	Bilateral	3	2	1	1	1.06	Autoimmune thyroiditis	B	II
86	695038	30	F	Swelling in the neck	Benign thyroid lesion	B	Left	2	2	2	3	2.03	Colloid goitre	B	II
87	661962	58	F	?MNG	Benign thyroid lesion	B	Left	2	2	2	3	1.14	Nodular goitre	B	II

s.no	UHID NO	Age	Gender	Clinical Diagnosis	USG diagnosis	USG Diagnosis	Side of lesion	TIRADS	ACR -TIRADS	ASTERIA CRITERIA	RAGO CRITERIA	EI -Mean	Pathological diagnosis	B/M	BETHESDA Scoring
88	701946	52	F	K/c/o medullary carcinoma	Neoplastic	M	Right	6	4	3	4	3.47	Medullary carcinoma thyroid	M	VI
89	705646	27	F	MNG	Adenomatous nodule	B	Bilateral	2	3	2	3	2.19	Lymphocytic thyroiditis	B	II
90	701257	35	F	Thyroid swelling	MNG	B	Bilateral	2	2	2	2	1.3	Colloid goitre	B	I
91	607882	80	F	MNG	MNG	B	Bilateral	2	3	2	2	1.64	Autoimmune thyroiditis	B	II
92	700484	30	F	MNG	Benign cystic lesion	B	Right	1	1	1	2	1.21	Colloid goitre	B	II
93	705612	19	F	Thyroid swelling	? Neoplastic	PM	Left	4A	4	1	2	1.97	Lymphocytic thyroiditis	B	II
94	708187	45	F	Thyroid swelling	Benign thyroid lesion	PB	Right	2	3	3	2	3.1	Papillary carcinoma thyroid classic type	M	VI
95	707458	57	M	? Lymphadenopathy	? Neoplastic	PM	Right	4B	5	2	2	0.81	Colloid goitre	B	II
96	478051	35	F	? Post thyroidectomy status	Recurrent goitre	B	Left	2	3	2	1	2.08	Colloid goitre	B	II
97	714299	31	F	Thyroid swelling	Likely Benign	PB	Left	2	3	2	1	2	Benign thyroid lesion	B	II
98	637624	50	F	? MNG	MNG	B	Bilateral	2	3	2	2	1.4	Colloid goitre	B	II
99	712481	45	F	? Thyroid swelling	Mixed solid/cystic lesion	PB	Right	2	3	2	3	1.8	Colloid goitre	B	II
100	714759	34	F	Solitary thyroid nodule	Spongiform	B	Right	1	2	2	3	0.81	Benign thyroid lesion	B	II
101	710215	67	F	? Neoplastic	Neoplastic	PM	Bilateral	5	5	4	5	3.3	Follicuar carcinoma of thyroid	M	VI
102	410506	50	F	?MNG	Mixed echogenicity nodules	PB	Bilateral	4A	4	3	2	1.35	Nodular goitre	B	II

s.no	UHID NO	Age	Gender	Clinical Diagnosis	USG diagnosis	USG Diagnosis	Side of lesion	TIRADS	ACR -TIRADS	ASTERIA CRITERIA	RAGO CRITERIA	EI -Mean	Pathological diagnosis	B/M	BETHESDA Scoring
103	716786	60	F	Thyroid swelling	Solitary thyroid nodule	PB	Right	3	3	2	1	0.52	Lymphocytic thyroiditis	B	II
104	717397	18	F	Swelling in the neck	Thyroiditis	B	Bilateral	3	3	2	1	0.97	Benign thyroid lesion	B	II
105	679376	27	F	? MNG	Thyroiditis	B	Bilateral	3	3	4	1	1.72	Nodular goitre	B	II
106	743612	72	F	?MNG	MNG	B	Bilateral	2	3	2	3	0.82	Lymphocytic thyroiditis	B	II
107	735574	32	F	Thyroid swelling	Heterogenous nodule	B	Right	3	3	2	4	1.31	Lymphocytic thyroiditis	B	II
108	734228	71	F	Swelling in the neck	Likely benign	B	Bilateral	2	3	2	3	0.87	Lymphocytic thyroiditis	B	II
109	731683	65	F	Thyroid swelling	Benign lesion	B	Bilateral	2	3	2	3	2.03	Colloid goitre	B	II
110	728975	30	F	Post op - left hemithyroidectomy	Likely neoplastic	PM	Right	4A	4	2	2	2.8	Nodular goitre	B	II
111	743598	46	F	?MNG	Likely benign	B	Biletral	1	1	2	3	0.78	Lymphocytic thyroiditis	B	II
112	746535	25	F	Thyroid swelling	Thyroiditis	B	Bilateral	2	3	2	1	0.61	Lymphocytic thyroiditis	B	II
113	743653	44	M	Swelling in the neck	Cystic lesion	B	Left	2	2	1	1	0.83	Colloid goitre	B	II
114	629625	60	F	Thyroid swelling	MNG	B	Bilateral	2	3	2	1	0.37	Nodular goitre	B	II
115	739547	45	F	?MNG	Thyroiditis	B	Bilateral	3	3	2	3	0.71	Lymphocytic thyroiditis	B	II
116	740050	25	F	Thyroid swelling	Thyroiditis	B	Bilateral	3	3	3	3	0.42	Lymphocytic thyroiditis	B	II

s.no	UHID NO	Age	Gender	Clinical Diagnosis	USG diagnosis	USG Diagnosis	Side of lesion	TIRADS	ACR -TIRADS	ASTERIA CRITERIA	RAGO CRITERIA	EI -Mean	Pathological diagnosis	B/M	BETHESDA Scoring
117	566895	45	F	Swelling in the neck	Thyroiditis	B	Bilateral	3	3	2	3	0.25	Benign thyroid lesion	B	II
118	713466	26	F	Thyroid swelling	MNG	B	Bilateral	2	3	1	1	1.61	Papillary carcinoma (oncocytic variant)	M	VI
119	716691	50	F	?MNG	Cystic lesion	B	Left	1	2	1	2	0.57	Nodular goitre	B	II
120	743520	38	F	Thyroid swelling	MNG	B	Bilateral	2	3	3	3	2.06	Lymphocytic thyroiditis	B	II
121	755611	28	F	Thyroid swelling	Colloid nodule	B	Left	2	2	2	1	1.9	Colloid goitre	B	II
122	756973	30	F	Thyroid swelling	Likely Benign	PB	Left	2	3	3	4	3.86	Follicular variant of papilary carcinoma	M	VI
123	753656	29	F	Solitary thyroid nodule	MNG	B	Bilateral	3	3	2	1	2.19	Papillary carcinoma thyroid classic type	M	VI
124	742330	56	M	Solitary thyroid nodule	MNG	B	Bilateral	2	2	2	3	3.68	Nodular goitre	B	II
125	742625	42	F	MNG	MNG	B	Bilateral	2	3	2	3	1.65	Nodular goitre	B	II
126	750907	39	F	Goitre	MNG	B	Bilateral	3	3	2	3	0.88	Autoimmune thyroiditis	B	II
127	741154	25	F	Thyroid swelling	Nodule with colloid degeneration	B	Bilateral	2	2	2	2	1.28	Benign thyroid lesion	B	II
128	751403	35	F	Thyroid enlargement	Spongiform	B	Left	1	1	2	2	1.4	Benign thyroid lesion	B	II
129	751606	55	M	Swelling in the neck	MNG	B	Bilateral	1	1	2	1	0.54	Colloid cyst	B	II
130	756964	32	F	Solitary thyroid nodule	Likely Benign	PB	Left	3	3	2	3	1.46	Lymphocytic thyroiditis	B	II
131	746354	28	F	Thyroid swelling	Likely Benign	PB	Right	2	3	2	2	1.65	Benign thyroid lesion	B	II

s.no	UHID NO	Age	Gender	Clinical Diagnosis	USG diagnosis	USG Diagnosis	Side of lesion	TIRADS	ACR -TIRADS	ASTERIA CRITERIA	RAGO CRITERIA	EI -Mean	Pathological diagnosis	B/M	BETHESDA Scoring
132	748228	23	F	Thyroid swelling	Likely neoplastic	PM	Right	4A	5	4	5	3.85	Papillary carcinoma thyroid classic type	M	VI
133	450682	55	F	? Thyroid malignancy	Neoplastic	M	Right	4B	5	4	5	5.86	Follicular variant of papilary carcinoma	M	VI
134	541540	25	F	? Thyroiditis	Thyroiditis	B	Bilateral	1	2	2	1	0.78	Hashimoto's thyroiditis	B	II
135	758410	53	F	Thyroid swelling for evaluation	Thyroiditis	B	Bilateral	3	2	2	1	1.66	Benign thyroid lesion	B	II
136	763079	68	F	?MNG	MNG	B	Bilateral	3	2	1	1	0.77	Nodular goitre	B	II
137	762900	40	F	? Thyroid swelling	Benign thyroid nodule	B	Right	2	1	2	3	1.96	Nodular goitre	B	II
138	765854	50	F	Thyroid swelling for evaluation	Benign thyroid nodule	B	Right	3	2	1	2	0.78	Nodular goitre	B	II
139	684653	55	F	Swelling in the neck	Benign thyroid lesion	B	Left	2	2	2	1	1.7	Benign thyroid lesion	B	II
140	749312	38	F	? Thyroid swelling	Cystic thyroid nodule	B	Left	2	1	2	1	0.96	Colloid cyst	B	II